UNIVERSITÀ DEGLI STUDI DI MESSINA

DIPARTIMENTO DI

SCIENZE CHIMICHE, BIOLOGICHE, FARMACEUTICHE ED AMBIENTALI

DOTTORATO DI RICERCA IN SCIENZE CHIMICHE
CICLO XXXIV (CHIM/06)

Molecular and supramolecular behaviour of tubular macrocycles

PhD student Marco Milone

Supervisor:
Prof. Melchiorre F. Parisi

Coordinator:
Prof. Paola Dugo

2018 – 2021

INDEX

Chapter 4

OVERLOOK

The topics covered in this PhD thesis concern the synthesis, the structural features and the molecular and supramolecular properties of tubular-shaped compounds, more specifically it focuses on macrocycles of the calix[4]arene and pillar[*n*]arene families.

After an introduction on the general aspects of supramolecular chemistry, some representative properties of the most common families of macrocyclic compounds are briefly surveyed (Chapter 1).

In Chapter 2, the synthesis of a new tubular derivative (**UC4T**) belonging to the calixarene sub-family of calix[4]tubes is reported and its structural properties are discussed both in solution (NMR studies) and in the solid state (X-ray crystal analysis) in relation to its propensity to bind metal ions and form polycapsular assemblies.

Chapter 3 explores the use of suitably functionalised pillar[5]arenes (**QP5$_{C4}$**/**QP5$_{C10}$**) as potential precursors for the formation of self-diagnosing smart polymers by way of exploiting the optical response generated by a supramolecular inclusion complex with a fluorophore derivative. The chapter also discusses the formation of a pseudo[1]rotaxane species and its solvent-dependent properties.

Chapter 4 deals with the formation of host-guest complexes in aqueous media. It describes the synthesis of a novel water-soluble pillar[6]arene (**WSP6**) that has been shown to interact with two model drugs, in one case to form surfaces with antibacterial and anti-adhesive properties, and in the other acting as a cargo molecule for drug release from a discrete system.

CHAPTER 1

1.1 The Supramolecular Chemistry

Chemistry is the science of matter and its transformations, it is the science of transfers and interactions; chemistry is the bridging science between the laws of physics and the rules of life, and life itself is its ultimate expression. Indeed, it plays a pivotal role in our understanding of material phenomena and our ability to act upon and modify them. Chemical synthesis is the art through which new molecules and new materials with novel properties can be produced.

Over the years, molecular chemistry has developed a wide range of sophisticated and powerful methods for building increasingly complex molecular structures by forming or breaking covalent bonds between atoms in a controlled and precise manner. Thus, molecular chemistry has established control over covalent bonding, but beyond this lies a field whose goal is to achieve control over weak intermolecular forces rather than strong covalent ones, the field of supramolecular chemistry. This type of chemistry deals with organised entities of even greater complexity resulting from the association of two or more chemical species, held together in effect primarily by intermolecular forces (Figure 1.1).[1]

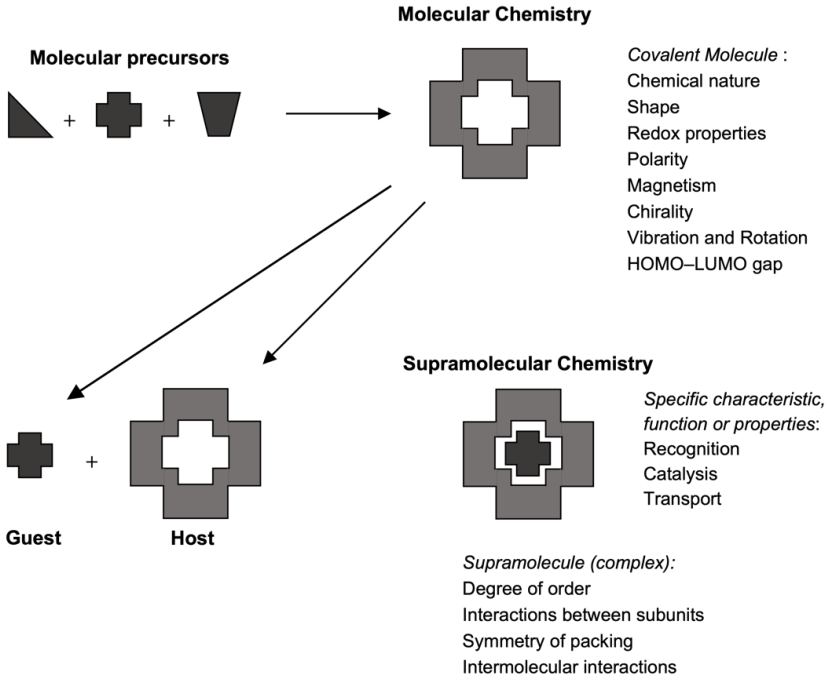

Figure 1.1. Comparison between the scope of molecular and supramolecular chemistry (adapted from ref 2).

As Professor Jean-Marie Lehn wrote, it is a sort of «*molecular sociology*»[2]: "*non-covalent interactions define the intermolecular component bond, the action and reaction, in brief, the behaviour of the molecular individuals and populations"*. He has, in fact, tailored a perfect definition for this discipline, that is «*chemistry beyond the molecule*». Supramolecular chemistry is, in fact, a highly interdisciplinary scientific field, dealing with the chemical, physical and biological characteristics of chemical species of greater complexity than the molecules themselves, held together and organised by means of intermolecular (non-covalent) interactions. In a sense, one could say that supramolecular chemistry expands into a supramolecular science, drawing on the physics of organised condensed matter and exporting its concepts to the biology of large molecular assemblies (Figure 1.2).

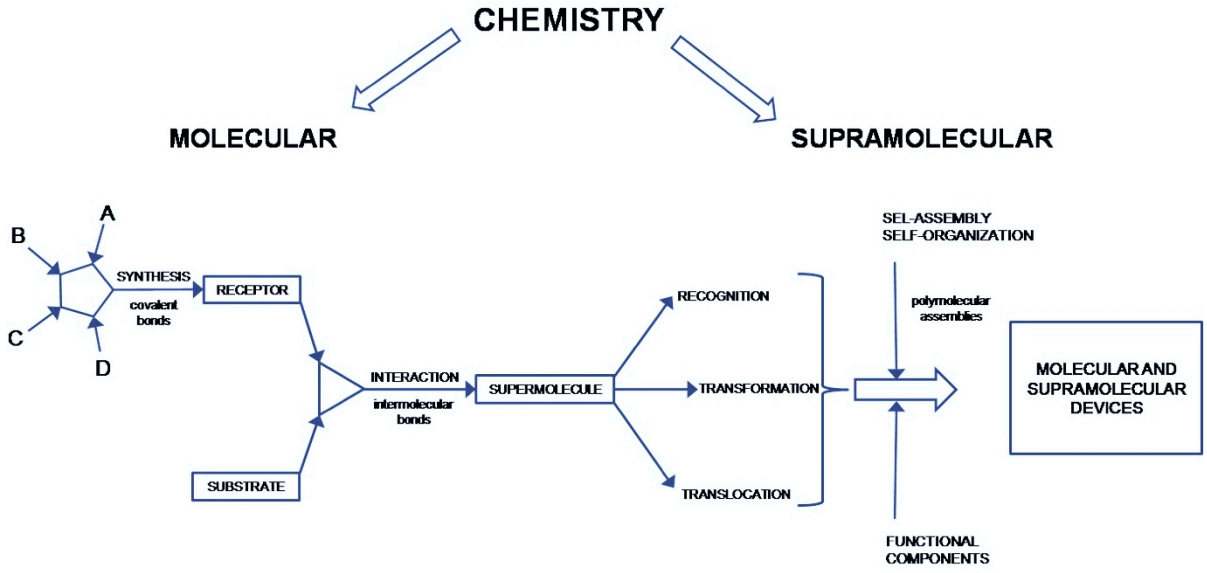

Figure 1.2. From molecular to supramolecular chemistry: molecules, supermolecules, molecular and supramolecular devices (adapted from ref. 2).

The rapid expansion of supramolecular chemistry, however, has led to an enormous variety of chemical systems that can be called supramolecular. For example, a fully covalent molecule comprising a chromophore (light-absorbing moiety), a spacer and a redox centre could be considered supramolecular because the chromophore and redox centre are able to absorb light or change the oxidation state, whether they are part of the supramolecular entity or not. Similarly, much work has focused on developing synthetic self-assembling pathways to large molecules or molecular arrays. These systems often self-assemble using a variety of interactions, some of which are clearly non-covalent (*e.g.*, hydrogen bonds) while others possess a significant covalent component (*e.g.*, metal-ligand interactions).

However, if supramolecular chemistry is considered in its simplest definition as involving a non-covalent bond or a complexation event, the nature of the bond itself must certainly be

defined. In this view, we generally consider a molecule (a 'host') binding another molecule (a 'guest') to produce a 'guest-host' or supermolecule complex ('übermoleküle').[3,4] In common knowledge, the host is represented by a large molecule or aggregate (such as a natural enzyme or a synthetic cyclic compound) that has a large central hole or cavity. On the other hand, the guest can be a monoatomic or inorganic ion, an ion pair or a more sophisticated molecule (such as a hormone, a pheromone or a neurotransmitter). More formally, the host is defined as the molecular entity that possesses convergent binding sites (*e.g.*, Lewis base donor atoms, hydrogen bond donors, etc.). The guest, conversely, possesses divergent binding sites (*e.g.*, a spherical metal cation, Lewis acid or a halogenide anion that accepts hydrogen bonds). In turn, a binding site is defined as a region of the host or guest capable of taking part in a non-covalent interaction.[5] Professor Donald J. Cram defined host-guest interaction as follows[6]: [...] *molecular complexes are usually held together by hydrogen bonding, by ion pairing, by π-acid to π-base interactions, by metal-to-ligand binding, by van der Waals attractive forces, by solvent reorganising, and by partially made and broken covalent bonds (transition states)* [...] *High structural organisation is usually produced only through multiple binding sites* [...] *A highly structured molecular complex is composed of at least one host and one guest component* [...]. Host and guest *molecules and ions* usually experience an attractive force between them and hence a stabilising binding free energy.

Thus, supramolecular chemistry is a recent subject that dates back to the late 1960s and early 1970s. Much of this discipline arose from the exceptional developments in macrocyclic chemistry during that decade, in particular the development of macrocyclic ligands for metal cations. It could be argued that this field began with the selective binding of alkaline metal cations by natural[7,8,9] as well as by synthetic macrocyclic and macropolycyclic ligands, the crown ethers[10,11] and the cryptands,[12,13] and reached its high points with the initial Nobel Prize win by Cram, Lehn and Pedersen in 1987 for research into the chemical basis of 'molecular recognition'[1b,14] (*i.e.*, how a receptor molecule selectively recognises and joins a substrate), and then in 2016 with further success by Feringa, Sauvage and Stoddart, also Nobel Prize laureates, in the design and development of molecular machines,[15] where the complexity of the systems increases dramatically.

Irrespective of the degree of complexity with which they are assembled, however supramolecular species are generally characterized both by the spatial arrangement of their components, their architecture or superstructure, and by the nature of the intermolecular bonds that hold these components together (Figure 1.3). They possess well-defined structural, conformational, thermodynamic, kinetic and dynamical properties. Various types of interactions may be distinguished, that present different degrees of strength, directionality,

dependence on distance and angles: metal ion coordination, electrostatic forces, hydrogen bonding, van der Waals interactions, donor-acceptor interactions, etc.

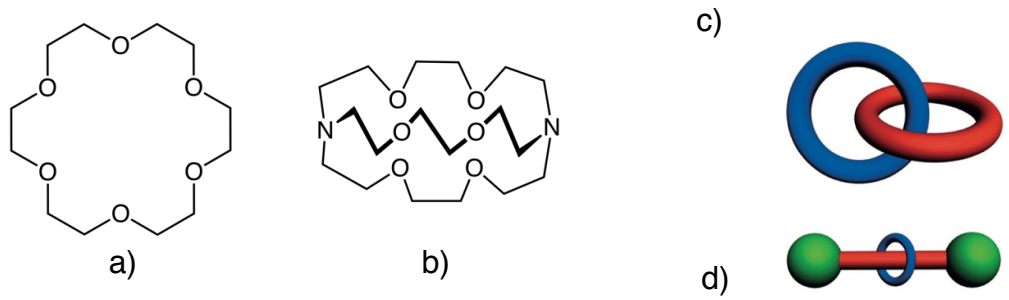

Figure 1.3. From "simple" structures of a) 18-crown-6 and b) [2.2.2]cryptand, to the schematic representations of the more complex c) catenanes and d) rotaxanes.

It is therefore clear that the main principle of this vast and fascinating branch of chemistry is the basic function of molecular recognition, that is defined by the energy and the information involved in the binding and selection of substrate(s) by a given receptor molecule; it may also involve a specific function.[13] In fact, since the mere binding is not recognition, it thus implies the storage and read out of some information, that could be stored in the architecture of the receptor or in its binding sites, and is read out by the formation and dissociation of the supermolecule. So, the basis of molecular recognition by a receptor towards a substrate is the concept of selectivity, which can be expressed in thermodynamic terms as the difference in free energy between the binding of a given substrate and those of other substrates, when interacting with a receptor. This selectivity is provided by many factors, for example the shape of both partners, the nature and number of the respective interacting binding sites and their spatial arrangement, and sometimes also the effect brought by the solvent medium in which interaction takes place. All of these factors could be resumed in the key-concept of complementarity (from the union of Greek words πλήρωμα: *complement*, and μέροσ: *part*), *i.e.*, when parts complement each other, and the complementarity defines the affinity between a receptor (host) molecule and a substrate (guest) partner.

Thus, molecular receptors are defined as organic structures held by covalent bonds, that are able to bind selectively ionic and/or molecular substrates by means of various intermolecular interactions, leading to an assembly of two or more species, a supermolecule,[2] and their design amounts to expressing in an organic molecule the above-mentioned principles of molecular recognition. The ideas of molecular recognition and receptor–substrate interaction have more and more insistently circulated in the chemical community, over the past forty years, ultimately leading to Professor Lehn's definition of *receptor chemistry*, *i.e.*, the chemistry of artificial receptor molecules. In this context, molecules have been synthesised

that perfectly interpret the role of host receptor: molecules that contain intramolecular cavities, clefts or pockets into which the substrate may fit. In such “concave” receptors the cavity is lined with binding sites directed towards the bound species. And so it was that macrocyclic compounds found their starring role on the grand stage of chemistry.

In fact, host–guest chemistry using macrocyclic compounds as hosts absolutely adheres to Lehn’s concept of supramolecular chemistry, because these are organized entities constructed from two or more chemical species by designed intermolecular interactions.

Some important macrocyclic compounds (Figure 1.4) used for the formation of supramolecular aggregates are cyclodextrins,[16] the aforementioned crown ethers,[10,11,17] cucurbit[*n*]urils,[18] calix[*n*]arenes (Section 1.2) and pillar[*n*]arenes (Section 1.3). Historically, the main reasons that have contribute to the widespread use of these molecules for a variety of applications are: (i) the ease of synthesis and derivatisation, (ii) a versatile purpose-suited functionality, (iii) their unique and singular host–guest properties which give them a high discrimination for a slight shape difference of the ideal guest, and the ability to form host–guest complexes in various media, such as aqueous, organic, bulk liquid, solid and gas phases in some cases; (iv) last but not least, their shape and all related characteristics, such as rigidity or flexibility, the presence or absence of symmetry and chirality, the biocompatibility (strictly dependent, of course, also on the type of functional groups present in the scaffold).

The last property is common for particular derivatives of these macrocyclic compounds, whose appropriate derivatisation allowed the development of supramolecular chemistry in an aqueous environment.

Name / Features	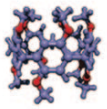 Pillar[n]arene	 Crown Ether	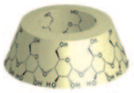 Cyclodextrin	 Calix[n]arene	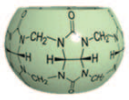 Cucurbit[n]uril
Synthesis/ Yield	◎	○	—	○	△
Functionality	◎	○	◎	○	△
Homologue	○ 5, 6 △(7-14)	◎12-21	○ α, β, γ-CD	○ 4, 6, 8 (5,7,9-20)	◎ 5-8 (10,14)
Shape	Pillar	Crown	Bucket	Calix	Pumpkin
Complexation (Aqueous)	○	△	○	○	◎
Complexation (Organic)	○	○	△	○	×
Original Property	Planar Chirality Symmetric	Flexible	Biocompatible Chirality Nonsymmetirc	Nonsymmetirc	Rigid Structure Symmetric

Figure 1.4. Comparison between the macrocyclic compounds. Symbol key: ◎ (very easy / high); ○ (easy / good); △ (hard / low); × (no evidence).

Certainly, of all of them, cyclodextrins have played a prominent role in the development of supramolecular aggregate formation in water, due to their high solubility in this solvent, and proven biocompatibility;[19] however, in later times, macrocycles such as calix[*n*]arenes and pillar[*n*]arenes have also been functionalised for the development of their chemistry in aqueous media. Their receptor properties are increasingly being exploited to bind harmful water-soluble molecules, or pharmacologically active molecules, or to bring poorly soluble molecules into aqueous solution, following the formation of host-guest type supramolecular aggregates.

The versatility of these macrocycles has enabled them to be employed in a wide range of chemical fields, in particular where their receptor properties can be used for the formation of supramolecular aggregates, both in organic solvents and in aqueous solutions, or their self-assembly capacities for the design of innovative materials.

In this doctoral thesis work, the concept of supramolecular aggregation is developed and applied to the fabrication of linear polymer structures, exploiting the self-assembling capabilities of tubular derivatives of calix[4]arenes (Chapter 2), or for the design of innovative smart materials, in the field of sensor technology, using chromophoric pillar[5]arene derivatives and their host abilities (Chapter 3). Finally, a discussion on the possibility of obtaining supramolecular aggregates of host-guest types also in aqueous solution, this time exploiting a water-soluble pillar[6]arene, whose characteristics allow its use for the manufacture of materials to a medical usage, or even the possibility of employment as a cargo molecule for the release of pharmacologically active molecules in a physiological environment (Chapter 4).

*1.2 Calix[*n*]arenes*

Calix[*n*]arenes are [1$_n$]-metacyclophanes consisting of *n* phenolic units (*n* ≥ 4) linked together, in their *ortho*-position, by methylene bridging groups. The chemistry of calixarenes started in the 40's, when Zinke and Ziegler foresaw the possibility to obtain cyclic oligomers by the condensation of *p*-alkylphenols and formaldehyde under alkaline conditions.[20] However, the most significant advances in this field have been obtained many years later the first report, and can be ascribed, above others, to the group of C. D. Gutsche. He and his collaborators[21] re-interpreted the results achieved by Zinke and planned the synthesis of the three cyclic oligomers (a tetramer, a hexamer and an octamer)[22] which constituted the original mixture obtained by Zinke. In addition, he proposed to name this class of macrocycles "calixarenes",[23] having noticed that, in the solid state, the cyclic tetramer adopts a conformation closely reminiscent of a Greek crater.[24] The use of this term was later extended to the higher oligomers, even though their overall conformations often diverge from the classical "calix" shape.

Given that the IUPAC nomenclature of this class of compounds would lead to the formulation of extremely complex names, there is a general agreement on the convention of indicating the number of phenolic units of the macrocycle[25] by placing a number in square brackets between the words "calix" and "arene", and specifying the substituents on the *para* position of the phenol units before the name of the calixarene. The position of the other substituents follows the numbering shown in Figure 1.5.

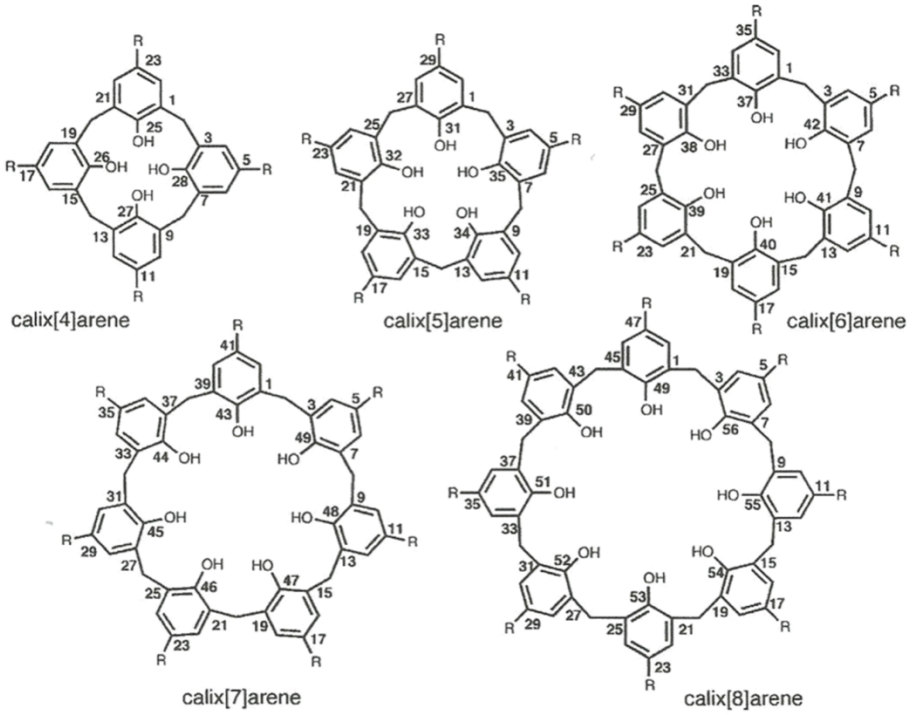

Figure 1.5. Numbering commonly used for calix[*n*]arenes nomenclature.

As far as their synthesis is concerned, the strategy designed by Zinke (the "one-pot" synthesis) is still the best method for the preparation of calixarenes composed of only one type of phenolic units. The size of the calixarene macrocycle produced from these cyclo-oligomerizations can be controlled by varying the reaction conditions (*e.g.,* solvent, temperature, type and number of equivalents of base, Scheme 1.1). The cyclic oligomers composed of an even number of phenolic units can be obtained in this manner on a large scale and with high yields (50–85%).[22]

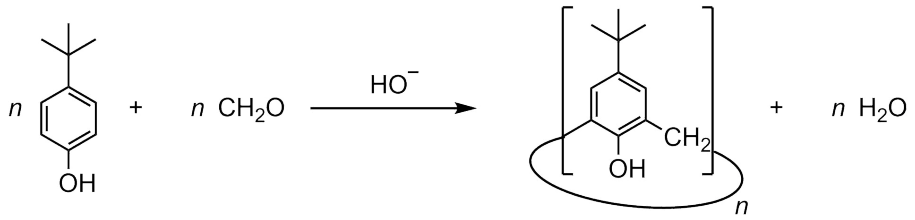

n	reaction conditions	yield (%)
4[22a]	NaOH / Ph_2O; 120–259 °C	49
5[26]	KOH / tetralin; 80–185 °C	10–15
6[22b]	KOH / xylene; reflux	83–88
8[22c]	NaOH / xylene; reflux	62–65

Scheme 1.1. Synthesis of *p-tert*-butylcalix[*n*]arenes.

Conversely, the yields of the pentamer (15–20%)[26] and the heptamer (11–17%)[27] are modest. Larger calixarenes can be obtained in higher yields when the condensation reaction is performed under acidic catalysis.[28] As an alternative to the "one-pot" synthesis, multiple step synthetic procedures have been described. This "multi-step" synthesis involves the repeated condensation of *p*-alkylphenol residues to obtain a suitably-sized linear oligomer, which is ultimately subjected to intramolecular cyclization[29] (Scheme 1.2). Such an approach presents the obvious advantage that different substituents can be introduced *ab initio* at the *para* position of the aryl residues on the calixarene skeleton, merely selecting different *p*-alkylphenols as reactants during the growth of the linear oligomer. The cyclization, often carried out under high dilution conditions, proceeds with good yields[30] but, given the large number of synthetic steps needed to produce the linear precursor, overall quantities of product are generally low.

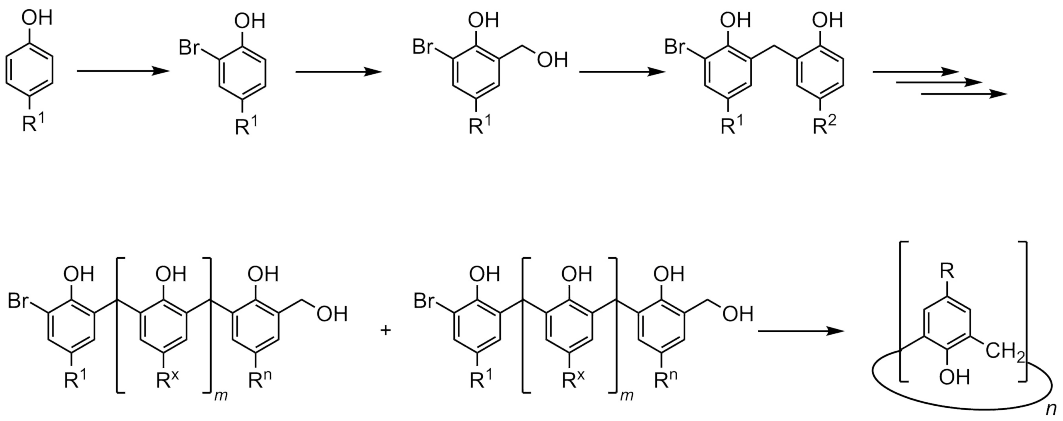

Scheme 1.2. “Multi-step” synthesis of calix[*n*]arenes.

Calixarenes are characterized by a marked conformational mobility, as a result of the rotation of the aryl residues around the CH_2ArCH_2 σ-bonds. This motion may occur via two different pathways, generally termed “lower-rim-through-the-annulus” and “upper-rim-through-the annulus”, where the *upper rim* is defined by the substituents in the *para* position of the aryl rings, and the *lower rim* by the phenolic oxygens (Figure 1.6). Therefore, in the former case it is the phenolic oxygens which swing through the macrocycle cavity, whereas in the latter it is the aryl groups that rotate inward the cyclic structure.

Of course, such conformational movement of aromatic units through the cavity may not occur simultaneously, involving all phenolic residues. When this does not happen, calixarenes may exist in different conformations, depending on the number of flipped aromatic units. In the particular case of calix[4]arenes, these macrocycles can give rise to three different conformations, shown in Figure 1.7.

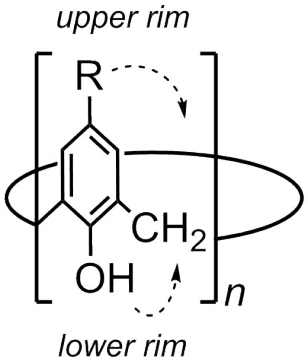

Figure 1.6. Mechanism of conformational interconversion of calix[*n*]arenes.

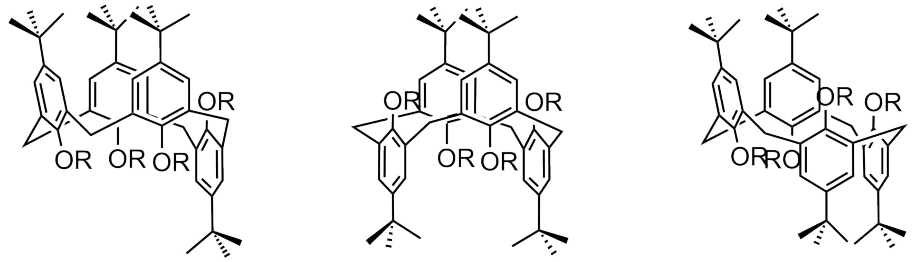

Figure 1.7. Possible conformations for *p-tert*-butylcalix[4]arene derivatives after *through-the-annulus* motion of one or two aromatic units .

VT NMR studies on calix[4]- and calix[5]arene showed that, at higher temperatures, the topologically non-equivalent protons of the bridging methylenes resonate as a singlet, and that upon cooling the singlets evolves to an AX system. This has been explained assuming fast interconversion at higher temperatures between two equivalents *cone* conformations (showed in Figure 1.8 for calix[4]arene).[31] Free energy barrier for the conformational interconversion is 15.7 kcal/mol (in $CDCl_3$) for *p-tert*-butylcalix[4]arene[25] and 13.2 kcal/mol for the *p-tert*-butylcalix[5]arene.[25]

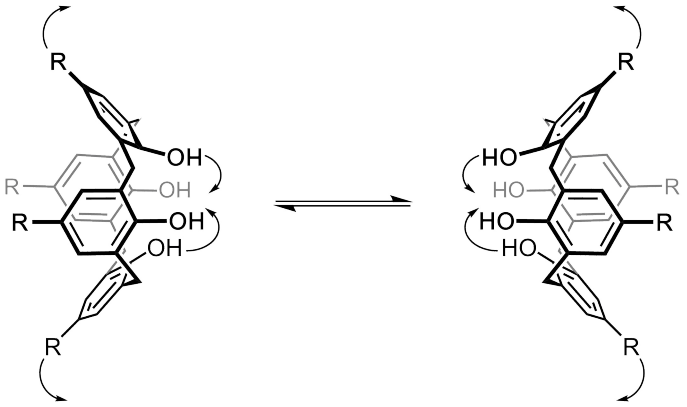

Figure 1.8. Interconversion of calix[4]arenes.

Conversely, in the solid state, as well as, in solution at lower temperatures, calix[4]-[32] and calix[5]arenes[33] adopt a *cone* conformation stabilized by intramolecular hydrogen bonds between the phenolic hydroxyl groups (Figure 1.9). Similarly, the larger (and more fluxional) *p-tert*-butylcalix[6]arene adopts a similar *cone* conformation in the solid state.[34]

The conformational mobility of the calixarene derivatives is a function both of the size of the macrocycle and of the size and nature of the substituents at the upper and lower rims. These motions can be slowed down or stopped altogether by introducing bulky groups at either of the two rims to obtain locked conformational isomers.

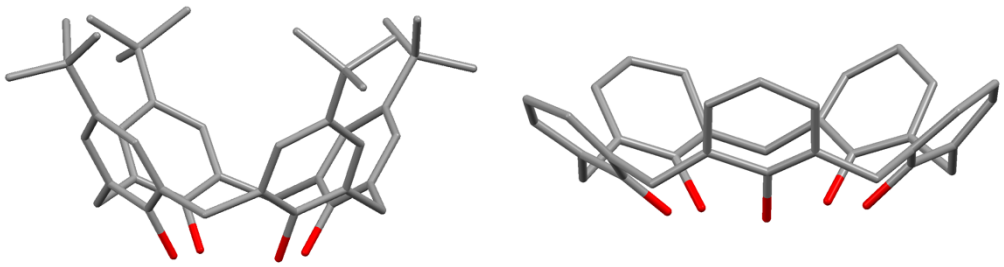

a b

Figure 1.9. X-ray crystal structures of a) *p-tert*-butylcalix[4]arene[32] and b) calix[5]arene[33] adopting a *cone* conformation. Hydrogens were removed for simplicity.

In calix[4]arenes, given the small size of the macrocycle, the intra-annular swing of the upper rim is inhibited even when the substituents in the *para* position is a hydrogen atom, whereas the lower rim swinging – which is the only motion allowed in unsubstituted calix[4]arenes – is blocked by attaching to the phenolic oxygens substituents larger than ethyl groups.[35] In the case of calix[6]arenes, even *tert*-butyl groups do not inhibit the upper-rim-through-the-annulus rotation.[36]

1.2.1 Selective functionalization of calix[4]arenes

Chemical modification of calixarenes does not only permit the synthesis of new host molecules by the introduction of additional functional groups, but it also allows control of the conformation of calixarenes and hindrance of conformational inversion.

Calixarenes derived from phenol can undergo modification in two main ways: 1) by the introduction of residues (functional groups) at the phenolic hydroxy groups; 2) by (electrophilic) substitution in the *p*-position with respect to the phenolic hydroxy group (subsequent to elimination of the *tert*-butyl group originally present).

1.2.1.1 Lower rim manipulation

In the case of calix[4]arenes, the reaction of all the OH groups with monofunctional reagents to give ether or ester derivatives has some interesting aspects: since larger substituents (*e.g.,* acetyl, propyl) cannot pass through the macrocycle, it is possible to isolate them as stable conformers.[37]

The regioselective reaction of single hydroxy groups in calixarenes is important for many purposes, in particular for the construction of larger molecules starting from several calixarene building units.[38] One of the first examples of selective functionalization to be described was that of the tribenzoate of the unsubstituted calix[4]arene.[39] The remaining OH

group can undergo etherification; thus, monoethers are accessible after hydrolysis of the ester groups.[40]

Direct monoalkylation has been carried out using an excess of the alkylating agent and K_2CO_3 in CH_3CN or CsF in DMF as a very weak base,[41] but also with NaH in toluene[42] or with $Ba(OH)_2$ in DMF.[43] The controlled cleavage of 1,3-diethers or tetraethers with either one or three equivalents of trimethylsilyl iodide offers another possible alternative.[44] Monoesters were also obtained in a similar manner from 1,3-diesters by reaction with imidazole.[45] The direct formation of triethers was achieved by using $BaO/Ba(OH)_2$ in DMF.[37b,46]

The best results in the selective *O*-alkylation (as in *O*-acylation[45,47]) of calix[4]arenes were obtained by reaction of two equivalents of a relatively weak base.[48] A variety of 1,3-diethers were thus obtained in good yields, also to the respect of the corresponding tetraethers. These results can also be readily understood on a theoretical basis[38] since the most stable anion (stabilized by two intramolecular hydrogen bonds) of the monoether formed in the first step is obtained by deprotonation of the opposing hydroxy group (Scheme 1.3).

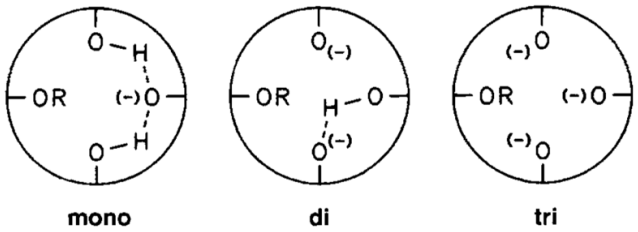

Scheme 1.3. Anions of a calix[4]arene monoether.

Dialkylation with a stoichiometric amount of the alkylating agent in the presence of an excess of a strong base (*e.g.*, NaH in DMF/THF) would on the other hand have to occur via the 2,4-dianion or via the trianion, from which the formation of the 1,2-diether should also be favoured for statistical reasons. Nevertheless, the yields of 1,2-diethers are in general lower. An alternative route to 1,2-diethers is the selective cleavage of neighbouring ether groups by $TiBr_4$.[49]

1.2.1.2 Upper rim manipulation

The calixarenes derived from *tert*-butylphenol are obtained particularly readily since the *tert*-butyl group can easily be removed by $AlCl_3$-catalyzed transalkylation in the presence of a suitable acceptor such as toluene or phenol.[50] This reaction[51] plays a key role in calixarene chemistry, as a large variety of calixarenes with different substituents in the *p*-positions can be obtained by subsequent electrophilic substitution.

Virtually, all the common reaction possible for phenol (or its ethers) have been carried out for calixarenes or their alkyl ether derivatives.

Among these could be mentioned:

- halogenation[52]
- nitration[53] and *ipso*-nitration[54]
- sulfonation[55] and *ipso*-sulfonation[56]
- sulfochlorination[57]
- chloromethylation[58]
- aminomethylation[59]
- acylation[60]
- coupling with diazonium salts[61]

Nitro compounds have also been obtained via the sulfonic acids[55a] or the nitroso compounds.[53] Claisen rearrangements of allyl ethers[39,50] and Fries rearrangements[62] have also been carried out.

The substituents thus introduced can undergo further reactions, for example the isomerization and/or ozonolysis of allyl groups,[50] haloform reactions of acetyl groups,[52b] Suzuki coupling reaction,[63] and more reduction of nitro-,[64] azo-,[65] or acyl groups,[60] as well as further substitution at chlorosulfone[57] and chloromethyl groups.[66]

Again, it is very desirable not to substitute all the *p*-positions, but only certain of them, in a selective way. This selectivity can be achieved by direct functionalization of OH groups, as this regiochemical information can be transferred to the *p*-positions, since phenol units are more reactive than their ether or ester derivatives.[38]

1.2.2 Calix[4]arene ionophoric properties

One of the most attractive features of calix[4]arenes is their cuplike structure, adopted both in solution and in the solid state. As a result, the calix[4]arene cavity is able to host and discriminate ions of complementary size.

Several studies, corroborated by crystallographic analyses, have shown the formation of calix[4]arene-metal ion complexes in the solid state. Early examples include a titanium-*p*-*tert*-butylcalix[4]arene[67] complex and a larger adduct where two Eu^{3+} atoms are bound to two *p*-*tert*-butylcalix[4]arene molecules.[68] This macrocycle also forms complexes with silicon(IV)[69] to give 'koilands' and with Al^{3+} and Zn^{2+} to form similar bis-calixarenes.[70, 71] *p*-*tert*-Butylcalix[4]arene forms a stable *endo*-cavity complex with caesium,[72] and a study on the complexation of its monoanionic form with alkali metals showed that the stability constants increase in the order $Li^+ < Na^+ < K^+ < Rb^+ < Cs^+$.[73]

The earliest examples of lower rim-substituted calix[4]arenes investigated for their complexation properties towards metal ions were the ethyleneoxy (–CH_2CH_2OR) derivatives, which showed only a modest cation binding capacity.[74] On the other hand, calix[4]arene bearing *n*-propyl substituents showed a strong affinity for K^+ and Ag^+ when in the 1,3-alternate conformation, while a weaker interaction was observed for the other conformers.[75] This finding on the 1,3-alternate conformer being able to form tighter complexes was attributed to a combined effect due to the concomitant interaction of the cation with the ethereal oxygens and the π-donor aryl rings of the calixarene.

1.2.3 Self-assembly of calix[4]arenes

Self-assembly is the spontaneous non-covalent association of two or more molecules into stable aggregates, under equilibrium conditions.[76] Intermolecular forces are capable of effectively organizing multicomponent supramolecular assemblies in a reversible and accurate fashion. As on many other occasions, chemistry attempts to imitate nature, where this type of association is involved in the formation of, for example, cell membranes, double-stranded nucleic acids and viruses; whereas in the chemical field self-assembly provides a novel, rapid way to construct complex nanostructures, receptor systems, catalysts and new materials. Calixarenes, in particular, had a great impact in the history of self-assembly,[25,29,37c,77] due to their relatively rigid structure and unique shape, combined with a well-developed synthetic chemistry that makes these macrocycles extremely convenient platforms for elaboration.[78] Indeed, a calixarene scaffold could be used in the design of well-defined assemblies by functionalization with multiple hydrogen bonding sites, a highly directional and specific force that is near-ubiquitous in self-assembly. The insertion of these sites can be done either at the upper or at the lower rim of the calixarene.[79] However, much stable dimers could be obtained from 1,3-*alternate* calix[4]arenes functionalized with two ureido-bearing moieties,[80] since there is a synergic effect of eight hydrogen bonds participating in the self-assembly process. Furthermore, when appropriate curvature and carefully engineered positioning of hydrogen bonding sites are implemented, calixarenes self-assembling system generates capsules, which are, by definition, receptors with enclosed cavities, formed through the reversible non-covalent interactions between two or more subunits.[81] Dimeric calix[4]arene tetraurea capsules could be obtained in this way, in which a seam of sixteen intramolecular hydrogen bonds at the upper rim is obtained, performing an head-to-tail assemble of the eight (four from each hemisphere) urea moieties (Figure 1.10).[82]

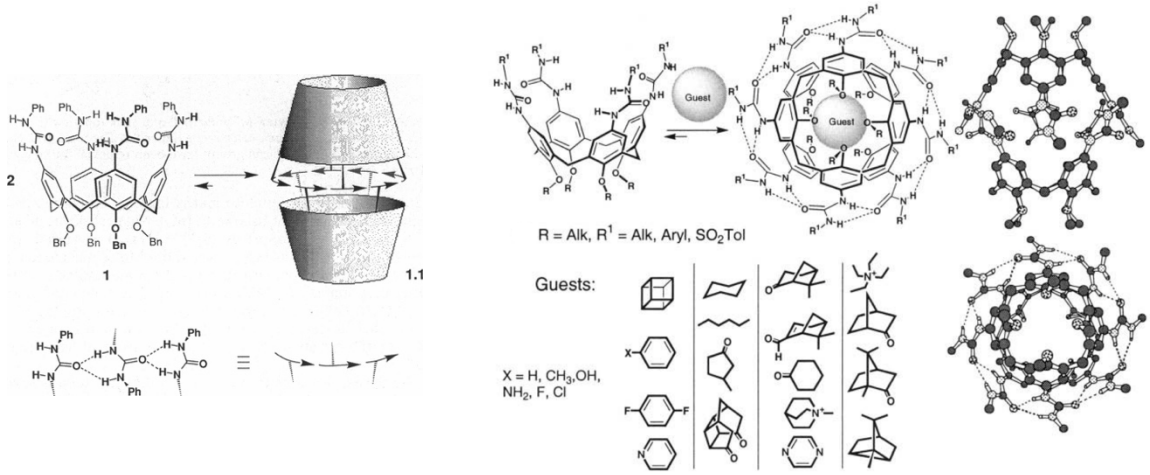

Figure 1.10. Hydrogen-bonded dimeric capsules of calix[4]arene tetraureas and their guests, with arrows representing ureas hydrogen-bonded in a head-to-tail topology. Bn, benzyl. On the right the X-ray crystal structure of the dimeric capsule.[82a]

Such an arrangement gives a rigid cavity capable to accommodate one benzene-sized guest molecule.[83] Homodimeric capsules made up as follows are meso and therefore achiral, possessing an S_8 symmetry in which however each individual calixarene is chiral because of the specific orientation of urea groups in the hydrogen-bonded assemble. As a consequence, guests on the inside of the cage formed by assembled structure preferentially adopt a particular favoured orientation.[84]

In addition, although the homodimeric capsule is achiral, if a chiral guest is offered (only one enantiomer) the whole complex became chiral. Indeed, the two halves are now diastereomeric and they show different signals in NMR spectra. Instead, if the guest is a racemic mixture, two diastereomeric capsules are formed.

When two calix[4]arene tetraureas are covalently linked at their lower rims, hydrogen bonding results in a polymer chain of capsules, also known as *polycapsules* (or *polycaps*).[85] These interesting aggregates form only when a properly-sized guest with the opportune shape is present and, like seen before with capsule aggregates, in competitive hydrogen bond-disrupting solvents such DMSO and MeOH, the polycaps dissociate. Whereas the treatment with an excess of simple dimeric capsule results in a breakdown of polycapsular structure in favour of dumbbell-shape assembly.

When the monomers are functionalized with long alkyl groups, the spaces between polymer chains are filled, and the resulting polycaps (at higher concentrations) self-organize into polymeric liquid crystals.[86]

1.3 Pillar[n]arenes

The discovery of pillar[*n*]arenes was, as with many entities in supramolecular chemistry, by chance. In 2008, the synthesis of phenol-formaldehyde resins using a featureless phenolic derivative, 1,4-dimethoxybenzene, led to the report of these fascinating macrocycles in the literature.[87] Pillar[*n*]arenes are highly symmetrical cyclo-oligomer, in which *n* indicates the number of aromatic units linked together to form a cavity.

The chemical structure is very similar to that of a calix[*n*]arene (Figure 1.11). However, one of the most important differences is the position of the methylene bridges. In calix[*n*]arenes, their units are connected by methylene bridges linked at the *meta* position (2,6-positions) of phenolic units. However, in this macrocycle, the units were connected by methylene bridges between the *para* position (2,5-positions). The different positions of these molecular links are very important and greatly affect the structure of the macrocycle. In the case of calix[*n*]arenes, owing to the *meta*-bridge linkage, their structures are open-ended and calix-shaped, and this peculiarity was the reason for their name. In contrast, because of the *para*-bridge linkage, the macrocycle obtained by Ogoshi is not a calix-shaped structure but rather a pillar-shaped structure.

Historically, reaction of phenolic derivatives with aldehydes has afforded various macrocyclic compounds,[88] more or less serendipitously; however, in order to obtain these kinds of molecules there are basically two key-factors. One is controlling the reaction point of phenolic derivatives to inhibit the formation of three-dimensional network polymers. The other is, instead, the inhibition of the linear polymer formation with concomitant acceleration of macrocyclization.

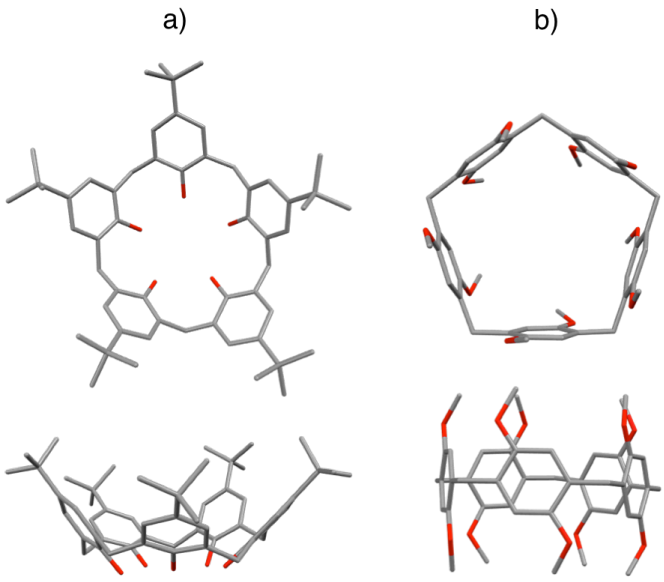

Figure 1.11. Top and side view of: a) *p-tert*-butylcalix[5]arene; b) 1,4-dimethoxypillar[5]arene.

Nowadays, more than a decade after Ogoshi's first report, pillar[*n*]arenes are recognized as key players in supramolecular chemistry: their symmetrical architecture and the electron-donating cavities are very intriguing and confer these macrocycles some special and interesting physical, chemical and host-guest properties.

Regardless the various functionalization, pillararenes display some specific characteristics: (i) despite of their simple structures, they exhibit outstanding host-guest properties and planar chirality (Figure 1.12);[89] (ii) due to their prismatic geometry, these macrocycles show very symmetrical pillar-shaped architectures from a side view (Figure 1.13).

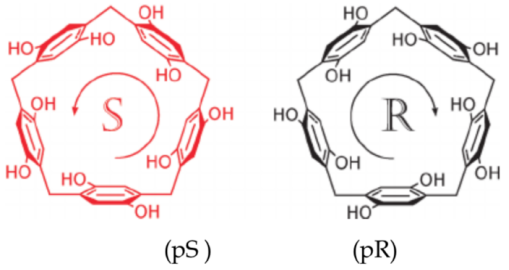

Figure 1.12. Planar chirality of pillar[5]arene

Viewed from the top, pillar[5]- and pillar[6]arenes in the specific, display a regular cyclic pentagonal and hexagonal structure, respectively. The pentameric macrocycle has a cavity size of approximatively 4.7 Å (almost analogous to 4.7 Å of α-cyclodextrin and 5.8 Å of cucurbit[6]uril). α-Cyclodextrin and cucurbit[6]uril can bind linear alkanes and simple aromatic compounds,[90] so these guests will also fit in the cavities of pillar[5]arenes.

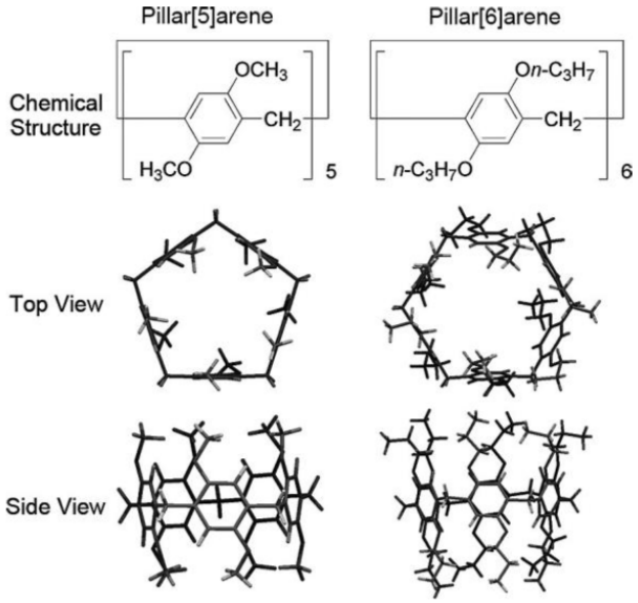

Figure 1.13. Chemical and X-ray crystal structures of dimethoxypillar[5]arene and *per*-propylated pillar[6]arene. (Adapted from ref. 84f)

In fact, these macrocycles form complexes with linear alkanes containing electron-poor systems, such as amine, ammonium, cyano and halogen groups, as well as simple aromatic compounds such as pyridinium and viologen derivatives. (iii) Ease of functionalization at both rims by different synthetic approaches, allowing the construction of a variety of pillararene-based supramolecular assemblies.

The first synthesis of pillar[5]arene **1**, reported in 2008,[87] is a condensation of 1,4-dimethoxybenzene with paraformaldehyde and an appropriate Lewis acid as catalyst, therefore the symmetrical 1,4-dimethoxypillar[5]arene (DMpillar[5]arene) **2** was selectively obtained (Scheme 1.4).

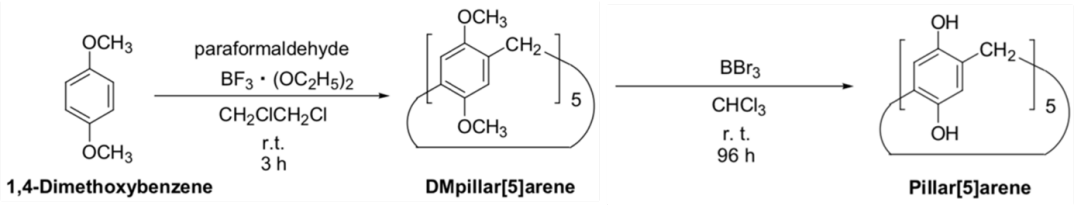

Scheme 1.4. Synthetic procedure to obtain **1**.

Various Lewis acid were used for this reaction, and with BF_3•OEt_2 the cyclic pentamer was obtained in 22% yield. Then, pillar[5]arene **1** was obtained by deprotection of the methoxy groups of DMpillar[5]arene with a 30% yield.[87]

Subsequently, many authors changed the firstly reported synthetic procedure to improve the yield of the cyclization reaction, decreasing consequently the total reaction time and also trying to obtain different sizes of pillararenes' cavities (*e.g.,* pillar[6]arenes).[91] As a further development of synthetic strategies, different methodologies were developed in order to obtain mono-, di-, tetra-, up to *per*-functionalized pillar[*n*]arenes.[92]

*1.3.1 Synthesis and functionalization of pillar[*n*]arenes*

Several methodologies have been developed for the synthesis and functionalization of pillar[*n*]arenes. For macrocyclic compounds functionalization is very important, because it can change their solubility and physical properties.[93] Substituents have, for example, a large effect on the conformation of pillar[*n*]arenes: the introduction of bulky or rigid π-conjugated moieties can inhibit the rotation of the aromatic units around the bond formed by the methylene bridges in pillar[5]arene. Moreover, position-selective group substitution of these molecules has expanded the possibility for material application.[93a-b,94]

The synthesis of pillar[5]arenes following the condensation of 1,4-dimethoxybenzene and paraformaldehyde in the presence of catalysis provided by a Lewis acid, which has now become the general method for preparing these macrocycles, has already been mentioned. It has been noted, in particular, that the use of $FeCl_3$ or $SnCl_4$ results in higher yields of linear polymers than of the pentamer cyclic derivative; on the other hand, with BF_3•OEt_2 in the presence of an appropriate solvent such as 1,2-dichloroethane (*vide infra*) the yields with which pillar[5]arene is obtained are decidedly higher (71%).[91b]

A further synthetic method to obtain highly symmetric pillar[5]arenes is the cyclization of 1,4-dialkoxy-2,5-di(alkoxymethyl)benzenes in the presence of refluxing *p*-toluenesulphonic acid (Scheme 1.5).[95] With this strategy, pillar[6]arene was obtained for the first time.[96]

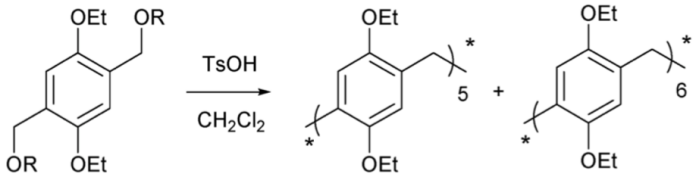

Scheme 1.5. Synthesis of 1,4-dialkoxypillar[5,6]arenes by cyclization reaction of 1,4-diakoxy-2,5-di(alkoxymethyl)benzenes.

Alkoxypillar[5,6]arenes can also be obtained by cyclo-oligomerisation of 2,5-dialkoxybenzyl alcohols or bromides (Scheme 1.6a).[91f] In fact, the shaping of pillar[*n*]arenes proceeds under dynamic covalent bond formation,[91g] as trimer macrocyclization tried to selectively produce pillar[6]arene, provided instead the pentameric derivative in higher yields (Scheme 1.6b), a phenomenon that can be explained by the cleavage of a methylene bridge from the structure, due to dynamic growth conditions.

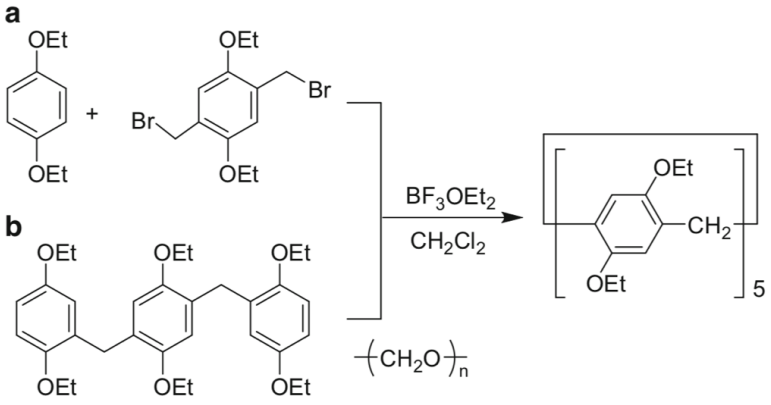

Scheme 1.6. Formation of pillar[5]arene via a) the cyclo-oligomerization of 2,5-dialkoxybenzylbromide and *p*-dialkoxybenzene; b) the macrocyclization of a trimer.

Cyclo-oligomerisation reaction between different monomers can also be used in order to obtain pillar[5]arenes with differently substituted aromatic units (co-pillararenes),[92d] as shown in Scheme 1.7.

It has already been discussed the possibility to readily produce pillar[5]arenes bearing ten OH moieties by treatment of preformed macrocycle with ten alkoxy groups with an excess of BBr_3.[87] The amount of BBr_3 and reaction temperature used in these deprotection reactions are important factors in terms of obtaining pillar[5]arenes with OH groups at specific positions.[97] Thus, treatment of *per*-methylated pillararenes with an excess of BBr_3 in anhydrous $CHCl_3$ yields the corresponding pillar[*n*]arenes (Scheme 1.8c) in a quantitative manner. Subsequent alkylation of the phenolic hydroxyls also enables a variety of derivatives to be obtained. By controlling the amount of BBr_3 and the reaction temperature, it is also possible to synthesise pillar[5]arene derivatives partially hydroxylated at specific positions (Scheme 1.8a).

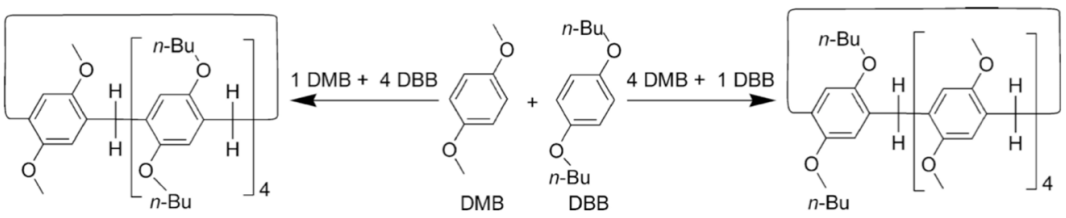

Scheme 1.7. Synthesis of co-pillar[5]arene derivatives.

However, another useful method for the introduction of reactive OH groups into pillar[*n*]arenes is the sequential oxidation/reduction method (Scheme 1.8b).[98] The oxidation of one of the 1,4-dialkoxybenzene units in pillar[5]arene afforded a macrocycle bearing a benzoquinone unit. The subsequent reduction of this derivative afforded a pillar[5]arene bearing two OH groups on the same unit. Thus, the main advantage of this method lies in the fact that it can be used to selectively produce pillar[5]arenes bearing two phenolic groups on the same unit, while the use of BBr_3 for the deprotection of the alkoxy groups in pillar[5]arenes generally results in the formation of a mixture of multi-deprotected pillar[5]arenes. In addition, further oxidation of preformed pillar[5]arenes afforded macrocycles containing two benzoquinone units. The subsequent reduction of these moieties afforded pillar[5]arenes bearing four OH groups at specific positions.[98a]

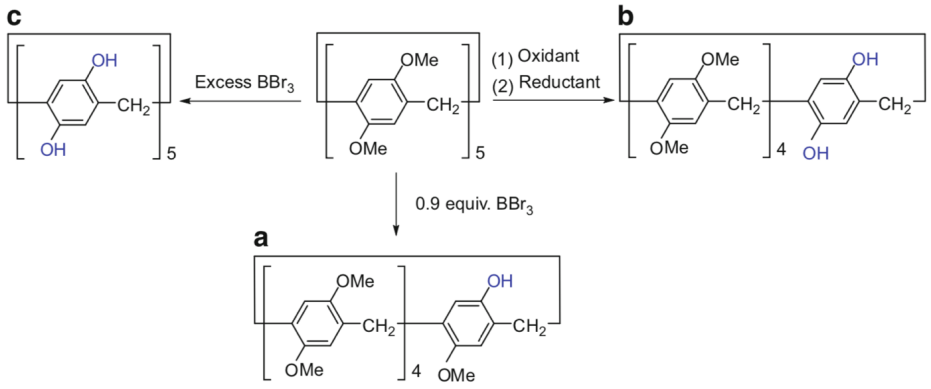

Scheme 1.8. Synthesis of pillar[5]arene derivatives a) mono-hydroxylated; b) with a single hydroquinone unit; c) *per*-hydroxylated.

The deprotection of alkoxy moieties with BBr_3 and the subsequent sequential oxidation/reduction pathway can therefore provide access to pillar[5]arenes bearing one, two, three, four and ten OH groups. Thus, a wide variety of pillar[5]arene derivatives can be produced by the etherification of OH groups with alkyl compounds bearing good leaving groups, in the presence of an appropriate base. Etherification, as a result, represents a straightforward and reliable process that can be readily applied to the functionalization of pillar[5]arenes with one up to ten OH groups. Such compounds can themselves be prepared by the deprotection of the corresponding alkoxy groups using the methods described above. Etherification has also been used for the functionalization of larger pillar[*n*]arene homologs with OH groups.[99]

Another powerful protocol for the synthesis of functionalized pillar[*n*]arenes involves the cyclization of 1,4-dialkoxybenzenes bearing a variety of different functional groups. For example, the formation of pillar[5]- and pillar[6]arenes with bromine functionalization can be achieved by cyclo-oligomerization of 1,4-dialkoxybenzene monomers containing two bromide moieties (Scheme 1.9a); indeed, deca- and dodecabromides are good building blocks for the preparation of various functionalized pillar[5]- and pillar[6]arenes, such as water-soluble cationic pillar[5]- and pillar[6]arenes, synthesized by the reaction of deca- and dodecabromides with amine compounds (see Section 4.2, Chapter 4). Pillar[5]arenes containing one or two bromide functions have also been prepared by the co-cyclization of a 1,4-dialkoxybenzene molecule with another 1,4-dialkoxybenzene carrying several alkoxy groups.[92d,100] The first example of a pillar[5]arene with one bromide group, prepared using a co-cyclization method, was reported by Stoddart *et al.*,[92a] also reporting the preparation of a similar pillar[5]arene containing only one bromide group (Scheme 1.9b).

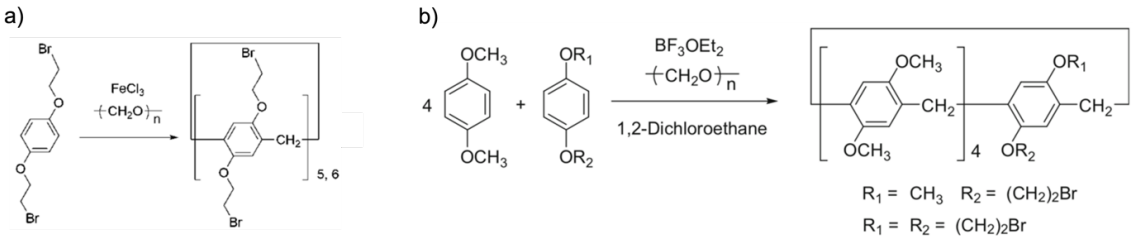

Scheme 1.9. a) cyclization of 1,4-dialkoxybenzenes bearing two bromide moieties to produce deca- and dodecabromides; b) co-cyclization of two different 1,4-dialkoxybenzene monomers with paraformaldehyde to produce pillar[5]arenes bearing one and two bromide moieties.

1.3.2 Solvent effect

The type of solvent used for the preparation of pillar[*n*]arenes can have a pronounced impact on the number of repeating units incorporated in the pillar[*n*]arene structure. The effect of the solvent clarified the high yields obtained for the synthesis of DMpillar[5]arene.[101] By using 1,2-dichloroethane as a solvent, pillar[5]arene was produced as the major product (up to 81% under the optimized conditions). In contrast, the yields were low when the reaction was carried out in dichloromethane (26%), chloroform (15%) or 1,1,2,2-tetrachloroethane (7%), that can be used as solvents for the synthesis of higher pillar[*n*]arene homologs, under kinetically controlled conditions (Figure 1.14).[102] Pillar[6]arene can be selectively obtained by using bulky hydrocarbons (*e.g.*, chlorocyclohexane) as solvent,[103] because these compounds are good guest molecules for pillar[6]arenes. In fact, when chlorocyclohexane was used as a solvent, pillar[6]arene was produced as the major product (87 %), together with a small amount of pillar[5]arene (3 %).

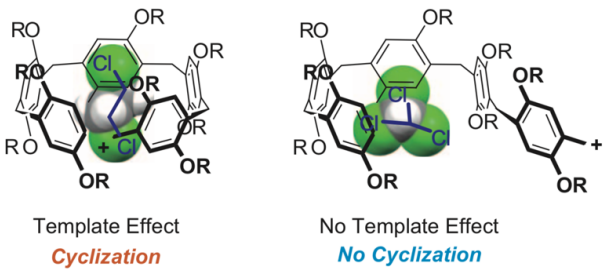

Figure 1.14. a) Linear shaped 1,2-dichloroethane acts as template for cyclic pentamers, pillar[5]arenes; b) Branched chloroform cannot act as a template for particular pillar[n]arene homologs.

Based on these observations, it was possible to elucidate the mechanism responsible for the formation of pillar[*n*]arenes. Linear solvents, like 1,2-dichloroethane, act as template molecules for the formation of pillar[5]arene, whereas branched chloroform failed as a template for the synthesis of specific pillar[*n*]arenes, resulting in a mixture of homologs and

polymers. In contrast, bulky solvents such as chlorocyclohexane are useful for the selective synthesis of pillar[6]arene (Figure 1.15). Thus, template solvents allowed to obtain pillar[5]- and pillar[6]arenes under thermodynamic conditions, whereas larger pillar[*n*]arenes homologs ($n > 6$) have, so far, been picked up only under kinetic conditions.[102]

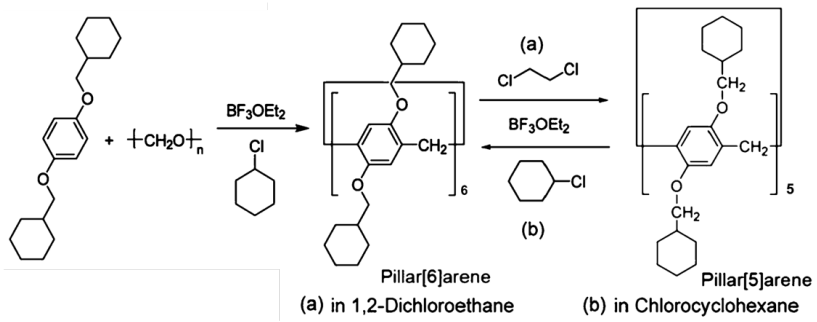

Figure 1.15. Selective synthesis of pillar[6]arene and reversible interconversion in its pentameric homolog.

1.3.3 Host-guest properties of pillar[n]arenes

Electrostatic potential plays an important role in molecular recognition properties of the macrocycles. In contrast to what is shown by calix[*n*]arenes, which have a slightly negative-charged cavity, the innermost portion of the cavity of pillar[5]- and pillar[6]arenes is characterised by a pronounced negative charge. In fact, the tubular cavity of these derivatives can count on the contribution of all the π-electrons offered by the aromatic portions of the macrocycle (Figure 1.16).

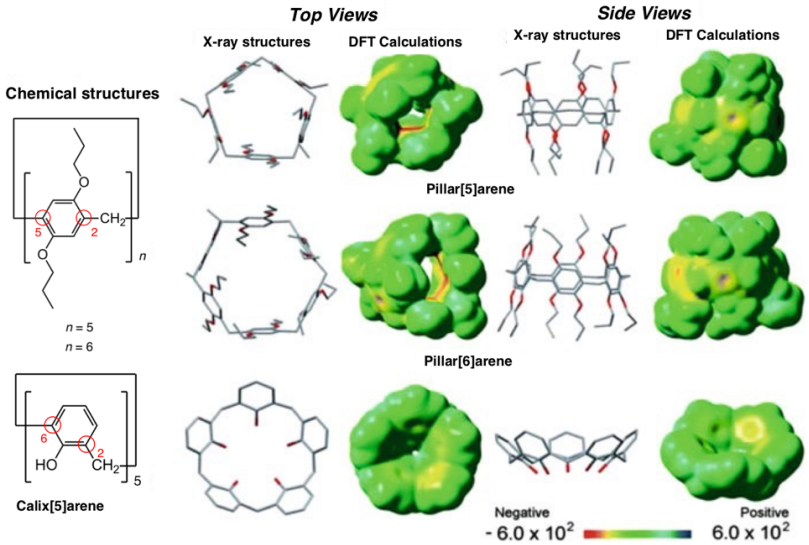

Figure 1.16. Comparison between calculated electrostatic potential (DFT B3LYP/6-31G(d,p)) in a.u. of the cavity of pillar[5]arene (up), pillar[6]arene (middle) and calix[5]arene (bottom), and their respective top and side view of X-ray crystal structures. (Adapted from ref. 104)

For this reason, although they do not show too strong a selectivity, they are able to complex neutral molecules but preferentially interact with linear guests that have a positive charge in their structure. In fact, the driving force behind the complexation process is the formation of multiple CH-π interactions between the linear alkyl chain of the guest and the electrons in the aromatic cavity. However, the association constants for the formation of host-guest complexes between these macrocycles and simple linear alkanes neutrally charged are lower than respective ones with positive or electron-withdrawing (EW) ending-groups molecules. [105] Also the length of the alkyl chain have a pronounced effect on the complexation ability of the guest molecule, thus was proved the good affinity between a C4 linear alkane with two EW terminal groups, because of the hydrophobicity of aliphatic moiety which is good to fit in the cavity of pillar[5]arene. And this is also the reason why pillar[5]arenes, in particular, prefer to form complexes with linear guest molecules, rather than with branched or cyclic molecules.[106]

In addition, it is possible to manage the complexation abilities of pillar[5]arenes via the installation of appropriate functional groups on both rims of their macrocyclic structures. For example, the introduction of one or two carboxylic acid moieties led to a considerable enhancement of the affinity between these macrocyclic host molecules and linear alkyl guests bearing one or two amino or ammonium groups.[107] In fact, the high binding constant values showed by such host-guest partners were attributed to the formation of electrostatic interactions between the ammonium cations and the carboxylate anions, together with the above mentioned formation of CH–π interactions (Figure 1.17).

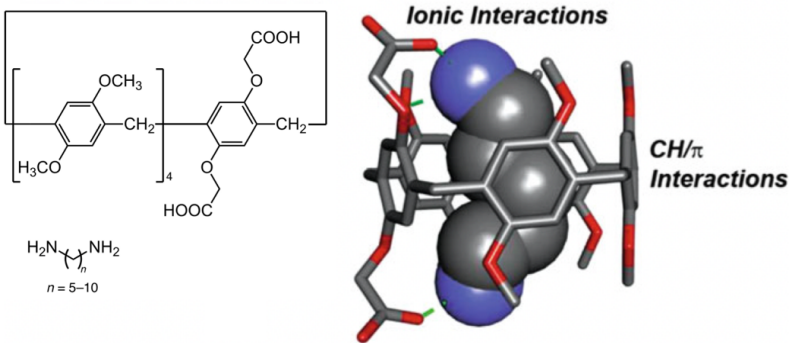

Figure 1.17. a) pillar[5]arene dicarboxylate and various diamines; b) X-ray crystal structure of the host-guest complex between cadaverine and the pillar[5]arene diacid derivative. (Adapted from ref. 99b)

The receptor properties are also modified as the width of the cavity formed by the aromatic units of the pillar[*n*]arenes changes. Moving from the 4.7 Å cavity size of pillar[5]arenes to the 6.7 Å cavity size of pillar[6]arenes, it opens up a wider choice of partner guest molecules (in

contrast, selectivity decreases). In fact, cyclohexameric homologues are able to form host-guest complexes with polyaromatic compounds and also with positively charged bulky hydrocarbons.[108]

1.3.4 Pillar[n]arene-based supramolecular assemblies

Due to their solubility in a large variety of solvents, low toxicity and specific recognition towards many model substrates, pillar[*n*]arenes have been widely used for the development of various interesting supramolecular systems, including nanomaterials,[109] chemosensors,[110] transmembrane channels,[111] and supramolecular polymers.[112] Additionally, the remarkable ability to recognise and selectively include both polar and neutral molecules within their cavities has led to the use of these macrocycles as molecular receptors specific to certain chemical species, suggesting various applications in different areas of research; in the biological field, for example, they have been used both for the recognition of biomolecules,[113] and in the selective delivery of drugs.[114] The ease in the functionalization and in the modulation of non-covalent host-guest interactions through external stimuli makes pillararenes particularly versatile in the preparation of smart materials. Indeed, they have received great attention in fabricating attractive supramolecular entities, such as rotaxanes[115] and catenanes.[116] Particularly interesting and fascinating in this respect are the mono-functionalized pillar[5]arenes. Such derivatives can form variable arrays via different threading modes of the guest units into their cavities. The assemblies will be self-inclusion complexes when intramolecular behaviours occur, otherwise inter-molecular assembly will result in the formation of oligomers, especially cyclic dimers, and supramolecular polymers (at high concentration), which are also named daisy chains[117,118] (Figure 1.18).

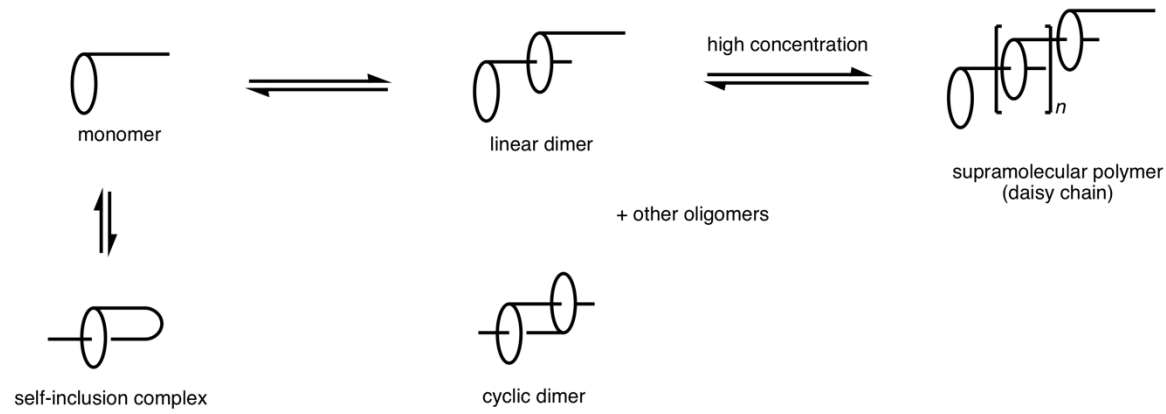

Figure 1.18. The equilibrium of the self-assembly of mono-functionalized pillararenes. (Adapted from ref. 119)

Intramolecular behaviour, and therefore also the formation of self-inclusion complexes, can be highly solvent-dependent.[120] It has been shown that the pillar-bound functionality is able to enter the macrocyclic cavity in a given solvent; however, as the medium changes, there is a phenomenon of escape of the previously included chain. Stable self-inclusion complexes have also been formed at high concentrations in solution, and even in the solid state.[121] Also the position and the nature of the substituents on the side chain covalently linked to the pillararenic framework is important for the self-inclusion phenomenon.[122]

However, depending on concentration, mono-functionalised pillar[5]arenes may organise themselves into structures other than the pseudo[1]rotaxane one resulting from the phenomenon of intra-cavity self-inclusion of the side chain bound to the macrocyclic scaffold. Indeed, in parallel to functionalization with appropriate akin ligands, they can form oligomeric or polymeric assemblies,[112,123] whose aggregation is mainly driven by the formation of CH-π interactions. On the other hand, the construction of stimuli-responsive supramolecular polymers is always attractive to supramolecular chemists. Such polymers have been prepared with pillar-based functional units, which can respond to external stimuli or to a change in some parameter.[124] In addition, based on the highly selective multiple host–guest recognition system, depending on the differences among the cavity sizes of pillar[5]arenes and pillar[6]arenes, it was also pursued the construction of artificial self-sorting systems,[108b] mimicking natural living organisms.

1.3.5 Pillar[n]arene-based hybrid materials

The next step was to combine the unique properties of pillar[*n*]arenes with the structural features provided by inorganic materials, in order to obtain hybrid systems that could combine the receptor capacities of these macrocycles with the robustness of inorganic matrixes. Hybrid materials thus assembled exhibit composite functions as well as complementary and optimized properties,[125] and also overcome the limitations of single-component materials, presenting abundant new features in terms of optical, mechanical, electrical and electrochemical properties. In fact, above mentioned properties made such materials particularly suitable for the construction of stimuli-responsive devices, in which the pillararenic macrocycle is immobilised on the inorganic surface, resulting in a sensor on a solid support.

For example, pillar[5]arenes have been used for the preparation of metal-organic frameworks[126] (MOFs),[127] and the first reported supramolecular-organic framework based on pillararene-scaffold unit has been shown to have a marked ability to reversibly trap CO_2.[128]

Another important application of MOFs has been pioneered in the biomedical field for the release of bioactive molecules, where the problem of early release of the drugs from the isolated inorganic framework is greatly outweighed by the affinity of these molecules for pillar[5]arene cavity.[129]

Furthermore, a water-soluble pillar[5]arene (**WP5**) was immobilised on the surface of silver nanoparticles (Silver-NPs) for the visual detection of toxic spermine and its analogues (Figure 1.19).[130] Whereas the first water-soluble pillar[6]arene form a pH-controllable host-guest complex with a pyridinium guest immobilised on multi-wall nanotubes (MWNTs),[99b,131] as well as another pillar[5]arene was anchored on the surface of graphene oxide to provide a biocompatible hybrid material.[132] Other biocompatible hybrid systems, with specific capacities for the selective release of pharmacologically active molecules,[133] have been obtained by exploiting a water-soluble pillar[5]- and pillar[6]arene as channel stopper molecules present in mesoporous silica nanoparticles capable of trapping drugs such as doxorubicin (**Dox**); release is guaranteed by detachment of the macrocycles from the structure following an external stimulus (lowering of the pH, presence of a competing guest, etc.).

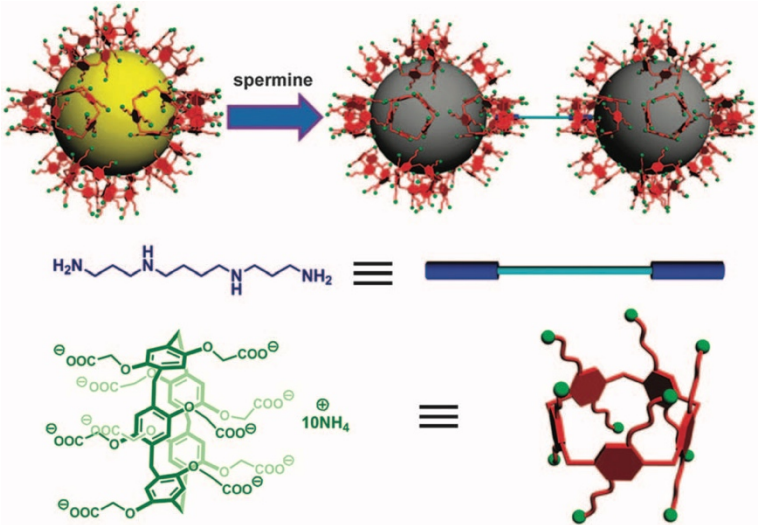

Figure 1.19. Schematic representation of the application of the **WP5**-stabilized silver nanoparticles in visual detection of spermine.[130]

1.4 References

[1] (a) Lehn J.M., *Angew. Chem.*, **1988**, *100*, 91; (b) Lehn J.M., *Angew. Chem. Int. Ed. Engl.*, **1988**, *27*, 89.

[2] Lehn J.M., *Supramolecular Chemistry: Concepts and Perspectives*, **1995**, VCH.

[3] (a) Wolf K.L., Frahm H., Harms H., *Z. Phys. Chem.*, **1937,** *Abt. B 36,* 237; (b) Wolf K.L., Dunken H., Merkel K., *Z. Phys. Chem.*, **1940,** *Abt. B 46,* 287; (c) Wolf K.L., Wolff R., *Angew. Chem.*, **1949,** *61,*191.

[4] Kyba E.P., Helgeson R.C., Madan K., Gokel G.W., Tarnowski T.L., Moore S.S., Cram D.J., *J. Am. Chem. Soc.*, **1977**, *99*, 2564.

[5] Steed J.W., Atwood J.L., *Supramolecular Chemistry, 2nd edition*, **2009**, John Wiley & Sons, Ltd.

[6] Cram D.J., *Angew. Chem. Int. Ed. Engl.*, **1986**, *25*, 1039.

[7] (a) Ovchinnikov Y.A., Ivanov V.T., Skrob A.M., *Membrane Active Complexones,* **1974**, Elsevier, New York; (b) Pressman B.C., *Annu. Rev. Biochem.*, **1976**, *45*, 501.

[8] (a) Brockmann H., Geeren H., *Justus Liebigs Ann. Chem.*, **1957,** *603,* 217; (b) Shemyakin M.M., Aldanova N.A., Vinogradova E.I., Feigina M.Y., *Tetrahedron Lett.*, **1963,** 1921; (c) Moore C., Pressman B.C., *Biochem. Biophys. Res. Commun.*, **1964,** *15,* 562; (d) Pressman B.C., *Proc. Natl. Acad. Sci. USA*, **1965,** *53,* 1077; (e) Mueller P., Rudin D.O., *Biochem. Biophys. Res. Commun.*, **1967**, *26,* 398; f) Andreoli T.E., Tieffenberg M., Tosteson D.C., *J. Gen. Biol.*, **1967,** *50,* 2527; (g) Shemyakin M.M., Ovchinnikov Y.A., Ivanov V.T., Antonov V.K., Skrob A.M., Mikhaleva I.I., Evstratov A.V., Malenkov G.G., *ibid.* **1967,** *29,* 834; (h) Pressman B.C., Harris E.J., Jagger W.S., Johnson J.H., *Proc. Natl. Acad. Sci. USA*, **1967,** *58,*1949.

[9] (a) Beck J., Gerlach H., Prelog V., Voser W., *Helv. Chim. Acta*, **1962,** *45,* 620; (b) Stefanác Z., Simon W., *Chimia*, **1966,** *20,* 436; *Microchem. J.*, **1967,** *12,* 125; (c) Kilbourn B.T., Dunitz J.D., Pioda L.A.R., Simon W., *J. Mol. Biol.*, **1967,** *30,* 559.

[10] Pedersen C.J., *J. Am. Chem. Soc.*, **1967,** *89,* 7017.

[11] Pedersen C.J., *Angew. Chem.,* **1988**,*100,* 1053*; Angew. Chem. Int. Ed. Engl,* **1988**, *27,* 1053.

[12] (a) Dietrich B., Lehn J.M., Sauvage J.P., *Tetrahedron Lett.*, **1969**, 2885; (b) Dietrich B., Lehn J.M., Sauvage J.P., Blanzat J., *Tetrahedron*, **1973**, *29,* 1629; Dietrich B., Lehn J.M., Sauvage J.P., *ibid.* **1973**, *29,* 1647.

[13] Lehn J.M., *Struct. Bonding*, **1973**,*16,* 1.

[14] (a) Cram D.J., *Angew. Chem. Int. Ed. Engl.*, **1988**, *27*, 1009; (b) Pedersen C.J., *Angew. Chem. Int. Ed. Engl.*, **1988**, *27*, 1021.

[15] (a) Feringa B.L., *Angew. Chem. Int. Ed.*, **2017***, 56*, 11060*;* (b) Stoddart J.F., *Angew. Chem. Int. Ed.*, **2017***, 56*, 11094; (c) Sauvage J.P., *Angew. Chem. Int. Ed.*, **2017***, 56*, 11080.

[16] (a) Villiers A., *C. R. Fr. Acad. Sci.*, **1891**, 435; (b) Crini G., *Chem. Rev.*, **2014**, *114*, 10940; (c) Rekharsky M.V., Inoue Y., *Chem. Rev.*, **1998**, *98*, 1875; (d) Szejtli J., *Chem. Rev.,* **1998**, *98*, 1743; (e) Crini G., *Chem. Rev.,* **2014**, *114*, 10940.

[17] Gokel G.W., Leevy W.M, Weber M.E., *Chem. Rev.,* **2004**, *104*, 2723.

[18] (a) Lee J.W., Samal S., Selvapalam N., Kim H.J., Kim K., *Acc. Chem. Res.*, **2003**, *36*, 621; (b) Lagona J., Mukhopadhyay P., Chakrabarti S., Isaacs L., *Angew. Chem. Int. Ed.*, **2005**, *44*, 4844; (c) Isaacs L., *Acc. Chem. Res.*, **2014**, *47*, 2052; (d) Behrend R., Meyer E., Rusche F., *Justus Liebigs Ann. Chem.*, **1905**, *339*, 1; (e) Freeman W.A., Mock W.L., Shih N.Y., *J. Am. Chem. Soc.*, **1981**, *103*, 7367; (f) Kim J., Jung I.S., Kim S.Y., Lee E., Kang J.K., Sakamoto S., Yamaguchi K., Kim K., *J. Am. Chem. Soc.*, **2000**, *122*, 540.

[19] (a) Zang J., Ma P.X., *Advanced Drug Delivery Reviews,* **2013**, *65*, 1215; (b) Irie T., Uekama K., *J. Pharm. Sci.*, **1997**, *86*, 147; (c) Murakami Y., Kikuchi J.I., Hisaeda Y., Hayashida O*., Chem. Rev.,* **1996**, *96*, 721; (d) Brewster M.E., Loftsson T., *Adv. Drug Delivery Rev.*, **2007**, *59*, 645.

[20] Zinke A., Ziegler E., *Ber.*, **1944**, *77*, 264.

[21] Gutsche C.D., Dhawan B., No K.H., Muthukrishnan R., *J. Am. Chem. Soc.*, **1981**, *103*, 3782.

[22] (a) Gutsche C.D., Iqbal M., *Org. Synth.*, **1990**, *68*, 234; (b) Gutsche C.D., Dhawan B., Leonis M., Stewart D., *Org. Synth.*, **1990**, *68*, 238; (c) Munch J.H., Gutsche C.D., *Org. Synth.*, **1990**, *68*, 243.

[23] Gutsche C.D., Muthukrishnan R., *J. Org. Chem.*, **1978**, *43*, 4905.

[24] Andreetti G.D., Ungaro R., Pochini A., *J. Chem. Soc.*, *Chem. Commun.*, **1979**, 1005.

[25] Gutsche C.D., *Calixarenes* "Monograph in Supramolecular Chemistry"; Stoddart J.F., Ed., The Royal Society of Chemistry: Cambridge, **1989**.

[26] (a) Steward D.R., Gutsche C.D., *Org. Prop. Proc. Int.*, **1993**, *25*, 137; (b) Iwamoto K., Araki K., Shinkai S., *Bull. Chem. Soc. Jpn.*, **1994**, *67*, 1499.

[27] Vocanson F., Lamartine R., Lantieri P., Longeray R., Gauvrit J.Y., *New J. Chem.*, **1995**, *19*, 825.

[28] Steward D.R., Gutsche C.D., *J. Am. Chem. Soc.*, **1999**, *121*, 4136.
[29] (a) Hayes B.T., Hunter R.F., *J. Appl. Chem.*, **1958**, *8*, 743; (b) Kammerer H., Happel G., Mathiasch B., *Makromol. Chem.*, **1981**, *182*, 1685; (c) Böemer V., Vicens J. in *"Calixarenes: A Versatile Class of Macrocyclic Compounds"* eds. J. Vicens and V. Böemer, Kluwer Academic, Dordrecht, **1991**, *39*.
[30] No K.H., Gutsche C.D., *J. Org. Chem.*, **1982**, *47*, 2713.
[31] Gutsche C.D., Bauer L.J., *J. Am. Chem Soc.*, **1985**, *107*, 6063.
[32] (a) Andreetti G.D., Ungaro R., Pochini A., *J. Chem. Soc.*, *Chem. Commun.*, **1979**, 1005; (b) Andreetti G.D., Ungaro R., Pochini A., *J. Chem. Soc.*, *Perkin Trans.*, **1983**, 1773.
[33] Coruzzi M., Andreetti G.D., Bocchi V., Pochini A., Ungaro R., *J. Chem. Soc.*, *Perkin Trans.*, **1982**, 1133.
[34] Andreetti G.D., Ugozzoli F., Casnati A., Ghidini E., Pochini A., Ungaro R., *Gazz. Chim Ital.*, **1989**, *119*, 47.
[35] Araki K., Iwamoto K., Shinkai S., Matsuda T., *Chem. Lett.*, **1989**, 1747.
[36] (a) Otsuka H., Araki K., Sakaki T., Nakashima K., Shinkai S., *Tetrahedron Lett.*, **1993**, *34*, 7275; (b) van Duynhoven J.P.M., Janssen R.G., Verboom W., Franken S.M., Casnati A., Pochini A., Ungaro R., de Mendoza J., Nieto P.M., Prados P. Reinhoudt D.N., *J. Am. Chem. Soc.*, **1994**, *116*, 5814.
[37] (a) Iwamoto K., Araki K., Shinkai S., *Tetrahedron*, **1991**, *47*, 4325; (b) Iwamoto K., Shinkai S., *J. Org. Chem.*, **1992**, *57*, 7066; (c) Böhmer V., *Angew. Chem. Int. Ed. Engl.*, **1995**, *34*, 713.
[38] van Loon J.D., Verboom W., Reinhoudt D.N., *Org. Prep. Proced. Int.* **1992**, *24*, 437.
[39] (a) Gutsche C.D., Lin L.G., *Tetrahedron*, **1986**, *42*, 1633; (b) Shang S., Khasnis D.V., Burton J.M., Santini C.J., Fan M.M., Small A.C., Lattman M., *Organometallics*, **1994**, *13*, 5157.
[40] King A.M., Moore C.P., Samankumara Sandanayake K.R.A., Sutherland I.O., *J. Chem. Soc.*, *Chem. Commun.*, **1992**, 582.
[41] Groenen L.C., Ruel B.H.M., Casnati A., Verboom W., Pochini A., Ungaro R., Reinhoudt D.N., *Tetrahedron*, **1991**, *47*, 8379.
[42] (a) Iwamoto K., Araki K., Shinkai S., *Tetrahedron*, **1991**, *47*, 4325; (b) Iwamoto K., Yanagi A., Arimura T., Matsuda T., Shinkai S*., Chem. Lett.*, **1990**, 1901; (c) Iwamoto K., Yanagi A., Araki K., Shinkai S., *ibid.*, **1991**, 473.
[43] (a) Iwamoto K., Araki K., Shinkai S., *Tetrahedron*, **1991**, *47*, 4325; (b) Iwamoto K., Shinkai S., *J. Org. Chem.*, **1992**, *57*, 7066; (c) Böhmer V., *Angew. Chem. Int. Ed. Engl.*, **1995**, *34*, 713.
[44] Casnati A., Arduini A., Ghidini E., Pochini A., Ungaro R., *Tetrahedron*, **1991**, *47*, 2221.
[45] See K.A., Fronczek F.R., Watson W.H., Kashyap R.P., Gutsche C.D., *J.* Org. *Chem.*, **1991**, *56*, 7256.
[46] (a) Barrett A., McKervey M.A., Malone J.F., Walker A., Arnaud-Neu F., Guerra L., Schwing-Weill M.J., Gutsche C.D., Stewart D.R., *J. Chem. Soc.*, *Perkin Trans. 2*, **1993**, 1475; (b) Souley B., Asfari Z., Vicens J., *Pol. J. Chem.*, **1993**, *67*, 763; (b) Gutsche C.D., Dhawan B., Levine J.A., No K.N., Bauer L.J., *Tetrahedron*, **1983**, *39*, 409; (c) Iwamoto K., Fujimoto K., Matsuda T., Shinkai S., *Tetrahedron Lett.*, **1990**, *31*, 7169; (d) Iwamoto K., Araki K., Shinkai S., *J. Org.* Chem., **1991**, *56*, 4955.
[47] (a) Gutsche C.D., See K.A., *J. Org. Chem.*, **1992**, *57*, 4527; (b) Shu C., Liu W., Ku M., Tang F., Yeh M., Lin L., *ibid.*, **1994**, *59*, 3730.
[48] (a) Collins E.M., McKervey M.A., Harris S.J., *J. Chem. Soc.*, *Perkin Trans. 1*, **1989**, 372; (b) van Loon J.-D., Arduini A., Verboom W., Ungaro R., vim Huminel G.J., Harkema S., Reinhoudt D.N., *Tetrahedron Lett.*, **1989**, *30*, 2681; (c) v. Loon J.-D., Arduini A., Coppi L., Verboom W., Pochini A., Ungaro R., Harkema S., Reinhoudt D.N., *J. Org. Chem.*, **1990**, *55*, 5639; (d) Collins E.M., McKervey M.A., Madigan E., Moran M.B., Owens M., Ferguson G., Harris S.J., *J. Chem. Soc.*, *Perkin Trans. 1*, **1991**, 3137.
[49] (a) Arduini A., Casnati A., Dodi L., Pochini A., Ungaro R., *J. Chem. Soc.*, *Chem. Commun.*, **1990**, 1597; (b) Yamamoto H., Sakaki T., Shinkai S., *Chem. Lett.*, **1994**, 469.
[50] Gutsche C.D., Levine J.A., Sujeeth P.K., *J. Org. Chem.*, **1985**, *50*, 5802.
[51] Kämmerer H., Happel G., Böhmer V., Rathay D., *Monatsh. Chem.*, **1978**, *109*, 767.
[52] (a) Gutsche C.D., Pagoria P.F., *J. Org. Chem.*, **1985**, *50*, 5795; (b) Conner M., Janout V., Regen S.L., *J. Org. Chem.*, **1992**, *57*, 3744; (c) Hamada F., Bott S.G., Orr G.W., Coleman A.W., Zhang H.M., Atwood J.L., *J. Incl. Phenom. Mol. Recogn.*, **1990**, *9*, 195; (d) Arduini A., Pochini A., Rizzi A., Sicuri A.R., Ungaro R., *Tetrahedron Lett.*, **1990**, *31*, 4653; (e) Arduini A., Pochini A., Sicuri A.R., Secchi A., Ungaro R., *Gazz. Chim. Ital.*, **1994**, *124*, 129; (f) Timmerman P., Verboom W., Reinhoudt D.N., Arduini A., Grandi S., Sicuri A.R., Pochini A., Ungaro R., *Synthesis*, **1994**, 185.
[53] No K., Noh Y., *Bull. Korean Chem.* Soc., **1986**, *7*, 314.
[54] Atwood J.L., Bott S.G., *Water Soluble Culixarene Salts. A Class of Compounds with Solid-State Structures Resembling Those of Clays.* in ref. 10c.

[55] (a) Shinkai S., Araki K., Tsubaki T., Arimura T., Manabe O., *J. Chem. Soc.*, *Perkin Trans. 1*, 1987, 2297 – 2299; (b) Casnati A., Ting Y., Berti D., Fabbi M., Pochini A., Ungaro R., Sciotto D., Lombardo G.G., *Tetrahedron*, **1993**, *49*, 9815.
[56] (a) Verboom W**.**, Durie A., Egberink R., Asfari Z., Reinhoudt D.N., *J. Org. Chem.*, **1992**, *57*, 1313; (b) Brake M., Böhmer V., Krilmer P., Vogt W., Wortmann R., *Supramol. Chem.*, **1993**, *2*, 65.
[57] (a) Morzherin Y., Rudkevich D.M., Verboom W., Reinhoudt D.N., *J. Org. Chem.*, **1993**, *58*, 7602; (b) Shinkai S., Kawdbata H., Matsuda T., Kawaguchi H., Manage O., *Bull. Chem. Sor. Jpn.*, **1990**, *63*, 1272.
[58] Almi M., Arduini A., Casnati A., Pochini A., Ungaro R., *Tetrahedron*, **1989**, *45*, 2177.
[59] (a) Gutsche C.D., Nam K.C., *J. Am. Chem. Soc.*, **1988**, *110*, 6153 – 6162; (b) Gutsche C.D., Alam I., *Tetrahedron*, **1988**, *44*, 4689.
[60] (a) Shinkai S., Nagasaki T., Iwamoto K., Ikeda A., He G.X., Matsuda T., Iwamoto M., *Bull. Chem. Soc. Jpn.*, **1991**, *64*, 381; (b) Huang Z.T., Wang C.Q., *Chem. Ber.*, **1994**, *127*, 519.
[61] (a) Shinkai S., Araki K., Shibita I., Manabe O., *J. Chem. Soc.*, *Perkin Trans. 1*, **1989**, 195 – 196; (b) Yeh M., Tang F., Chen S., Liu W., Lin L., *J. Org. Chem.*, **1994**, *59*, 754.
[62] (a) No K., Noh Y., Kim Y., *Bull. Korean Chem. Soc.*, **1986**, *7*, 442; (b) Arimura T., Shinkai S., Matsuda T., Hirata Y., Satoh H., Manabe O., *Bull. Chem. Soc. Jpn.*, **1988**, *61,* 3733.
[63] (a) Juneja R.K., Robinson K.D., Johnson C.P., Atwood J.L., *J. Am. Chem. Soc.*, **1993**, *115*, 3818; (b) Wong M.S., Nicoud J.F., *Tetrahedron Lett.*, **1993**, *34*, 8237; (c) Paek K.S., Ihm H.J., No K.H., *Bull. Korean Chem. Soc.*, **1994**, *15*, 422.
[64] (a) van Loon J.D., Heida J.F., Verboom W., Reiuhoudt D.N., *Recl. Trav. Chim. Pays-Bas*, **1992**, *111,* 353; (b) Beer P.D., Drew M.G.B., Hazlewood C., Hesek D., Hodacova J., Stokes S.E., *J. Chem. Soc.*, *Chem. Commun.*, **1993**, 229.
[65] (a) Morita Y., Agawa T., Kai Y., Kanehisa N., Kasai N., Nomura E., Taniguchi H., *Chem. Left.*, **1989**, 1349; (b) Morita Y., Agawa T., Nomura E., Taniguchi H., *J. Org. Chem.*, **1992**, *57*, 3658.
[66] (a) Nagasaki T., Sisido K., Arimura T., Shinkai S., *Tetrahedron*, **1992**, *48,* 797. (b) Hardd T., Rudzinski J.M., Shinkai S., *J Chem. Soc.*, *Perkin Trans. 2*, **1992**, 2109; (b) Almi M., Arduini A., Casnati A., Pochini A., Ungaro R., *Tetrahedron*, **1989**, *45*, 2177; (c) Arduini A., Pochini A., Rizzi A., Sicuri A.R., Ugozzoli E., Ungaro R., *Tetrahedron*, **1992**, *48*, 905.
[67] Olmstead M.M., Sigel G., Hope H., Xu X., Power P.P., *J. Am. Chem. Soc.*, **1985**, *107*, 8087.
[68] (a) Furphy B.M., Harrowfield J.M., Ogden M.I., Skelton B.W., White A.H., Wilner F.R., *J. Chem. Soc.*, *Dalton Trans.*, **1989**, 2217; (b) Harrowfield J.M., Ogden M.I., White A.H., Wilner F.R., *Aust. J. Chem.*, **1989**, *42*, 949.
[69] (a) Delaigue X., Hosseini M.W., Leize E., Kieffer S., Van Dorsselaer A., *Tetrahedron Lett.*, **1993**, *34*, 7561; (b) Hajek F., Graf E., Hosseini M.W., De Cian A., Fischer J., *ibid.*, **1997**, *38*, 4555.
[70] (a) Atwood J.L, Bott S.G., Jones C., Raston C.L., *J. Chem. Soc.*, *Chem. Commun.*, **1992**, 1349; (b) Atwood J.L., Junk P.C., Lawrence S.M., Raston C.L., *Supramol. Chem.*, **1996**, *7*, 15.
[71] Gardiner M.G., Lawrence S.M., Raston C.L., Skelton B.W., White A.H., *J. Chem. Soc.*, *Chem. Commun.*, **1996**, 2491
[72] Harrowfield J.M., Ogden M.I., Richmond W.R., White A.H., *J. Chem. Soc.*, *Chem. Commun.*, **1991**, 1159.
[73] Abidi R., Baker M.V., Harrowfield J.M., Ho D.S., Richmond W.R., Skelton B.W., White A.H., Varnek A., Wipff G., *Inorg. Chim. Acta*, **1996**, *246*, 275.
[74] (a) Bocchi V., Foina D., Pochini A., Ungaro R., Andreetti G.D., *Tetrahedron*, **1982**, *38*, 373; (b) Ungaro R., Pochini A., Andreetti G.D., Ugozzoli F., *J. Inclusion Phenom.*, **1985**, *3*, 409.
[75] (a)Ikeda A., Shinkai S., *J. Am. Chem. Soc.*, **1994**, *116*, 3102; (b) Ikeda A., Shinkai S., *Tetrahedron Lett.*, **1992**, *33*, 7385; (c) Xu W., Puddephatt R.J., Muir K.W., Torabi A.A., *Organometallics*, **1994**,*13*, 3054.
[76] (a) Whitesides G.M., Mathias J.P., Seto C.T., *Science*, **1991**, *254*,1312; (b) Lawrence D.S., Jiang T., Levett M., *Chem. Rev.*, **1995**, *95,* 2229; (c) Philp D., Stoddart J.F., *Angew. Chem., Int. Ed. Engl.*, **1996**, *35*, 1154.
[77] (a) Gutsche C.D., *Calixarenes Revisited,* Royal Society of Chemistry, Cambridge, **1998**; (b) Shinkai S., *Tetrahedron*, **1993**, *49,* 8933; (c) Timmerman P., Verboom W., Reinhoudt D.N., *Tetrahedron*, **1996**, *52*, 2663; (d) Böhmer V., Kraft D., Tabatabai M., *J. Incl. Phenom.*, **1994**, *19,* 17.
[78] (a) Higler I., Timmerman P., Verboom W., Reinhoudt D.N., *Eur. J. Org. Chem.*, **1998**, 2689; (b) Rudkevich D.M., Rebek J. Jr., *Eur. J. Org. Chem.*, **1999**, 1991.
[79] (a) van Loon J.D., Janssen R.G., Verboom W., Reinhoudt D.N., *Tetrahedron Lett.*, **1992**, *33,* 5125; (b) Andreu C., Beerli R., Branda N., Conn M., de Mendoza J., Galan A., Huc I., Kato Y., Tymoschenko M., Valdez C., Wintner E., Wyler R., Rebek J. Jr., *Pure Appl. Chem.*, **1993**, *65,* 2313; (c) Vreekamp R.H., Verboom W.,

Reinhoudt D.N., *Red. Trav. Chim. Pays-Bas*, **1996**, *115,* 363; (d) Koh K., Araki K., Shinkai S., *Tetrahedron Lett.*, **1994**, *35,* 8255; (e) Vreekamp R.H., Verboom W., Reinhoudt D.N., *J. Org. Chem.*, **1996**, *61,* 4282; (f) Higler I., Grave L., Breuning E., Verboom W., de Jong F., Fyles T.M., Reinhoudt D.N., *Eur. J. Org. Chem.*, **2000**, 1727; (g) Arduini A., Fabbi M., Mantovani M., Mirone L., Pochini A., Secchi A., Ungaro R., *J. Org. Chem.*, **1995**, *60,* 1454; (h) Struck O., Verboom W., Smeets W.J.J., Spek A.L., Reinhoudt D.N., *J. Chem. Soc., Perkin Trans. 1*, **1997**, 223.

[80] Gonzalez J.J., Prados P., de Mendoza J., *Angew. Chem., Int. Ed. Engl.*, **1999**, *38,* 525.

[81] Conn M.M., Rebek J. Jr., *Chem. Rev.*, **1997**, *97,* 1647.

[82] (a) Shimizu K.D., Rebek J. Jr., *Proc. Nail. Acad. Sci. USA*, **1995**, *92,* 12403; (b) Mogck O., Böhmer V., Vogt W., *Tetrahedron*, **1996**, *52*, 8489; (c) Castellano R.K., Rudkevich D.M., Rebek J. Jr., *J. Am. Chem. Soc.*, **1996**, *118,* 10002; (d) Scheerder J., Vreekamp R.H., Engbersen J.F.J., Verboom W., Reinhoudt D.N., *J. Org. Chem.*, **1996**, *61*, 3476.

[83] Mogck O., Paulus E.F., Böhmer V., Thondorf I., Vogt W., *Chem. Commun.*, **1996**, 2533.

[84] Hamann B.C., Shimizu K.D., Rebek J. Jr., *Angew. Chem., Int. Ed. Engl.*, **1996**, *35*, 1326.

[85] (a) Castellano R.K., Rudkevich D.M., Rebek J. Jr., *Proc, Natl. Acad. Sci. USA*, **1997**, *94,* 7132; (b) Castellano R.K., Rebek J. Jr., *J. Am. Chem. Soc.*, **1998**, *120*, 3657.

[86] Castellano R.K., Nuckolls C., Eichhorn S.H., Wood M.R., Lovinger A.J., Rebek J. Jr., *Angew. Chem., Int. Ed. Engl.*, **1999**, *38*, 2603.

[87] Ogoshi T., Kanai S., Fujinami S., Yamagishi T., Nakamoto Y., *J. Am. Chem. Soc.,* **2008**, *130*, 5022.

[88] Gutsche C.D., *Calixarenes*, The Royal Society of Chemistry, Cambridge, **1989**.

[89] (a) Ogoshi T., Kitajima K., Aoki T., Fujinami S., Yamagishi T., Nakamoto Y., *J. Org. Chem.,* **2010**, *75*, 3268; (b) Ogoshi T., Shiga R., Yamagishi T., Nakamoto Y., *J. Org. Chem.,* **2011**, *76*, 618; (c) Ogoshi T., Masaki K., Shiga R., Kitajima K., Yamagishi T., *Org. Lett.,* **2011**, *13*, 1264.

[90] (a) Rekharsky M.V., Inoue Y., *Chem. Rev.,* **1998**, *98*, 1875; (b) Harada A., Hashidzume A., Yamaguchi H., Takashima Y., *Chem. Rev.,* **2009**, *109*, 5974; (c) Wenz G., Han B.H., Müller A., *Chem. Rev.,* **2006**, *106*, 782; (d) Lee J.W., Samal S., Selvapalam N., Kim H.J., Kim K., *Acc. Chem. Res.,* **2003**, *36*, 621.

[91] (a) Ogoshi T., Kitajima K., Yamagishi T.A., Nakamoto Y., *Org. Lett.,* **2010,** *12*, 636; (b) Ogoshi T., Aoki T., Kitajima K., Fujinami S., Yamagishi T.A., Nakamoto Y., *J. Org. Chem.,* **2011**, *76*, 328; (c) Ogoshi T., Shiga R., Yamagishi T.A., Nakamoto Y., *J. Org. Chem.,* **2011**, *76*, 618; (d) Cao D., Kou Y., Liang J., Chen Z., Wang L., Meier H., *Angew. Chem. Int. Ed.,* **2009**, *48*, 9721; (e) Kou Y., Tao H., Cao D., Fu Z., Schollmeyer D., Meier H., *J. Org. Chem.,* **2010**, *75*, 6464; (f) Ma Y., Zhang Z., Ji X., Han C., He J., Zeper A., Chen W., Huang F., *Eur. J. Org. Chem.*, **2011**, *27*, 5331; (g) Holler M., Allenbach N., Sonet J., Nierengarten J.F., *Chem. Commun.,* **2012**, *48*, 2576.

[92] (a) Strutt N.L., Forgan R.S., Spruell J.M., Botros Y.Y., Stoddart J.F., *J. Am. Chem. Soc.,* **2011**, *133*, 5668; (b) Ogoshi T., Demachi K., Kitajima K., Yamagishi T., *Chem. Commun.,* **2011**, *47*, 7164; (c) Ogoshi T., Kitajima K., Fujinami S., Yamagishi T., *Chem. Commun.,* **2011**, *47*, 10106; (d) Zhang Z.B., Xia B.Y., Han C.Y., Yu Y.H., Huang F.H., *Org. Lett.,* **2010**, *12*, 3285; (e) Ogoshi T., Yamafuji D., Kotera D., Aoki T., Fujinami S., Yamagishi T., *J. Org. Chem.,* **2012**, *77*, 11146; (f) Ogoshi T., Yamagishi T., *Eur. J. Org. Chem.,* **2013**, 2961.

[93] (a) Khan A.R., Forgo P., Stine K.J., D'Souza V.T., *Chem. Rev.*, **1998**, *98*, 1977; (b) Engeldinger E., Armspach D., Matt D., *Chem. Rev.*, **2003**, *103*, 4147; (c) Bellia F., La Mendola D., Pedone C., Rizzarelli E., Saviano M., Vecchio G., *Chem. Soc. Rev.*, **2009**, *38*, 2756.

[94] (a) Takahashi K., Hattori K., Toda F., *Tetrahedron Lett.*, **1984**, *25*, 3331; (b) Ikeda H., Nagano Y., Du Y., Ikeda T., Toda F., *Tetrahedron Lett.*, **1990**, *31*, 5045; (c) Gutsche C.D., Dhawan B., Levine J.A., Hyun No K., Bauer L.J., *Tetrahedron*, **1983**, *39*, 409; (d) Beer P.D., *Chem. Commun.*, **1997**, 2377, (e) Ho Z., Ku M., Shu C., Lin L., *Tetrahedron*, **1996**, *52*, 13189; (f) Shirakawa S., Kimura T., Murata S., Shimizu S., *J. Org. Chem.*, **2009**, *74*, 1288; (g) Colasson B., Reinaud O., *J. Am. Chem. Soc.*, **2008**, *130*, 15226; (h) Zhao N., Lloyd G.O., Scherman O.A., *Chem. Commun.*, **2012**, *48*, 3070; Lucas D., Minami T., Iannuzzi G., Cao L., Wittenberg J.B., Anzenbacher P., Isaacs L., *J. Am. Chem. Soc.*, **2011**, *133*, 17966.

[95] Kou Y., Tao H., Cao D., Fu Z., Shollmeyer D., Meier H., *Eur. J. Org. Chem.*, **2010**, 6464.

[96] Cao D.R., Kou Y.H., Liang J.Q., Chen Z.Z., Wang L.Y., Meier H., *Angew. Chem. Int. Ed.*, **2009**, *48*, 9721.

[97] (a) Ogoshi T., Demachi K., Kitajima K., Yamagishi T., *Chem. Commun.*, **2011**, *47*, 7164; (b) Han J., Hou X., Ke C., Zhang H., Strutt N. L., Stern C.L., Stoddart J.F., *Org. Lett.*, **2015**, *17*, 3260.

[98] (a) Ogoshi T., Yamafuji D., Kotera D., Aoki T., Fujinami S., Yamagishi T., *J. Org. Chem.*, **2012**, *77*, 11146; (b) Han C.Y., Zhang Z.B., Yu G.C., Huang F., *Chem. Commun.*, **2012**, *48*, 9876; (c) Wei P., Yan X., Huang F., *Chem. Commun.*, **2014**, *50*, 14105.
[99] (a) Ogoshi T., Kida K., Yamagishi T., *J. Am. Chem. Soc.*, **2012**, *134*, 20146; (b) Yu G., Xue M., Zhang Z., Li J., Han C., Huang F., *J. Am. Chem. Soc.*, **2012**, *134*, 13248; (c) Chi X.D., Xue M., *Chem. Commun.*, **2014**, *50*, 13754; (d) Yang J., Chi X., Li Z., Yu G., He J., Abliz Z., Li N., Huang F., *Org. Chem. Front.*, **2014**, *1*, 630; (e) Chi X.D., Xue M., *RSC Adv.*, **2014**, *4*, 37786; (f) Li Z.T., Yang J., Yu G.C., He J.M., Abliz Z., Huang F., *Chem. Commun.*, **2014**, *50*, 2841; (g) Shao L., Zhou J., Hua B., Yu G., *Chem. Commun.*, 2015, *51*, 7215; (h) Li Z.T., Yang J., Yu G.C., He J.M., Abliz Z., Huang F., *Org. Lett.*, **2014**, *16*, 2066; (i) Ma Y., Chi X., Yan X., Liu J., Yao Y., Chen W., Huang F., Hou J.L., *Org. Lett.*, **2012**, *14*, 1532.
[100] Han C., Yu G., Zheng B., Huang F., *Org. Lett.*, **2012**, *14*, 1712.
[101] Boinski T., Szumna A., *Tetrahedron*, **2012**, *68*, 9419.
[102] Hu X. B., Chen Z. X., Chen L., Zhang L., Hou J. L., Li Z. T., *Chem. Commun.*, **2012**, *48*, 10999.
[103] Ogoshi T., Ueshima N., Akutsu T., Yamafuji D., Furuta T., Sakakibara F., Yamagishi T., *Chem. Commun.*, **2014**, *50*, 5774.
[104] Ogoshi T., Yamagishi T., *Chem. Commun.*, **2014**, *50*, 4776.
[105] (a) Shu X., Chen S., Li J., Chen Z., Weng L., Jia X., Li C., *Chem. Commun.*, **2012**, *48*, 2967; (b) Shu X.Y., Fan J.Z., Li J., Wang X.Y., Chen W., Jia X.S., Li C., *Org. Biomol. Chem.*, **2012**, *10*, 3393; (c) Li C., Chen S., Li J., Han K., Xu M., Hu B., Yu Y., Jia X., *Chem. Commun.*, **2011**, *47*, 11294; (d) Han K., Zhang Y., Li J., Yu Y., Jia X., Li C., *Eur. J. Org. Chem.*, **2013**, 2057.
[106] Ogoshi T., Demachi K., Kitajima K., Yamagishi T., *Chem. Commun.*, **2011**, *47*, 10290.
[107] (a) Xia B.Y., Xue M., *Chem. Commun.*, **2014**, *50*, 1021; (b) Yu G.C., Hua B., Han C.Y., *Org. Lett.*, **2014**, *16*, 2486.
[108] (a) Li C., Shu X., Li J., Fan J., Chen Z., Weng L., Jia X., *Org. Lett.*, **2012**, *14*, 4126.
(b) Ogoshi T., Kayama H., Yamafuji D., Aoki T., Yamagishi T., *Chem. Sci.*, **2012**, *3*, 3221; (c) Yu G., Han C., Zhang Z., Chen J., Yan X., Zheng B., Liu S., Huang F., *J. Am. Chem. Soc.*, **2012**, *134*, 8711.
[109] (a) Yao Y., Xue M., Zhang Z., Zhang M., Wang Y., Huang F., *Chem. Sci.,* **2013**, *4*, 3667; (b) Yu G., Han C., Zhang Z., Chen J., Yan X., Zheng B., Liu S., Huang F., *J. Am. Chem. Soc.,* **2012**, *134*, 8711; (c) Yu G., Zhou X., Zhang Z., Han C., Mao Z., Gao C., Huang F., *J. Am. Chem. Soc.,* **2012**, *134*, 19489; (d) Yu G., Ma Y., Han C., Yao Y., Tang G., Mao Z., Gao C., Huang F., *J. Am. Chem. Soc.,* **2013**, *135*, 10310.
[110] Li C., Zhao L., Li J., Ding X., Chen S., Zhang Q., Yu Y., Jia X., *Chem. Commun.,* **2010**, *46*, 9016.
[111] Si W., Chen L., Hu X.B., Tang G., Chen Z., Hou J.L., Li Z.T., *Angew. Chem. Int. Ed.,* **2011**, *50*, 12564.
[112] Zhang Z., Luo Y., Chen J., Dong S., Yu Y., Ma Z., Huang F., *Angew. Chem. Int. Ed.,* **2011**, *50,* 1397.
[113] (a) Wang P., Li Z.T., Ji X.F., *Chem. Commun.*, **2014**, *50*, 13114; (b) Li C.J., Ma J.W., Zhao L., Zhang Y.Y., Yu Y.H., Shu X.Y., Li J., Jia X.S., *Chem. Commun.*, **2013**, *49*, 1924; (c) Hua B., Zhou J., Yu G.C., *Tetrahedron Lett.*, **2015**, *56*, 986.
[114] (a) Jie K.C., Zhou Y.J., Yao Y., Shi B.B., Huang F.H., *J. Am. Chem. Soc.*, **2015**, *137*, 10472; (b) Chi X.D., Ji X.F., Xia D.Y., Huang F.H., *J. Am. Chem. Soc.*, **2015**, *137*, 1440; (c) Chi X.D., Yu G.C., Shao L., Chen J.Z., Huang F.H., *J. Am. Chem. Soc.*, **2016**, *138*, 3168.
[115] (a) Strutt N.L., Forgan R.S., Spruell J.M., Botros Y.Y., Stoddart J. F., *J. Am. Chem. Soc.*, **2011**, *133*, 5668; (b) Ogoshi T., Yamafuji D., Aoki T., Kitajima K., Yamagishi T., Hayashi Y., Kawauchi S., *Chem. Eur. J.*, **2012**, *18*, 7493; (c) Ogoshi T., Yamafuji D., Aoki T., Yamagishi T., *Chem. Commun.*, **2012**, *48*, 6842; (d) Ogoshi T., Iizuka R., Kotera D., Yamagishi T., *Org. Lett.*, **2015**, *17*, 350; (e) Wei P.F., Yan X.Z., Li J.Y., Ma Y.J., Yao Y., Huang F.H., *Tetrahedron*, **2012**, *68*, 9179; (f) Dong S.Y., Han C.Y., Zheng B., Zhang M.M., Huang F.H., *Tetrahedron Lett.*, **2012**, *53*, 3668.
[116] (a) Kitajima K., Ogoshi T., Yamagishi T., *Chem. Commun.*, **2014**, *50*, 2925; (b) Ogoshi T., Akutsu T., Yamafuji D., Aoki T., Yamagishi T.A., *Angew. Chem. Int. Ed.*, **2013**, *52*, 8111; (c) Yan X.Z., Wei P.F., Li Z.T., Zheng B., Dong S.Y., Huang F.H., Zhou Q.Z., *Chem. Commun.*, **2013**, *49*, 2512.
[117] Fang L., Olson M.A., Benitez D., Tkatchouk E., Goddard W.A., Stoddart J.F., *Chem. Soc. Rev.*, **2010**, *39*, 17.
[118] Rotzler J., Mayor M., *Chem. Soc. Rev.*, **2013**, *42*, 44.
[119] T Ogoshi, *Pillararenes*, **2016**, *Monographs in Supramolecular Chemistry No. 18*, The Royal Society of Chemistry.
[120] (a) Ogoshi T., Demachi K., Kitajima K. Yamagishi T., *Chem. Commun.,* **2011**, *47*, 7164; (b) Zhang W., Liu L., Duan W., Zhou Q., Ma C., Huang Y., *Molecules*, **2019**, *24*, 2693.

[121] (a) Chen Y., Cao D., Wang L., He M., Zhou L., Schollmeyer D., Meier H., *Chem. Eur. J.*, **2013**, *19*, 7064; (b) Han Y., Huo G., Sun J., Xie J., Yan C., Zhao Y., Wu X., Lin C., Wang L., *Sci. Rep.*, **6**, 28748; (c) Jiang S., Han Y., Sun J., Yan C., *Tetrahedron*, **2017**, *73*, 5107.
[122] (a) Guan Y., Liu P., Deng C., Ni M., Xiong S., Lin C., Hu X., Ma J., Wang L., *Org. Biomol. Chem.*, **2014**, *12*, 1079; (b) Xia B., Xue M., *Chem. Commun.,* **2014**, *50*, 1021; (c) Tian H., Wang C., Lin P., Meguellati K., *Tetrahedron Letters*, **2018**, *59*, 3416; (d) Wu X., Gao L., Sun J., Hu X., Wang L., *Chinese Chemical Letters*, **2016**, *27*, 1655; (e) Zhang R., Wang C., Long R., Chen T., Yan C., Yao Y., *Front. Chem.*, **2019***, 7,* 508.
[123] (a) Strutt N.L., Zhang H., Giesener M.A., Leia J., Stoddart J.F., *Chem. Commun.*, **2012**, *48*, 1647; (b) Zhang Z., Yu G., Han C., Liu J., Ding X., Yu Y., Huang F., *Org. Lett.*, **2011**, *13*, 4818.
[124] (a) Xia B., Zheng B., Han C., Dong S., Zhang M., Hu B., Yu Y., Huang F., *Polym. Chem.*, **2013**, *4*, 2019; (b) Wang K., Wang C.Y., Wang Y., Li H., Bao C.Y., Liu J.Y., Zhang S.X.A., Yang Y.W., *Chem. Commun.*, **2013**, *49*, 10528; (c) Wang Y., Xu J.F., Chen Y.Z., Niu L.Y., Wu L.Z., Tung C.H., Yang Q.Z., *Chem. Commun.*, **2014**, *50*, 7001.
[125] Wight A.P., Davis M.E., *Chem. Rev.*, **2002**, *102*, 3589.
[126] (a) Qiu S., Xue M., Zhu G., *Chem. Soc. Rev.*, **2014**, *43*, 6116; (b) Zhou H.C., Kitagawa S., *Chem. Soc. Rev.*, **2014**, *43*, 5415.
[127] (a) Strutt N.L., Fairen-Jimenez D., Iehl J., Lalonde A.M.B., Snurr R.Q., Farha O.K., Hupp J.T., Stoddart J.F., *J. Am. Chem. Soc.*, **2012**, *134*, 17436; (b) Strutt N.L., Zhang H., Stoddart J.F., *Chem. Commun.*, **2014**, *50*, 7455.
[128] Tan L.L., Li H., Tao Y., Zhang S.X.A., Wang B., Yang Y.W., *Adv. Mater.*, **2014**, *26*, 7027.
[129] (a) Tan L.L., Li H., Zhou Y., Zhang Y., Feng X., Wang B., Yang Y.W., *Small*, **2015**, *11*, 3807; (b) Tan L.L., Li H., Qiu Y.C., Chen D.X., Wang X., Pan R.Y., Wang Y., Zhang S.X.A., Wang B., Yang Y.W., *Chem. Sci.*, **2015**, *6*, 1640.
[130] Yao Y., Zhou Y., Dai J., Yue S., Xue M., *Chem. Commun.*, **2014**, *50*, 869.
[131] Yang J., Yu G., Xia D., Huang F., *Chem. Commun.*, **2014**, *50*, 3993.
[132] Zhou J., Chen M., Xie J., Diao G., *ACS Appl. Mater. Interfaces*, **2013**, *5*, 11218. (b) Zhang H., Ma X., Nguyen K.T., Zeng Y., Tai S., Zhao Y., *ChemPlusChem*, **2014**, *79*, 462.
[133] (a) Sun Y.L., Yang Y.W., Chen D.X., Wang G., Zhou Y., Wang C.Y., Stoddart J.F., *Small*, **2013**, *9*, 3224; (b) Huang X., Du X., *ACS Appl. Mater. Interfaces*, **2014**, *6*, 20430; (c) Zhou T., Song N., Yu H., Yang Y.W., *Langmuir*, **2015**, *31*, 1454.

CHAPTER 2

2.1 Calix[4]arene tubular derivatives: Calix[4]tubes

Since their discovery, calix[*n*]arenes have attracted considerable interest, initially in synthetic organic chemistry, and subsequently in the supramolecular field. These macrocycles have undergone a wide range of functionalizations (see Section 1.2.1, Chapter 1), which have enabled them to be used in various fields, such as anion receptors,[1] fluorescent sensors,[2] multivalent ligands,[3] and also in the manufacture of chiral colourimetric recognition sensors,[4] polymers, [5] supramolecular nanostructures [6] and functional nanomaterials. [7] These macrocycles have also become very popular for the design of ion channels, based on those naturally occurring in biological systems.

The possibility of selective recognition of group 1 metals has led to combine calixarenes with crown ethers,[8] to yield calixcrowns. These derivatives have shown enhanced selectivity towards several ions.[9] The linkage of two calix[4]arenes with polyether bridges, through their lower rims, has allowed the shuttling of the sodium cation between the two ends of this calix[4]polyether (partial) tube.[10]

Subsequent to the formation of bis-calixarene barrels obtained by the Ziessel group,[11] Beer and co-workers developed a new class of ionophores selective for potassium ions, and reported the first synthesis of a calix[4]tube system (Figure 2.1).[12] Potassium ions were also shown to act in this case as templating agents for the formation of the quadruple bridge between the two calixarene units.

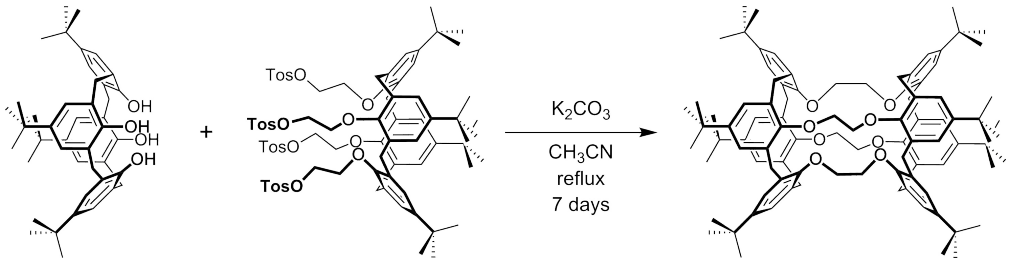

Figure 2.1. The synthesis of the first reported calix[4]tube by Beer *et al.*[12]

Potassium encapsulation into the cryptand-like cage provided by the four dioxyethylene bridges was also shown to happen in the solid state by X-ray crystal analysis,[12,13] whereas theoretical calculations elucidated the mechanism of such encapsulation, indicating that the cation enters the tube from one calixarene cavity and then reaches the central tubular cage.[14]

The optimization of the structural features of this tubular receptor,[13] eventually afforded the less rigid calix[4]semitubes[15] and the ditopic calix[4]semitube urea derivatives.[16] More recent advances regarding some additional structural modification of this tubular receptor also led to the rubidium uptake by asymmetric calix[4]-thiacalix[4]tubes[17] and to the tuning of the conformational equilibrium of functionalized calix[4]tubes controlled by intramolecular hydrogen bonding or electrostatic repulsion weak interactions.[18] So far, however, the upper rim functionalization of calix[4]tube to fabricate building blocks for the assembly of supramolecular arrays has lagged behind.

2.2 Synthesis and properties of octatolylurea-calix[4]tube UC4T

In a recent account, Gaeta *et al.* have reported the synthesis of octaamino-calix[4]tube **AC4T** and have shown the key role played by potassium ions in the non-covalent synthesis of discrete porphyrin-calix[4]tube nanostructures.[19] Building on these results, in connection with the current interest for linear supramolecular polymers,[20] it was decided to focus the attention on the synthesis of octaureido-calix[4]tubes for the potential development of more complex supramolecular structures.

Octatolylurea-calix[4]tube **UC4T** was obtained in a 60% yield by reacting the known octaamino-calix[4]tube **AC4T**[19] with *p*-tolylisocyanate in anhydrous dimethylsulfoxide (Scheme 2.1).

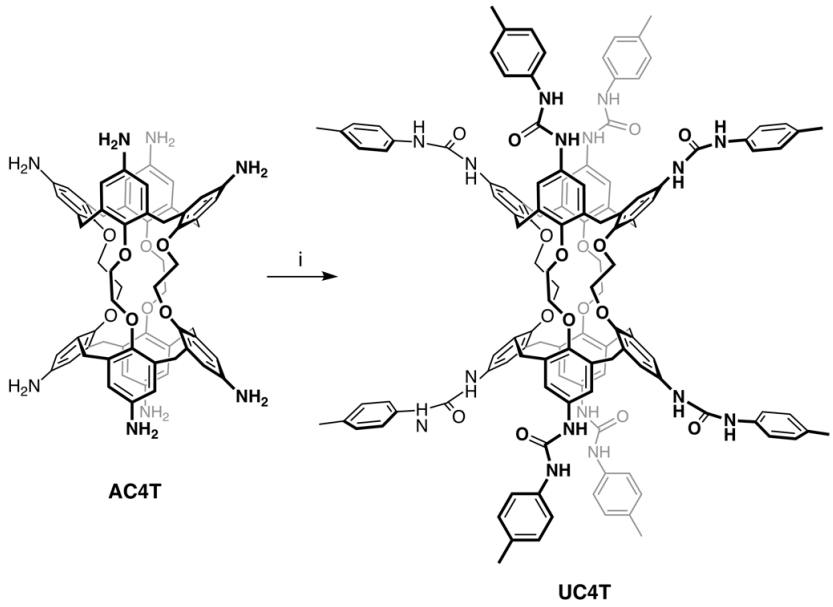

Scheme 2.1. Synthesis of **UC4T** starting from **AC4T**; (i) *p*-tolylisocyanate, dry DMSO, r.t., 3h.

The new **UC4T** calixtube derivative is an interesting monomeric unit potentially useful for the formation of linear supramolecular (poly)capsular assembly,[21] as it possess two divergent calix[4]arene cavities decorated with urea functionalities. However, for this to happen it is mandatory that the macrocycle cavities adopt a regular *cone* conformation so as the sealing between two or more calix[4]arene subunits can takes place through 16-hydrogen-bond arrays.[22] In addition, given that these macrocycles show, in solution and in the solid state,[12,13,14,19, 23] a fairly rigid C_{2v} symmetry, due to alternating *gauche-like* and *anti* conformations of the four linkers, a way must be found to overcome these conformational/structural handicaps.

Unfortunately, **UC4T** was found to be insoluble in all apolar and weakly polar solvents (chloroform, dichloromethane, benzene), that typically promote the formation of hydrogen-bonded dimers between calix[4]arenes functionalized at the upper rim with urea moieties, whereas it was readily soluble in highly polar dimethyl sulfoxide (DMSO). In analogy with the congener parent **AC4T**, the *p-tert*-butylated derivative and the other calix[4]arene tubes,[13,14,18,24] the two cavities of the octaurea calix[4]arene **UC4T** adopt in DMSO-d_6 solution a *flattened-cone* (alternatively defined *pinched-cone*) conformation, with two pairs of opposite aryl rings parallel to each other and the remaining two pointing outwards, as revealed by the presence, in the ^{1}H NMR spectrum, of four resonances for the NHs, two sharp singlets for the aromatic hydrogens (ArH), two different tolyl residues (TolH and CH_3), two singlets for OCH_2 groups and one AX system for the bridging methylenes ($ArCH_2Ar$) of the calixarene scaffold (Figure 2.2).

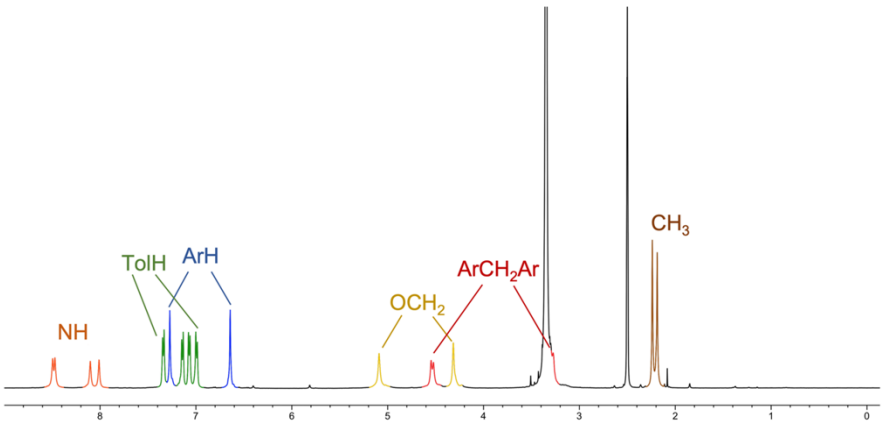

Figure 2.2. ^{1}H NMR spectrum of **UC4T** (500 MHz, DMSO-d_6, 298 K).

Figure 2.3 provides further evidence of an interconversion between two equivalent conformations in solution by showing the presence of ROESY chemical-exchanging cross-peaks, for the ArH, NH and OCH_2 resonances of **UC4T**.

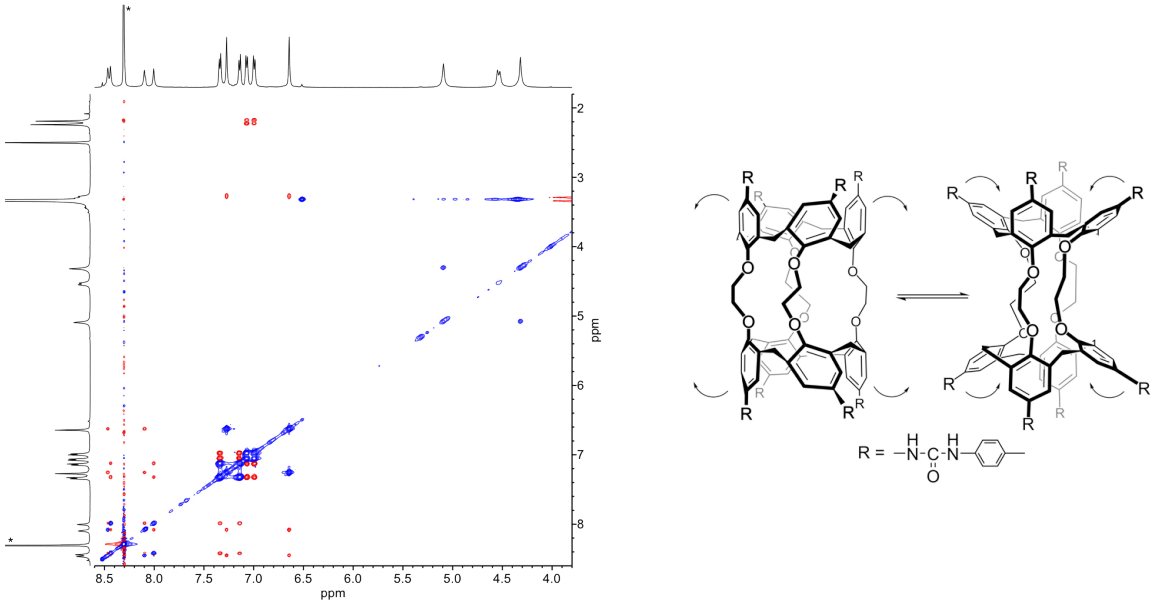

Figure 2.3. Left) Section of the ROESY spectrum of **UC4T** (500 MHz, DMSO-d_6, 298 K); right) schematic C_{2v} conformational interconversion occurring in DMSO solution (the asterisk refers to trace amount of $CHCl_3$ present in the NMR sample).

With the exception of a few examples of mechanically entangled capsular dimers,[25] DMSO – owing to its pronounced tendency to form hydrogen bonds with ureido moieties– is generally not a suitable solvent for the formation of capsular assembly between tetraurea-calix[4]arene derivatives, because it rapidly destroys the hydrogen-bond belt necessary for the self-assembly, even at low concentrations (2%), in apolar solvents. In our hands, **UC4T** (1 mM) in a $CDCl_3$/DMSO-d_6 (98:2, *v*/*v*) solvent mixture gave an opalescent suspension, and the ^{1}H NMR spectrum recorded after filtration of the undissolved material displayed an unexpected complexity (Figure 2.4).

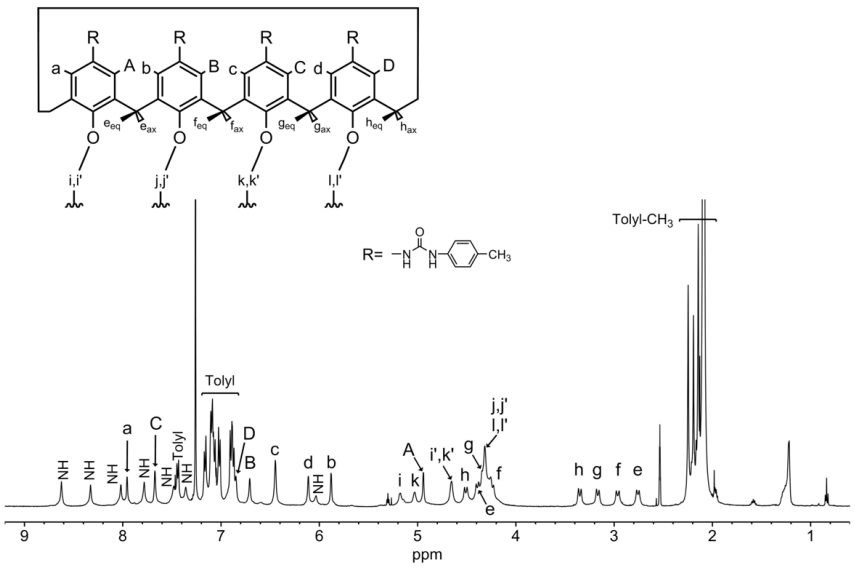

Figure 2.4. ^{1}H NMR spectrum (500 MHz, $CDCl_3$/DMSO-d_6 98:2, 298 K) of [**UC4T**] = 1 mM, after filtration.

Exhaustive 2D NMR analysis by COSY and HSQC experiments revealed the presence of eight resonances for the calixarene aromatic hydrogens showing *meta-coupling* cross-peaks, four non-equivalent signals for the tolyl residues, eight distinct resonances for the NHs, four different signals for the OCH_2 groups and four AX systems for the axial and equatorial hydrogen atoms of the methylene groups bridging the aromatic units. The addition of increasing amounts (up to ca. 8%) of DMSO-d_6 to the original solution, caused the appearance of a new set of resonances which first coexisted with the former ones and finally became predominant (Figure 2.5).

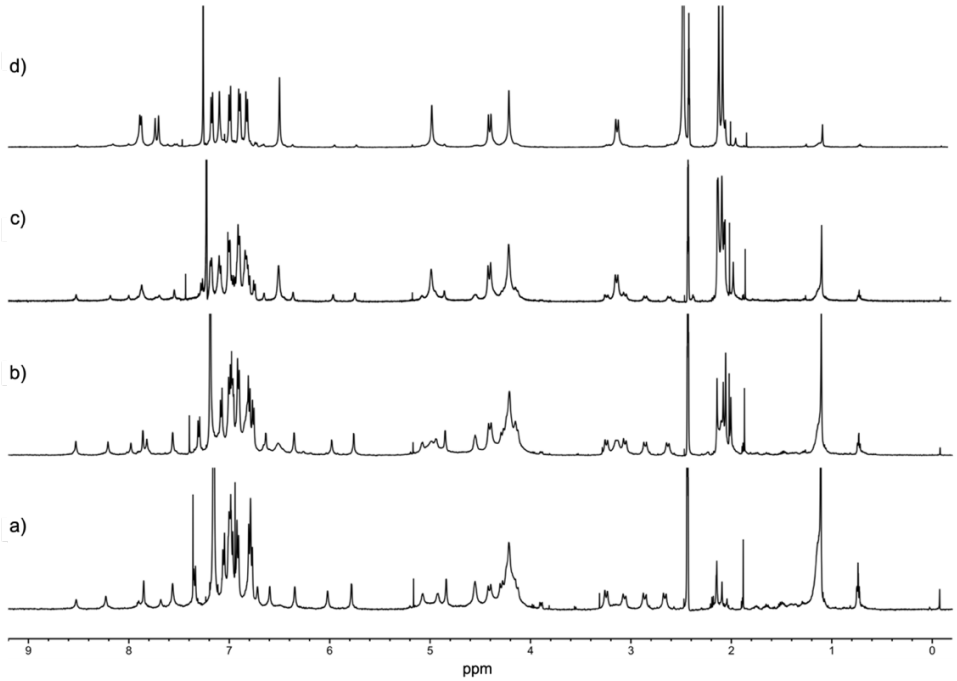

Figure 2.5. ^{1}H NMR spectrum (500 MHz, 298 K) of [**UC4T**] = 1 mM in: a) $CDCl_3$/DMSO-d_6, 98:2; b) $CDCl_3$/DMSO-d_6, 96:4; c) $CDCl_3$/DMSO-d_6, 94:6; d) $CDCl_3$/DMSO-d_6, 92:8.

The ROESY spectrum of **UC4T** (Figure 2.6), in a 98:2 $CDCl_3$/DMSO-d_6 mixture, shows close contacts between the hydrogen atoms of the bridging methylene groups and those present on the two flanking aryl rings (*i.e.*, A-e_{eq}-b, B-f_{eq}-c, C-g_{eq}-d and D-h_{eq}-a). Hydrogen atoms located on adjacent aryl rings (*i.e.*, A-b, B-c, C-d and D-a) do also show close contact with each other, suggesting that all these resonances belong to a single calix[4]arene asymmetric cavity.

Interestingly, red dashed circles in Figure 2.6 highlight that a chemical exchange is occurring in solution between bulk water and those interacting with **UC4T**. The conformational stability of **UC4T**, in the above-mentioned solvent mixture, was further confirmed by a series of VT-NMR experiments, carried out in the 243–323 K temperature range, which displayed overall similar spectral pattern (Figure 2.7).

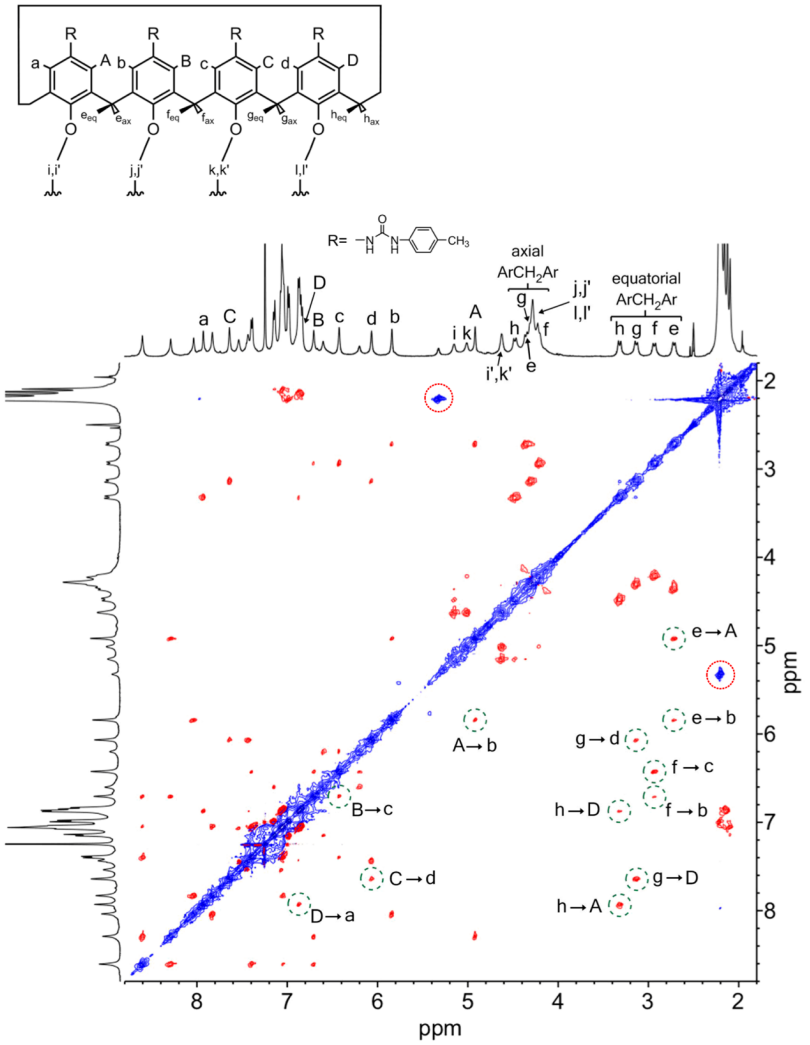

Figure 2.6. ROESY spectrum (500 MHz, 298 K) of [**UC4T**] = 1 mM in $CDCl_3$/DMSO-d_6 (98:2). Close contact peaks and exchange cross-peaks are shown in red and blue, respectively.

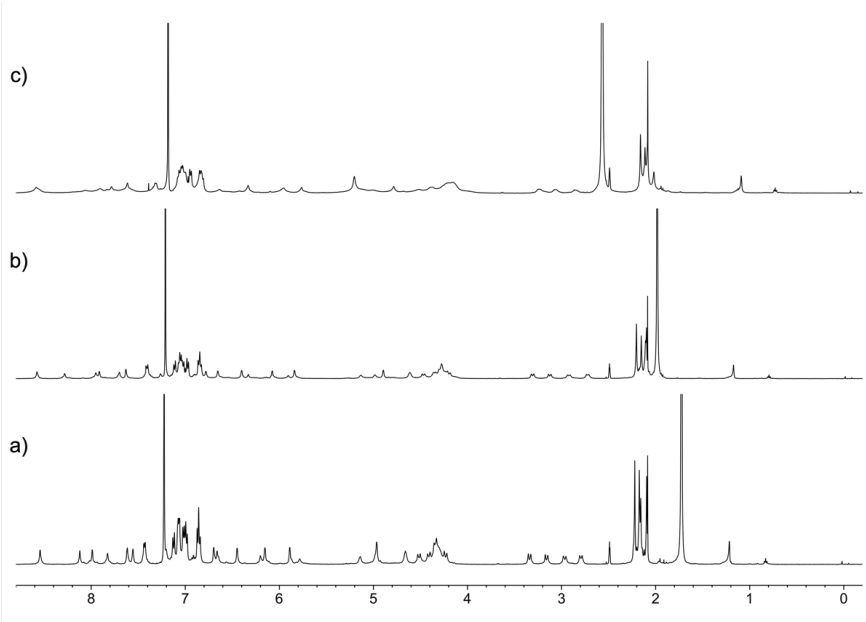

Figure 2.7. VT NMR analysis (500 MHz) of [**UC4T**] = 1 mM in $CDCl_3$/DMSO-d_6. 98:2 at: a) 328 K; b) 298 K and c) 243 K.

All the information gathered so far rule out the formation of dimeric or short oligomeric assemblies, because of the lack of signals accountable for the *end-group* cavities. Conversely, the set of resonances arising from a single calixarene cavity reasonably suggest the presence in the $CDCl_3$/DMSO-d_6, 98:2 solution of **UC4T** as a monomer or as a huge linear polymer.

To further understand the structural features of **UC4T,** a Diffusion-Ordered NMR SpectroscopY (DOSY) study was carried out at different concentrations of DMSO-d_6, in order to determine the "size" of the species present in $CDCl_3$/DMSO-d_6 solvent mixtures of different composition. The DOSY plot of the 2%-DMSO solution showed all the resonances of the spectrum lying on the same line, corresponding to a self-diffusion coefficient $D_{obs} \approx 3.8 \times 10^{-10}$ $m^2\ s^{-1}$ (Figure 2.8a). After the addition of DMSO-d_6 (up to *c.a.* 6% *v/v*), the spectrum showed the additional resonances of the **UC4T** *flattened-cone* conformer and the DOSY plot (Figure 2.8b) revealed the presence of two distinct sets of very close diffusion coefficients ruling out the formation, in the first place, of a long linear assembly. The decrease of the diffusion coefficient values (from *c.a.* 3.8×10^{-10} to *c.a.* 2.2×10^{-10} $m^2\ s^{-1}$) observed for the original species in the two solvent systems ($CDCl_3$/DMSO-d_6: 98:2 and 94:6, respectively) can be explained by taking into account the increase of solvent viscosity upon DMSO addition. This hypothesis is further corroborated by the lower value of diffusion coefficient detected for the residual $CHCl_3$ resonance at 7.26 ppm.

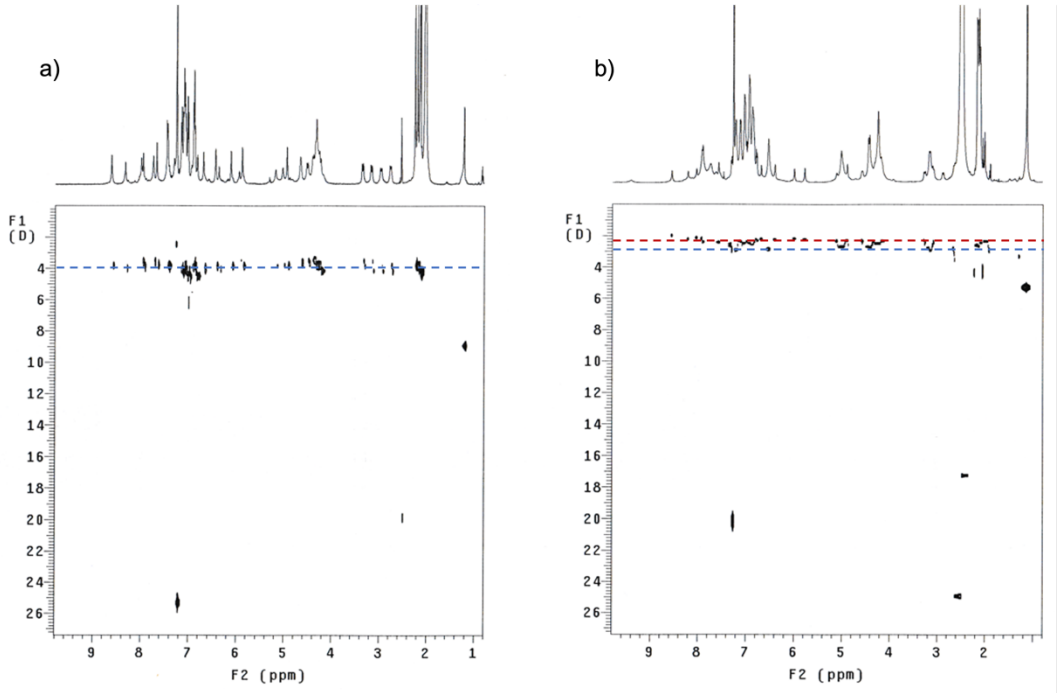

Figure 2.8. On the left side, DOSY spectrum of [**UC4T**] = 1 mM in $CDCl_3$/DMSO-d_6 98:2; on the right, DOSY spectrum of [**UC4T**] = 1 mM in $CDCl_3$/DMSO-d_6 94:6.

It has been reported that H-bonding or electrostatic interactions may affect the conformational distribution of calix[4]tube derivatives. For instances, a calix[4]tube distally substituted with adamantyl-ureido moieties shows, in $CDCl_3$, an equal population of two distinct *flattened-cone* conformations. The 50/50 population ratio remained the same upon heating up to 328 K, suggesting that hydrogen bonding between the urea moieties can withstand high temperatures. The subsequent addition of CF_3CO_2D, however, induced a substantial conformational rearrangement, consistent with a 90:10 ratio in favour of the *flattened-cone* conformer with the aryl residues bearing the ureido groups pointing outwards.[18] Our findings on the conformational equilibrium of **UC4T** in different $CDCl_3$/DMSO-d_6 mixtures clearly emphasize the prime role played by H-bonded solvent molecules to the conformational equilibrium of this unique calix[4]tube derivative. NMR data suggest that at lower DMSO concentrations, **UC4T** is frozen into an asymmetric conformation, most likely as a result of H-bond interactions. This asymmetric spectral pattern is seen over an 80-degree temperature range (Figure 2.7). The addition of increasing volumes of the polar solvent eventually switches the equilibrium towards the more flexible C_{2v}-C_{2v} interconverting *flattened-cone* conformations. To the best of our knowledge this is the first example of a symmetrically-substituted calix[4]tube derivative showing in solution a stable solvent-dependent asymmetric conformation. Any speculation about the formation of specific intra- (ureido-ureido) or intermolecular (ureido-DMSO) hydrogen-bond interactions, which might account for an asymmetric conformation in solution, is dangerous, as many of these intra- and intermolecular interactions may co-exist because of the concomitant presence of H-bond donor/acceptor ureido groups and of H-bond acceptor solvent molecules (DMSO). The two crystallographic structures of **UC4T** (see below), however, confirm the central role played by hydrogen bonding to polar molecules (DMSO, H_2O) in the orientations ("head-to-tail" or "head-to-head and tail-to-tail") of the **UC4T** ureido groups in the solid state.

Based on the above-mentioned findings, it was concluded that in a 98:2 $CDCl_3$/DMSO-d_6 solvent mixture, the formation of the desired **UC4T** (poly)capsular assembly is likely prevented by conformational constrains.

Bearing in mind the importance of cation encapsulation –inside the cryptand-like dioxyethylene cage– for an effective conformational rearrangement (from a C_{2v} to a C_{4v}) of a calix[4]tube derivative[12,19] and, at the same time, the symmetry requirement (C_{4v}) necessary to promote the capsular assembly of ureido-calix[4]arene derivatives (see Section 1.2.2, Chapter 1), KI and $BaCl_2$ were added to 98:2 $CDCl_3$/DMSO-d_6 solutions of **UC4T**, and ^{1}H NMR spectra were regularly recorded over a two-week period. Barium was selected as a potential guest for the polyether-cage of **UC4T** on the basis of its similar ionic radius (1,35 Å) to that of K^+ (1,38 Å).

In both instances, the initial pattern simplified with time (Figure 2.9, traces a–c and d–f in the case of KI and $BaCl_2$, respectively) and spectra progressively showed a merging of the OCH_2 resonances to a single broad signal and a downfield shift of the NH resonances[26] to 9.6 ppm. Such a trend could in principle be compatible with the encapsulation of the cation inside the dioxyethylene cage of **UC4T**, with a subsequent conformational rearrangement of the two calix[4]arene subunits, from a *flattened-cone* (C_{2v} symmetry) to a regular *cone* (C_{4v} symmetry), ultimately leading to the formation of dimeric (or higher order) capsular assemblies, held together by a seam of intermolecular H-bond between the ureido moieties. Unfortunately, as time went by, the two solutions yielded increasing amount of a powdery precipitate which eventually settled at the bottom of the NMR tube, preventing any further NMR study. Furthermore, no trace of **UC4T** was detected in the resulting supernatant solution after four weeks (spectra not shown).

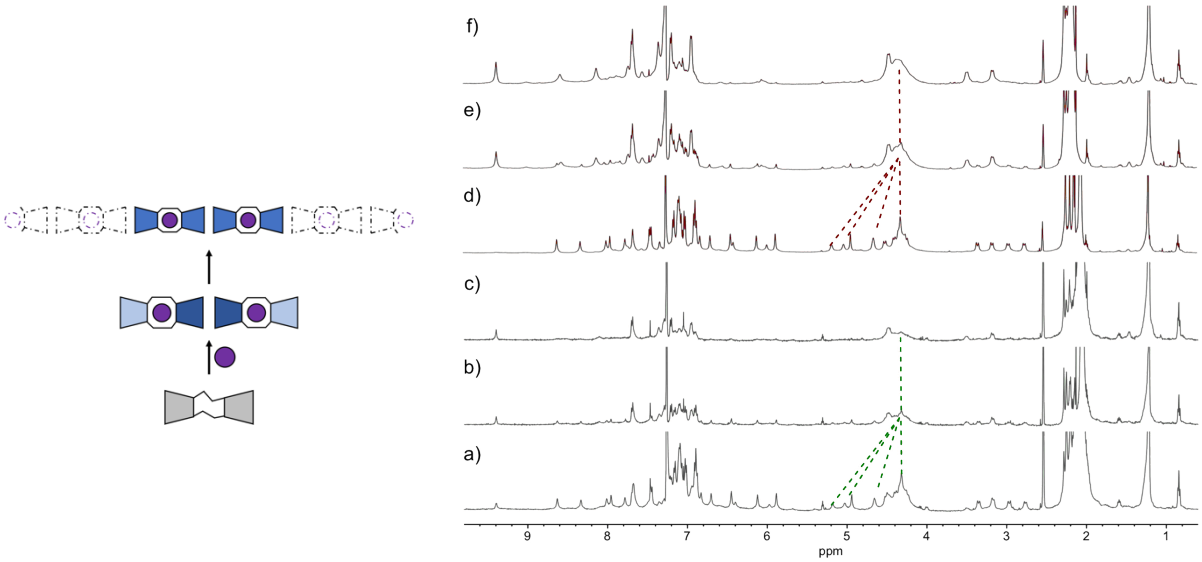

Figure 2.9. ^1H NMR spectra of [**UC4T**] = 1 mM in $CDCl_3$/DMSO-d_6, 98:2 after: a) 1 day after addition of KI (2 equiv.); b) 3 days after addition of KI; c) 7 days after addition of KI; d) 1 day after addition of $BaCl_2$ (2 equiv.); 7 days after addition of $BaCl_2$; 14 days after addition of $BaCl_2$. A schematic representation of the likely dimeric/oligomeric **UC4T** capsular assemblies formed upon K^+ and Ba^{2+} addition is shown on the left.

Attempts to isolate X-ray-grade crystals from these suspensions were to no avail. However, single crystals, suitable for X-ray investigation, were later obtained by slow evaporation of DMSO/chloroform solution of **UC4T.** Two different crystal forms (α and β) were obtained from two different crystallization trials, one in which the solution contained KI (with a resulting K^+/**UC4T** molar ratio of 1.2) and one in which it contained $BaCl_2{\cdot}2H_2O$ (with a resulting Ba^{2+}/**UC4T** molar ratio of 1.2). The X-ray structures show that both α and β forms have the

UC4T molecules located on crystallographic inversion centres without any metal ion coordinated by the central dioxyethylene cryptand-like cage. (Figure 2.10).

The divergent calix[4]arene units of the centrosymmetric **UC4T** molecule adopt a *flattened-cone* conformation in both crystal forms, which means that the two symmetry related calix[4]arene units are pinched on the same sides (Figure 2.11). In particular, two opposite aryl rings are more outwardly inclined (136 and 142° in α; 139 and 141° in β) with the other two nearly orthogonal (88 and 86° in α; 84 and 87° in β) with respect to the corresponding mean plane of the methylene bridging groups of the calixarene unit. Angles smaller (or larger) than 90° indicate that the aryl rings bearing the ureido moieties are inward (or outward) oriented with respect to the centre of the cone.

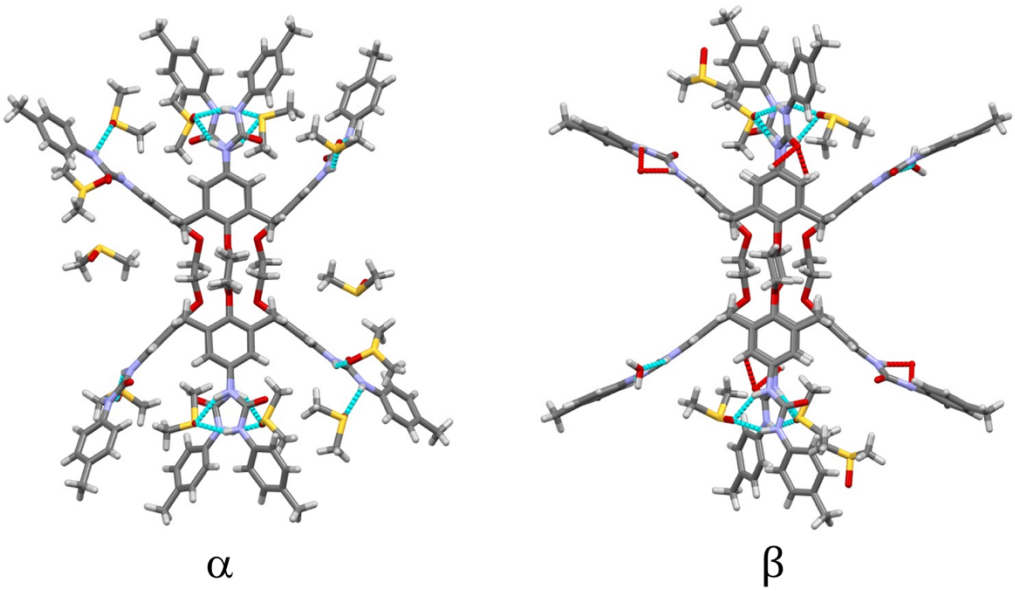

Figure 2.10. Stick representation of the α and β forms of **UC4T**. The atomic species are in CPK colours. For the sake of clarity, only one position of each disordered group is shown. H-bonds are depicted with dashed lines. The **UC4T** molecules are located on crystallographic inversion centres in both crystal forms. Inversion related solvent molecules are also shown.

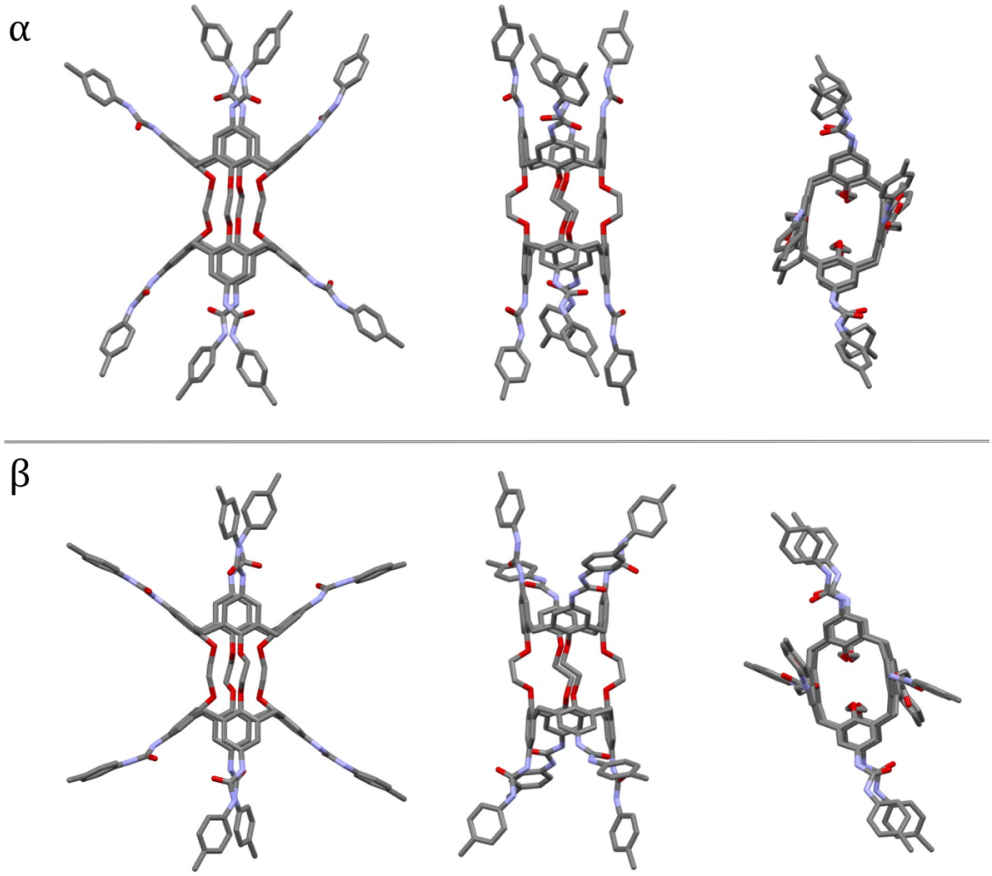

Figure 2.11. Orthogonal views of the α and β forms of **UC4T**. The atomic species are in CPK colours. For the sake of clarity, only one position of each disordered group is shown. The two divergent calix[4]arene units adopt a *flattened-cone* conformation in both crystal forms.

The *flattened-cone* conformation dramatically affects the relative positions of the four dioxyethylene groups positioned at the lower rim, with opposite (distal) pairs of O atoms pushed further apart on the pinched sides and closer together on the flattened sides (O···O distances of 3.27 and 5.43 Å for α and 3.26 and 5.39 Å for β). The consequence of this is that the pairs of O atoms connected by the ethylene bridges on the pinched sides are closer together (2.71 and 2.74 Å for α and β, respectively), while they are further apart on the other sides (3.61 and 3.63 Å for α and β, respectively). These geometrical features are consistent with the observed conformation of the ethylene bridging unit (Figure 2.11). The torsion angles of the C-O-C-C-O-C chains in the α form are 171° (trans), 20° (cis) and 171° (trans) (TCT) for the less extended chain and 104°/95° (anticlinal), 155°/160° (trans) and 112°/123° (anticlinal) for the two disordered positions (see the Experimental Section) of the more extended chain. For the β form, the corresponding chain conformations are 163° (trans), 36° (gauche) and 162° (trans) for the less extended chain and 98° (anticlinal), 154° (trans) and 116° (anticlinal) (ATA) for the more extended chain. Owing to the presence of an inversion centre, the symmetry related chains have the same torsion angles with opposite sign.

The orientation of the ureido groups is rather different in the two crystal forms. In the α form the neighbouring ureido groups are all head-to-tail oriented (carbonyl of one ureido group pointing towards the NH groups of an adjacent group in a clockwise or anticlockwise sense of rotation), while in the β form they are less symmetrically disposed with a general head-to-head (carbonyl towards carbonyl) and tail-to-tail (NH towards NH) orientation (Figure 2.12).

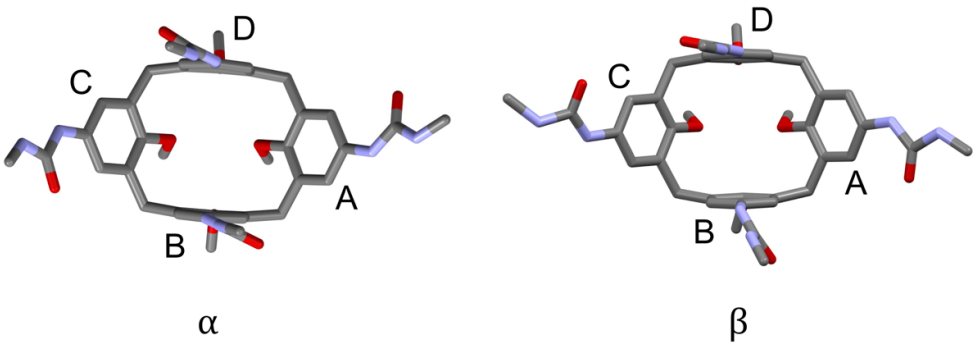

Figure 2.12. Top views of the ureido groups orientation in the α and β forms of **UC4T**. The atomic species are in CPK colours. For the sake of clarity, only the aromatic calix[4]arene unit and ureido groups are shown.

In the α form, in combination with the crystallographic inversion centre, a pseudo twofold axis passing in the middle of the pinched calix[4]arene units produces a pseudo C_{2h} point symmetry of the molecule (Figure 2.11). It should be noted that the bridging ethylene groups with a TCT chain conformation are compatible with a horizontal symmetry plane, however groups with a more extended ATA chain conformation are not compatible with C_{2h} symmetry. Interestingly, in the α form these more extended chains show a statistical disorder which can be rationalized in terms of the overlap of two equivalent molecules related by the pseudo horizontal plane. In the β form, the complete loss of the twofold axis due to the ureido group conformations reduces the point symmetry of the molecule to C_i.

Table 2.1 shows details of the different orientation and deformation of the ureido arms in the two crystal forms. The tilt of the ureido groups with respect to the corresponding calix-aryl moieties and with respect to the terminal tolyl rings is more regular in the α form (Figure 2.11). These values range from 12.2 to 28.2° in the α form and from 6.0 to 58.0° in the β form (Table 2.1). A significant bend of one arm toward the calix cup is observed in the α form (Figure 2.11), as indicated by the –2.68 Å out of plane distance of the tolyl group from the aromatic plane of the corresponding calix aryl group. The β form shows three arms bent significantly outward (Table 2.1). The partial loss of planarity of these aromatic systems is highly influenced by the intermolecular H-bond formation and crystal packing.

Table 2.1. Orientation of the ureido arms for the α and β crystal forms of **UC4T**. Dihedral angles between the planar ureido and aryl groups to which they are attached. Out of plane distance of the tolyl group from the aromatic plane of the corresponding calix aryl group. The negative (positive) sign indicates an inward (outward) bend of the arm with respect to the calix cup.

crystal form	ureido–calix–aryl (°)	ureido–arm–aryl (°)	calix–aryl–arm–Tolyl (°)	Out of plane distance (Å)
α, A	17.8	14.8	32.6	0.35
α, B	28.2	25.9	53.2	0.79
α, C	12.2	28.1	37.5	-2.68
α, D	21.9	26.7	45.0	0.44
β, A	6.0	10.6	16.0	1.41
β, B	58.0	50.9	58.0	4.19
β, C[a]	23.5	29.4 (47.1)	20.4 (69.5)	2.52 (-0.79)
β, D	12.6	21.8	34.4	0.24

[a] Values in parenthesis refer to the angles made with the second orientation of the external tolyl ring.

In the α form all the NH groups are involved in H-bonds with the co-crystallized DMSO solvent molecules. In particular, the two NH groups of the A arm are involved as H-bond donors with two O-atom acceptors of distinct DMSO molecules, while the other three ureido groups are involved in bifurcated H-bonds (two donors and one acceptor) with single DMSO molecules (Figure 2.13). On the contrary, the carbonyl groups of the ureido moieties are not involved in any H-bond interactions.

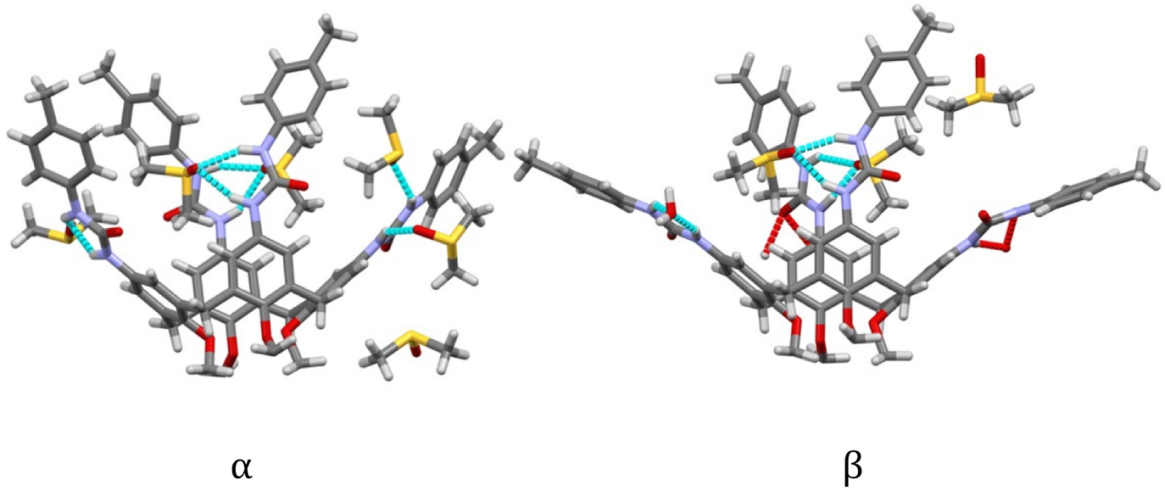

Figure 2.13. H-bonds found in the α and β forms of **UC4T**. The atomic species are in CPK colours. For the sake of clarity, only the crystallographically independent unit of **UC4T** and one position of each disordered group are shown. H-bonds are depicted with dashed lines, the cyan colour indicates H-bonds between **UC4T** and solvent molecules, while the red colour indicates H-bonds between **UC4T** molecules related by crystallographic symmetry.

In the β form only the ureido arms of the pinched rings (B, D) are involved in bifurcated H-bonds (two donors and one acceptor) with the co-crystallized DMSO solvent molecules. The

two NH groups of the A arm are involved as H-bond donors in a bifurcated interaction with a co-crystalized water molecule stoichiometrically added in the crystallization batch by means of the $BaCl_2 \cdot 2H_2O$ salt. The NH groups of the opposite ureido arm (C), which shows a two-position disorder of the tolyl ring, are involved in bifurcated H-bonds with the ureido carbonyl group of a pinched arm (B) of a symmetry related **UC4T** molecule (Figure 2.13). Therefore, this kind of bifurcated intermolecular H-bond, which involves two couples of ureido groups related by an inversion centre per molecule (one donor and one acceptor of H-bonds), produces a close packed 1D array of **UC4T** molecules interconnected by a complementary H-bond network along the *c* axis of the unit cell (Figure 2.14).

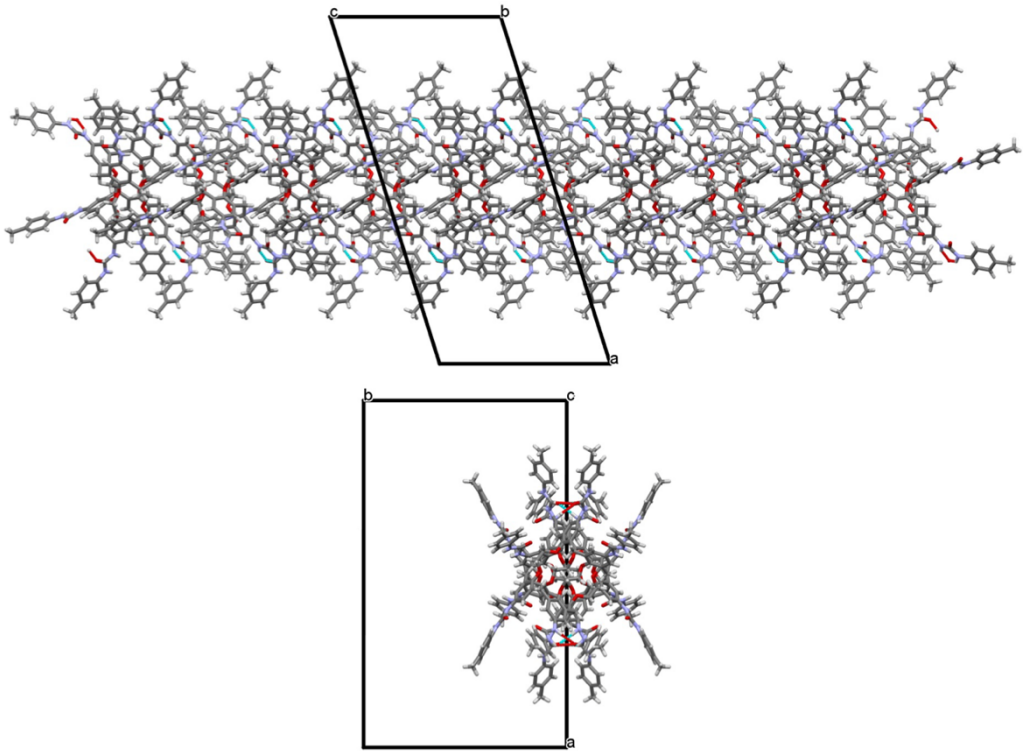

Figure 2.14. Side and top views of the close-packed 1D array of **UC4T** molecules interconnected by a complementary H-bond network (cyan dashed lines) observed along the c axis of the monoclinic unit cell of the β form.

These 1D arrays of **UC4T** molecules interconnected by a complementary H-bond network, are assembled in the β form through an almost face to face assembly of calix-caps (Figure 2.15). In particular, two facing **UC4T** molecules form a pseudo-capsule mainly delimitated by the ureido arms of the pinched sides of the calixarene moieties (Figure 2.15a). However, this pseudo capsule contains a partially inserted ureido arm of an adjacent molecule (Figure 2.15b). Overall, adjacent 1D arrays are interconnected by these pseudo-capsules, forming an interdigitation of ureido arms of the pinched rings of different arrays (Figure 2.15c). These 1D arrays are assembled in the C centred monoclinic lattice in such a way to produce large

parallel solvent channels as observed in the crystal packing of the β form (Figure 2.16, bottom). On the contrary, the α form shows a more closed packing with the small cavities filled by DMSO molecules (Figure 2.16, top). The parallel solvent channels observed in β form run along the *c* axis of the monoclinic unit cell (Figure 2.17) and are only partially filled by highly disordered solvent molecules.

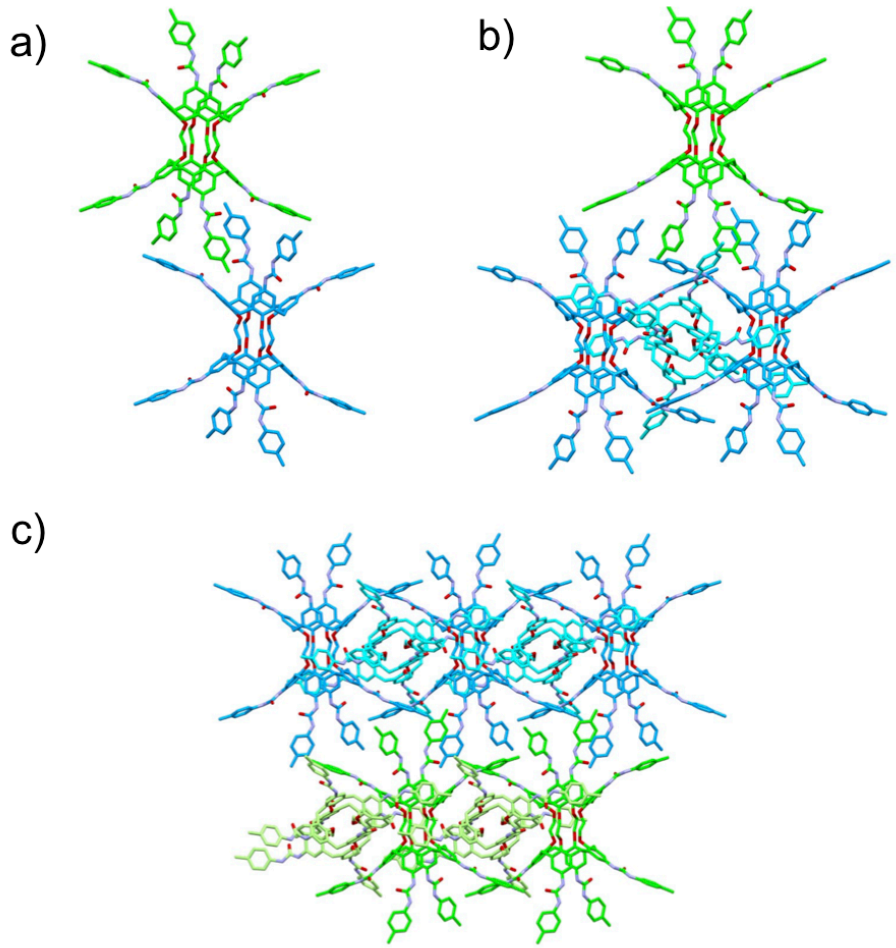

Figure 2.15. Assembly of 1D array of **UC4T** molecules interconnected by a complementary H-bond network observed in the β form. a) Two facing **UC4T** molecules form a pseudo capsule mainly delimitated by the ureido arms of the pinched rings. b) The pseudo-capsule contains a partially inserted ureido arm of an adjacent molecule. c) Adjacent 1D arrays are interconnected by these pseudo-capsules. Molecules of the same 1D array have the same colour.

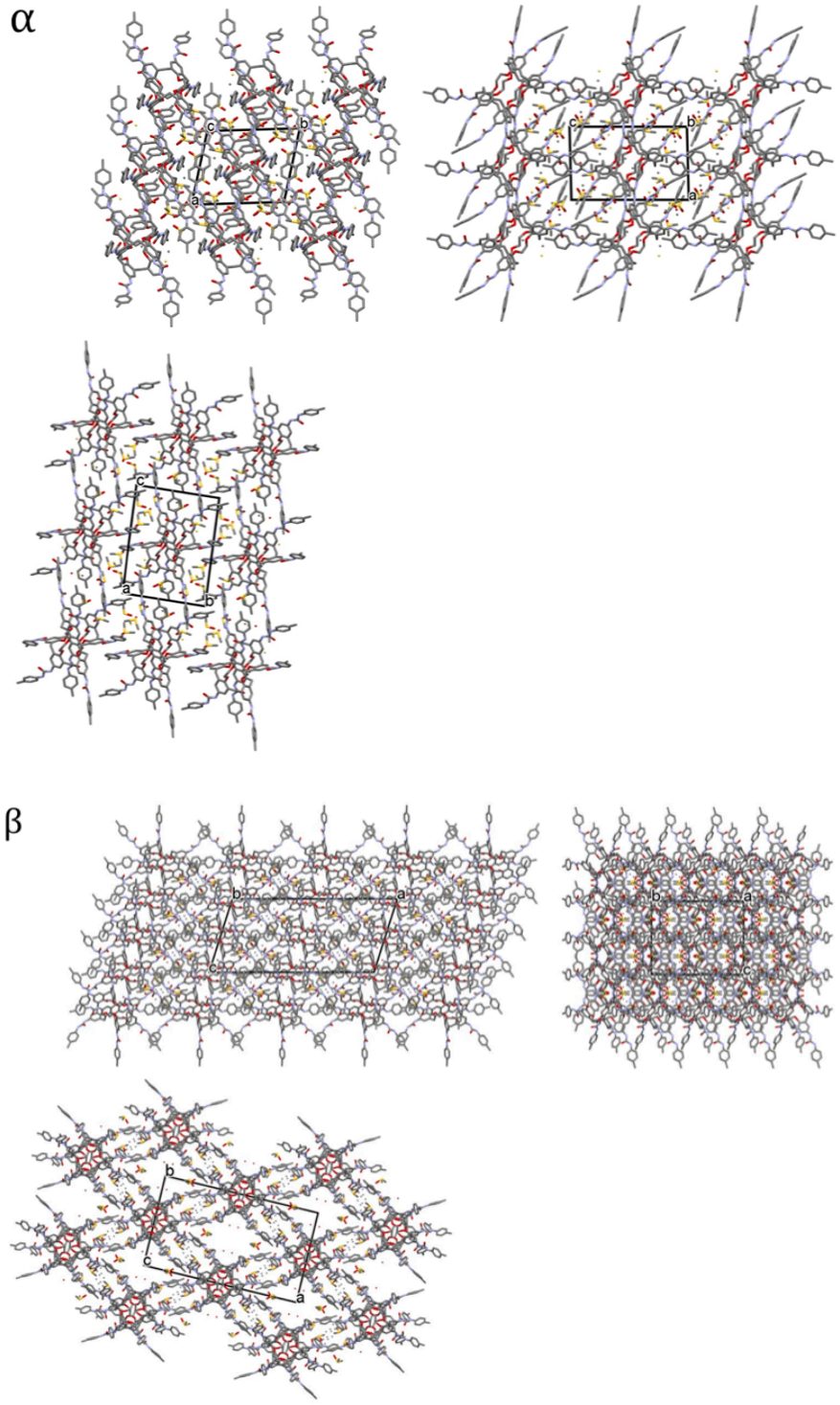

Figure 2.16. Orthogonal representation of the crystal packing of the triclinic α (top) and monoclinic β (bottom) forms of **UC4T.** The projections follow the convention used for the space groups in the International Tables of Crystallography.

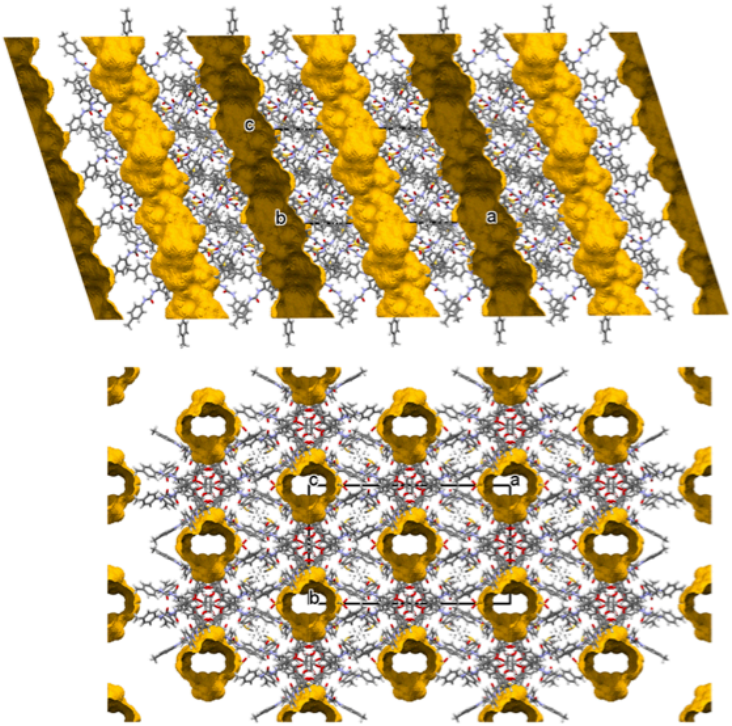

Figure 2.17. Side and top views of the solvent channel observed in the β form of **UC4T**. The solvent contact surface, calculated with a solvent probe radius of 1.4 Å (corresponding to a water molecule probe) and a grid spacing of 0.2 Å, delimitates an accessible water solvent volume corresponding to 14% of the total crystal volume.

Considering the crystal packing of **UC4T** molecules only (removing the solvent molecules from the structural model) the solvent accessible volumes of the two crystal forms (calculated with a solvent probe radius of 1.2 Å and a grid spacing of 0.2 Å) are quite close (38.5 and 42.0% of the crystal volume for α and β forms, respectively). However, by including in the structural model the more strongly coordinated solvent molecules H-bonded to ureido groups, the solvent accessible volumes decrease to 6.4 and 29.1% for α and β forms, respectively. On the other hand, with the complete structural models, which includes the solvent molecules entrapped in packing cavities, the solvent accessible volumes shrink to 0.6 and 16.1% for α and β forms, respectively. The residual accessible solvent volume observed in the α form corresponds to spherical cavities of 12.16 $Å^3$ located in the middle of the calix cups (Figure 2.18). These spherical cavities are present also in the β form together with the solvent channels.

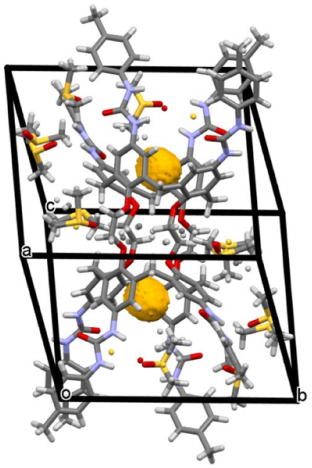

Figure 2.18. Solvent cavities observed in the α form of **UC4T**. The solvent contact surface, calculated with a solvent probe radius of 1.2 Å and a grid spacing of 0.2 Å, delimitates two symmetric spherical cavities of 12.16 Å^3 each located in the middle of the calix cups. They correspond to 0.6% of the total crystal volume.

Although a close parallel between liquid and solid state is impossible, X-ray data on the ability of **UC4T** to adopt different conformations depending on the extent and type of interactions with polar solvent molecules (*i.e.,* DMSO and H_2O) provide a clue for a reinterpretation of the NMR findings discussed earlier and more specifically on the asymmetric spectral pattern observed in Figure 2.4. It is reasonable to assume that in a 98:2 $CDCl_3$/DMSO-d_6 solution polar species, such as dimethylsulfoxide and adventitious water molecules, are able to stabilize an asymmetric conformation of **UC4T**, by efficiently interacting –via hydrogen-bonds– with the ureido groups. For instance, the average C_s symmetry imposed to a single cavity by the ATA extended arrangement of the ethylene bridges (Figure 2.19) would no longer exist if any of the ureido groups were to bind a water or a DMSO molecule via strong H-bonds. This would result in a complete loss of symmetry and would, as a result, give rise to the complex ^{1}H NMR spectrum observed in our study (Figure 2.4).

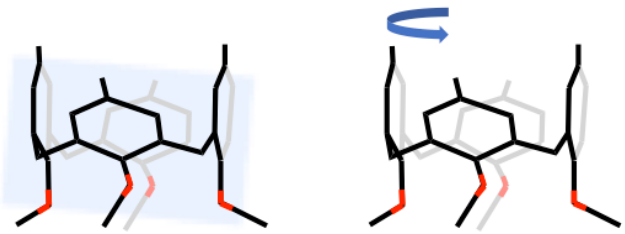

Figure 2.19. Presence of an average σ_h plane bisecting a single **UC4T** cavity in C_s symmetry (left); the loss of any symmetry element following non-covalent oriented interactions with DMSO or H_2O molecules (right).

On the other hand, In the presence of a higher concentration of polar solvent molecules, the dynamic interaction with “bulk” DMSO favours the more flexible and symmetric structure with calixarene cups displaying C_{2v} conformations.

In conclusion, the first symmetrically-substituted octaureido-calix[4]tube derivative (**UC4T**) showing in solution a stable solvent-dependent asymmetric conformation was obtained. The structure was confirmed also by X-ray crystal analysis, which showed the ability of **UC4T** to adopt different conformations in the solid state (α or β form), depending on the extent of interactions with polar solvent molecules (*i.e.,* DMSO and H_2O). These findings, alongside with the NMR data in solution indicate that in a 98:2 $CDCl_3$/DMSO-d_6 solvent mixture, the formation of the desired **UC4T** (poly)capsular assembly is likely prevented by conformational constrains.

2.3 Experimental Section

2.3.1 General procedures and instrumental description

Chemicals and reagents obtained from commercial sources were used as received. Anhydrous solvents were dried according to standard methods.[27] All moisture sensitive reactions were conducted under inert atmosphere (Ar or N_2) using glassware previously dried in an oven (T > 140 °C, 12–24 h). the course of reactions was followed by thin layer chromatography (TLC) on silica gel plates with fluorescent indicator (Polygram SIL G/UV254, Fluka Analytical, Sigma-Aldrich). Compounds were revealed by UV (λ = 254 nm) or by treatment with phosphomolybdic acid hydrate (5% in EtOH, w/v). Column chromatography was performed using silica gel (230–400 mesh, Kiesegel 60 Merck) as stationary phase. The extracted organic phases were dried on $MgSO_4$ and evaporated under reduced pressure using a rotary evaporator. Melting points were determined on a Kofler hot stage apparatus and are uncorrected. ^1H and ^{13}C NMR spectra were recorded on a VNMRs 500 Varian spectrometer at 298 K where not specified, at 500 and 125 MHz respectively. Chemical shifts are reported in ppm and are referenced to the residual solvent used ($CDCl_3$: δ_H 7.26 and δ_C 77.0 ppm; DMSO-d_6: δ_H 2.50 and δ_C 39.5 ppm). Chemical shifts (δ) are reported in ppm and coupling constants (J) are reported in Hz. Diffusion Ordered NMR SpectroscopY (DOSY), COSY, NOESY and ROESY studies were performed with a pulse-field gradient probe. DOSY spectra were recorded at 298 K using a Doneshot (DgcsteSl_cc) pulse sequence. Experimental parameters were optimized according to the sample under investigation. Diffusion gradients were incremented in 30 steps with gradient pulse amplitudes varying from 1.6 to 50 gauss/cm, the number of transients acquired for each increment ranging from 16 to 128, with a diffusion gradient length of 2–4 ms and diffusion delays in the 150–200 ms range. All measurements were performed in triplicate and the reported values are the mean ± standard deviation of the mean. 2D NOESY experiments were carried out using 200–400 ms mixing times, 16 transients for each increment (512 in total) and a relaxation time of 3 s.
^1H NMR peak assignments follow from 2D-COSY and C-H correlation experiments (HSQC, HMQC, HMBC). Two-dimensional adiabatic ROESY spectra in $CDCl_3$ and DMSO-d_6 were acquired with a standard pulse sequence over a sweep width of 6510 Hz using 2048 data points in the t_2 dimension and 1024 or 2048 increments in the t_1 dimension for different mixing times of τ_m = 400 and 200 ms at 298 K. A total of 32 scans were collected for each t_1 increment with an acquisition time of 0.2137 s followed by an additional relaxation delay of 2.5 s. When necessary, reactions were carried out under an argon atmosphere.

Mass spectra were acquired on a Q-Exactive Plus Orbitrap mass spectrometer (ThermoScientific - San Jose, USA) equipped with a heated electrospray ion source (HESI-II). Samples were dissolved in either CH_3OH or DMSO and solutions of appropriate concentrations were analyzed by flow injection mass spectrometry (FIA-MS). Sample solutions were injected, by means of an automated syringe, into an eluent flow of methanol, generated by a Vanquish UHPLC system (Thermo Fisher Scientific) and directly sent to the spectrometer at a flow rate of 100 μL/min. Prior to each series of acquisitions, the mass spectrometer was externally calibrated with the Negative Ion Calibration Solution (Thermo Fisher Scientific). The following operating parameters were used: resolution 140,000; sheath and auxiliary gas flow rate were 35 and 10 respectively; spray voltage 3.0 kV; capillary temperature 250 ° C; S-lens RF level 100. The autogain control (AGC) was optimized at 1e6 with a maximum injection time (maxIT) of 250 ms. Full scan data were processed with Xcalibur version 4.1 (ThermoScientific - San Jose, USA). High resolution mass spectra were acquired in negative ion mode and the identity of each analyte was confirmed by comparing the experimental data with both their theoretical molecular weight and their expected isotopic pattern.

Spectrometric analyses were performed by Dr Aldo Profumo, IRCCS Policlinico San Martino, National Institute for Cancer Research, Genova.

X-ray crystal analysis was carried out by Prof. Neil Hickey and Prof. Silvano Geremia, University of Trieste.

2.3.2 Synthetic procedures

Octatolylurea-calix[4]tube (**UC4T**): *p*-Tolylisocyanate (188 μL; 1,49 mmol) was added to a solution of **AC4T** (100 mg; 93 μmol) in anhydrous DMSO. After stirring for three hours at room temperature, acetone was added, the precipitate collected by suction filtration and suspended in refluxing acetone for 1h. **UC4T** was finally obtained as a white powder (120 mg; 60% yield). ^{1}H NMR (DMSO-d_6) δ 8.48 (s, 4H, NH), 8.46 (s, 4H, NH), 8.09 (s, 4H, NH), 8.00 (s, 4H, NH), 7.34 (d, J = 8 .1 Hz, tolyl, 8H), 7.26 (s, 8H, ArH), 7.14 (d, J = 8.1 Hz, tolyl, 8H), 7.07 (d, J = 8.1 Hz, tolyl, 8H), 6.99 (d, J = 8.1 Hz, tolyl, 8H), 6.63 (s, 8H, ArH), 5.08 (s, OCH_2, 8H), 4.53 (d, J = 12.2 Hz, $ArCH_2Ar$, 8H), 4.31 (s, OCH_2, 8H), 3.29 (d, J = 12.2 Hz, $ArCH_2Ar$, 8H), 2.23 (s, CH_3, 12H) and 2.18 (s, CH_3, 12H) ppm; ^{13}C NMR (DMSO-d_6) δ 153.3, 152.7, 152.3, 150.5, 137.3, 137.1, 135.4, 134.0, 133.3, 132.7, 130.4, 129.1, 118.9, 118.3, 118.05, 72. 9, 31.8, 20.3 ppm. HRMS (ESI/Orbitrap) m/z: $[M–H]^{2–}$ Calcd for $C_{128}H_{120}N_{16}O_{16}$, 1067.4455; Found, 1067.4481.

2.3.3 Single-crystal structure determination of α and β forms of UC4T

Single crystals suitable for X-ray investigation were obtained by slow evaporation of DMSO/chloroform solution obtained by dissolving 4 mg of **UC4T** in 20 μL in DMSO anhydrous to which was successively added 980 μL of chloroform. Two different crystal forms (α and β) were obtained from two different crystallization trials, one in which the DMSO solution contained KI (with a resulting K^+/**UC4T** molar ratio of 1.2) and one in which it contained $BaCl_2 \cdot 2H_2O$ (with a resulting Ba^{2+}/**UC4T** molar ratio of 1.2).

Data collection was carried out at the XRD1 beamline of the Elettra synchrotron (Trieste, Italy), employing the rotating-crystal method with a Dectris Pilatus 2M area detector. Single crystals were dipped in paratone cryoprotectant, mounted on a loop and flash-frozen under a nitrogen stream at a 100 K. Diffraction data were indexed and integrated using the XDS package,[28] while scaling was carried out with XSCALE.[29] Structures was solved using the SHELXT program[30] and refinement was performed with SHELXL-18/3,[31] operating through the WinGX GUI,[32] by full-matrix least-squares (FMLS) methods on F^2.

Non-hydrogen atoms were anisotropically refined with exclusion of atoms with a low occupancy factor, which were refined isotropically. Hydrogen atoms were added at the calculated positions and refined using the riding model. Due to the low reflection/parameters ratio, the β form was refined using the SIMU and ISOR cards together with several geometrical constraints (aromatic rings) and restraints (DMSO solvent molecules). Crystallographic data and refinement details are reported in **Table 2.2**.

The asymmetric unit of the triclinic α form (P-1 space group) contains a half **UC4T** molecule located on a centre of crystallographic symmetry, with 4.6 co-crystallized DMSO molecules located in 6 different crystallographic independent sites with partial occupancy factors (Figure 1a). Three of these solvent molecules also show a two-position disorder. Furthermore, two dioxyethylene bridging moieties of **UC4T** related by a centre of symmetry show two-position disorder.

The monoclinic β form (*C* 2/c space group) also shows the **UC4T** molecules located on crystallographic inversion centres. One terminal aryl group was found disordered over two almost orthogonal positions. Three different sites of co-crystallized DMSO molecules (for a total of 1.8 molecules) and one water molecule were modelled in the asymmetric unit of the electron density maps (Figure 1b). This crystal form is characterized by large solvent channels (15% of cell volume) partially filled by highly disordered solvent molecules. The diffused residual electron density present in these channels was corrected by the SQUEEZE procedure.[33] In these channels a total of 678 electrons per unit cell were found. This

corresponds to about two further disordered DMSO molecules per asymmetric unit.

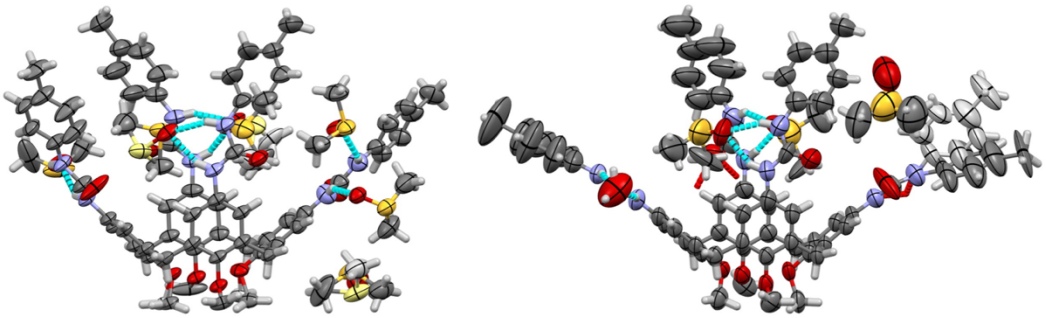

α β

Figure 2.20. Asymmetric unit with anisotropic ellipsoid representation of non-H atoms of the α and β forms of **UC4T**. Ellipsoids are shown at the 50% probability level. The atom species are in CPK colours with alternative positions of disordered groups in paler colours. H-bonds are evidenced with dashed lines.

Table 2.2. Crystal data and structure refinement for α and β forms of **UC4T**

	α	β
Empirical formula	C_{128} H_{120} N_{16} O_{16}, 9.2(C_2 H_6 O S)	C_{128} H_{120} N_{16} O_{16}, 7.6(C_2 H_6 O S), 2(H_2O)
Formula weight	2857.17	2768.19
Temperature (K)	100(2)	100(2)
Wavelength (Å)	0.7	1.0
Crystal system	Triclinic	Monoclinic
Space group	*P* -1	*C* 2/c
Unit cell dimensions (Å, °)	*a* = 12.729(9) *b* = 15.650(3) *c* = 19.849(5) α = 91.255(5) β = 91.14(3) γ = 103.68(3)	*a* = 40.093(14) *b* = 22.414(5) *c* = 18.799(3) α = 90 β = 107.521(12) γ = 90
Volume (Å^3)	3840(3)	16110(7)
Z	1	4
ρ_{calcd} (g/cm^3)	1.236	1.141
μ (mm^{-1})	0.193	0.393
F(000)	1514	5869
Reflections collected	81832	16433
Independent reflections	15039	6028
Data / restraints / parameters	15039 / 0 / 1019	6028 / 1336 / 794
GooF	1.007	1.104
Final *R* indices [I>2σ(I)]	R_1 = 0.1228 wR_2 = 0.3307	R_1 = 0.1409 wR_2 = 0.3645
R indices (all data)	R_1 = 0.1570 wR_2 = 0.3693	R_1 = 0.1539 wR_2 = 0.3809
CCDC code	######	######

2.4 References

[1] P. Lhoták, in Anion Sensing, *ed. I. Stibor, Springer Berlin Heidelberg, Berlin, Heidelberg*, **2005**, 65.
[2] Kim J.S., Quang D.T., *Chem. Rev.*, **2007**, *107*, 3780.
[3] Baldini L., Casnati A., Sansone F., Ungaro R., *Chem. Soc. Rev.*, **2007**, *36*, 254.Kubo Y., Maeda S.Y., Tokita S., Kubo M., *Nature*, **1996**, *382*, 522.
[4] Kubo Y., Maeda S.Y., Tokita S., Kubo M., *Nature*, **1996**, *382*, 522.
[5] (a) Guo D.S., Liu Y., *Chem. Soc. Rev.*, **2012**, *41*, 5907; (b) Sun R., Xue C., Ma X., Gao M., Tian H., Li Q., *J. Am. Chem. Soc.*, **2013**, *135*, 5990.Prins L.J., Timmerman P., Reinhoudt D.N., *Pure Appl. Chem.,* **1998**, *70*, 1459.
[6] Prins L.J., Timmerman P., Reinhoudt D.N., *Pure Appl. Chem.,* **1998**, *70*, 1459.
[7] Wei A., *Chem. Commun.*, **2006**, 1581.
[8] (a) Pedersen C.J., *J. Am. Chem. Soc.*, **1967**, *89*, 2495; (b) Pedersen C.J., *J. Am. Chem. Soc.*, **1967**, *89*, 7017.
[9] (a) Yamamoto H., Shinkai S., *Chem Lett,* **1994**, 1115; (b) Casnati A., Pochini A., Ungaro R., Bocchi C., Ugozzoli F., Egberink R.J.M., Struijk H., Lugtenberg R., de Jong F., Reinhoudt D.N., *Chem. Eur. J.*, **1996**, *2*, 43; (c) Casnati A., Pochini A., Ungaro R., Ugozzoli F., Arnaud F., Fanni S., Schwing M.J., Egberink R.J.M., de Jong F., Reinhoudt D.N., *J. Am. Chem. Soc.*, **1995**, *117*, 2767; (d) Arnaud-Neu F., Arnecke R., Böhmer V., Fanni S., Gordon J.L.M., Schwing-Weill M.J., Vogt W., *J. Chem Soc., Perkin Trans.*, **1996**, *2*, 1855.
[10] Ohseto F., Shinkai S., *J. Chem. Soc., Perkin Trans.*, **1995**, 1103.
[11] Ulrich G., Ziessel R., *Tetrahedron Lett.*, **1994**, *35*, 6299; (b) Ulrich G., Ziessel R., Manet I., Guardigli M., Sabbatini N., Fraternali F., Wipff G., *Chem. Eur. J.*, **1997**, *3*, 1815.
[12] Schmitt,P.; Beer P.D.; Drew M.G.B.; Sheen P.D.; *Angew. Chem. Int. Ed. Engl.*, **1997**, *36*, 1840.
[13] Matthews S.E., Felix V., Drew M.G.B., Beer P.D., *Org. Biomol. Chem.*, **2003**, *1*, 1232.
[14] Matthews S.E., Schmitt P., Felix V., Drew M.G.B., Beer P.D., *J. Am. Chem. Soc.*, **2002**, *124*, 1341.
[15] Webber P.R.A., Cowley A., Drew M.G.B., Beer P.D., *Chem. Eur. J.*, **2003**, *9*, 2439.
[16] Webber P.R.A., Beer P.D., *Dalton Trans.*, **2003**, 2249.
[17] Khomich E., Kashapov M., Vatsouro I., Shokova E., Kovalev V., *Org. Biomol. Chem.*, **2006**, *4*, 1555.
[18] Puchnin K., Cheshkov D., Zaikin P., Vatsouro I., Kovalev V., *New J. Chem.*, **2013**, *37*, 416.
[19] Gaeta M., Rodolico E. Fragalà, M. E., Pappalardo A., Pisagatti I., Gattuso G., Notti A., Parisi M.F., Purrello R., D'Urso A., *Molecules*, **2021**, *26*, 704.
[20] (a) Notti A., Pisagatti I., Nastasi F., Patanè S., Parisi M.F., Gattuso G., *J. Org. Chem.*, **2021**, *86*, 1676; (b) Manganaro N., Pisagatti I., Notti A., Pappalardo A., Patanè S., Micali N., Villari V., Parisi M.F., Gattuso G., *Chem. Eur. J.*, **2018**, *24*, 1097.
[21] Castellano R.K., Nuckolls C., Eichhorn S.H., Wood M.R., Lovinger A.J., Rebek J. Jr., *Angew. Chem., Int. Ed. Engl.*, **1999**, *38*, 2603.
[22] (a) Mogck O., Böhmer V., Vogt W., *Tetrahedron*, **1996**, *52*, 8489; (b) Pop A., Vysotsky M.O., Saadioui M., Böhmer V., *Chem. Commun.*, **2003**, 1124; (c) Broda F., Vysotsky M.O., Böhmer V., Thondorf I., *Org. Biomol. Chem.*, **2006**, *4*, 2424.
[23] Makha M., Nichols P.J., Hardie M.J., Raston C.L., *J. Chem. Soc., Perkin Trans 1*, **2002**, 354.
[24] (a) Buhdka J., Lhotak P., Stibor I., Michlova V.J., Sykova, J., Cisarova I., *Tetrahedron Lett.*, **2002**, *43*, 2857; (b) Puchnin K., Zaikin P., Cheshkov D., Vatsouro I., Kovalev V., *Chem. Eur. J.*, **2012**, *18*, 10954.
[25] Vysotsky M.O., Thondorfb I., Böhmer V., *Chem. Commun.*, **2001**, 1890.
[26] Mogck O., Böhmer V., Vogt W., *Tetrahedron*, **1996**, *52*, 25, 8489.
[27] Armarego W.L.F., *Purification of Laboratory Chemicals – Eighth Edition*, Butterworth-Heinemann (Elsevier), **2017**.
[28] Kabsch W., *Acta Crystallogr. Sect. D Biol. Crystallogr.*, **2010**, *66*, 125.
[29] Kabsch W., *Acta Crystallogr. Sect. D Biol. Crystallogr.*, **2010**, *66*, 133.
[30] Sheldrick G.M., *Acta Crystallogr.*, **2015**, *A71*, 3.
[31] Sheldrick G.M., *Acta Crystallogr.*, **2015**, *C71*, 3.
[32] Farrugia L.J., *J. Appl. Crystallogr.*, **2012**, *45*, 849.
[33] Spek A.L., *Acta Crystallogr. Sect. C*, **2015**, *71*, 9.

CHAPTER 3

3.1 Pillar[n]arene-based functional polymers

Functional polymers are defined as polymers with advanced mechanical, optical and/or electronic properties.[1] The properties of these materials are determined by the presence of additional functional groups other than those incorporated in the polymer chain. They combine the advantages of traditional polymers (ease of synthesis, processability and mechanical properties) with the characteristics attributed by the additional functional groups. In some cases, polymer chains can assemble into supramolecular aggregates. When the formation, or dissociation, of these assemblies is caused by a chemical or physical stimulus, the polymer takes on smart characteristics. Among other methods, it is possible to obtain this type of material using supramolecular cross-linking. The reversibility of non-covalent (host-guest) interactions has made these types of derivatives suitable for the development of self-healing and self-diagnostic materials.[2]

Two different synthetic strategies can be used to produce these materials. One involves the covalent anchoring of host and guest subunits to a preformed polymer matrix, while the other relies on the formation of polymerizable host and guest monomers to form co-polymers. In this context, macrocyclic derivatives (cyclodextrins, [3] cucurbit[*n*]urils, [4] resorcin[*n*]arene cavitands[5] and calix[*n*]arenes[6]) have already been used as functional monomers.

As mentioned earlier, due to the rigid electron-rich tubular structure of their cavity and the regular arrangement of alkoxy functionalizations, pillar[*n*]arenes have been used as monomer units for the development of supramolecular polymers[7,8,9,10] and various advanced functional materials. [11] Even more, recent studies have focused on the anchoring of pillar[*n*]arenes to polymeric matrices in order to obtain multi-responsive systems.[12]

In the following chapter is described the synthesis of two pillar[5]arene derivatives **QP5$_{C10}$** and **QP5$_{C4}$**, originally designed as potential host monomer for the development of supramolecular optically-responsive elastomers, but later studied (*i.e.*, **QP5$_{C10}$**) just as solvent-sensitive pseudo[1]rotaxane systems.

3.2 Synthesis and solution properties of ω-alkenyl pillar[5]arenes

Pisagatti *et al.*[13] not long ago have developed a reliable quartz-supported pillararene-based optical device for the sensing of "transparent" analytes. In particular, based on the known affinity of pillar[5]arenes towards linear (di)amines –both as such[14] and in the protonated[15] form– they synthesized a new pillararene-based sensing agent (**QP5**) for the detection of UV-inactive or dansyl-derivatized linear (di)amines and covalently grafted it –via a 7-chloro-4-quinolylazo moiety– to a silylated quartz substrate.

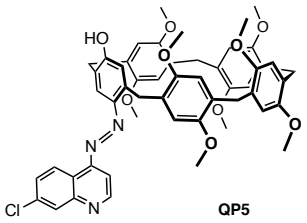

QP5

On a parallel ground, inspired by the work of Dalcanale and co-workers[16] on the use of a tetraphosphonato cavitand and a pyrene-containing *N*-methylpyridinium guest as active luminescent component for the preparation of a self-diagnostic elastomers, we reasoned that **QP5** could easy be transformed into a suitable polymerizable host component. A useful self-diagnostic supramolecular system should exhibit no fluorescence (OFF) when host and guest are associated but a detectable fluorescence emission (ON) of the guest when the host-guest complex dissociates allowing, in this way, the detection of a crack/fracture or an area of high strain (Figure 3.1). If poly(dimethylsiloxane) (PDMS) elastomer was to be used as the matrix, both the guest and the host should contain a terminal double bond, for cross-links purpose, and such alkenyl chains have to be long enough to allow sufficient conformational flexibility to the complex, thus avoiding its mechanical dissociation during the curing of the matrix, making the complex soluble and stable in the PDMS matrix.

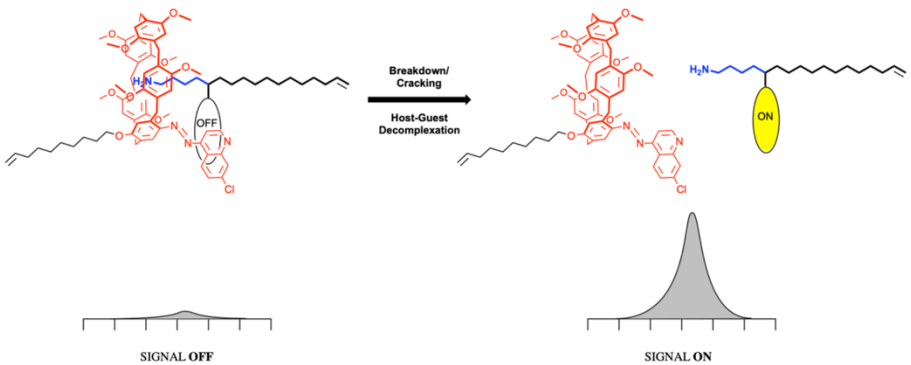

Figure 3.1. Figurative representation of how self-diagnostic supramolecular system should work.

Using as a starting point the evidence that the dansyl-cadaverine emission is progressively quenched by the addition of increasing amounts of pillar[5]arene host **QP5** (Figure 3.2), the novel pillar[5]arene **QP5$_{C10}$** and the dansyl-lysine ester **DL$_{C10}$** become the initial synthetic targets of the studies described in this chapter.

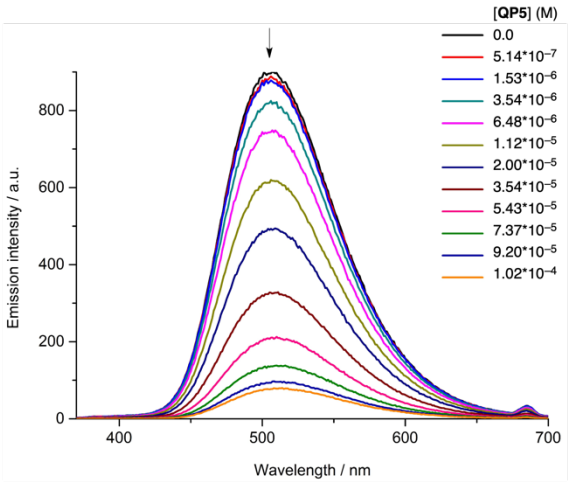

Figure 3.2. Emission titration spectra (λ_{exc} = 340 nm) of a tetrachloroethane (TCE) solution of [dansyl-cadaverine] = 9.9 × 10^{-6} M upon addition of increasing amounts of **QP5**.

Pillar[5]arene **QP5$_{C10}$** was synthesized from the known[13] hydroxy-derivative **QP5** by simple treatment with 9-decen-1-tosylate in the presence of potassium carbonate (Scheme 3.1).

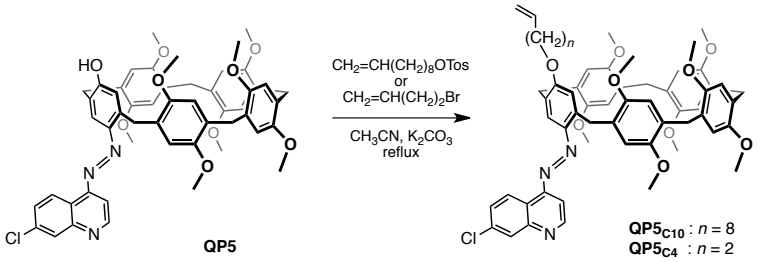

Scheme 3.1. Syntheses of pillar[5]arenes **QP5$_{C10}$** and **QP5$_{C4}$**.

Lysine was targeted as a potential precursor for the synthesis of a fluorogenic guest complementary to pillararene **QP5$_{C10}$** on the basis of its structural similarity to cadaverine [$H_2N(CH_2)_4CH(CO_2H)NH_2$) *vs.* $H_2N(CH_2)_5NH_2$] and its additional potential to undergo tripodal functionalization. As shown in Scheme 3.2 we introduced a dansyl group on the α-amino group, a sufficiently long ω-alkenyl chain (as an ester group) on the carboxyl group while we left the ε-amino moiety unaltered.

Dansyl groups have been widely employed as labelling agents of amines,[17] amino acids and peptides for detection purposes.[18] This fluorophore –owing to its high fluorescence quantum yields, large Stokes shifts and emission properties, strongly dependent from the surrounding

environment– has also been used for the preparation of a variety of macrocyclic chemosensors.[19,20,21] The terminal double bond was deemed necessary in view of a later incorporation of the host-guest complex into a given polymeric matrix[16] and, in this respect, a ten-carbon atom chain, was judged long enough to allow an easy anchoring onto the matrix and a sufficient conformational flexibility during the following complexation/decomplexation process between host and guest. On the other hand, the 4-aminobutyl moiety, as such[13,14] or on its protonated[15] form, was identified as a structural element likely recognized by the pillar[5]arene cavity of the host molecule.

The dec-9-en-1-yl ester of N_α-dansyl-L-lysine (**DL$_{C10}$**) was synthesized in four steps from L-Lys-OH (Scheme 3.2). Accordingly, treatment of lysine with 2-(*tert*-butoxycarbonyloxyimino)-2-phenylacetonitrile (BOC-ON), under controlled conditions (pH = 10.8–11.2),[22] gave the corresponding ε-protected derivative **1**, which was first reacted[23] with dansyl chloride to provide the N_α-dansyl-N_ε-Boc-Lys-OH intermediate **2** and then converted to the corresponding ester derivative **3a**, upon treatment with 9-decen-1-ol, in the presence of 1-hydroxybenzotriazole (HOBt) and 1-ethyl-3-(3′-dimethylaminopropyl)carbodiimide (EDCI).[24] Removal of the Boc-protecting group, under standard acidic conditions (trifluoroacetic acid (TFA) in CH_2Cl_2)[25] from the ε-amino group gave the desired dansylated amino ester.

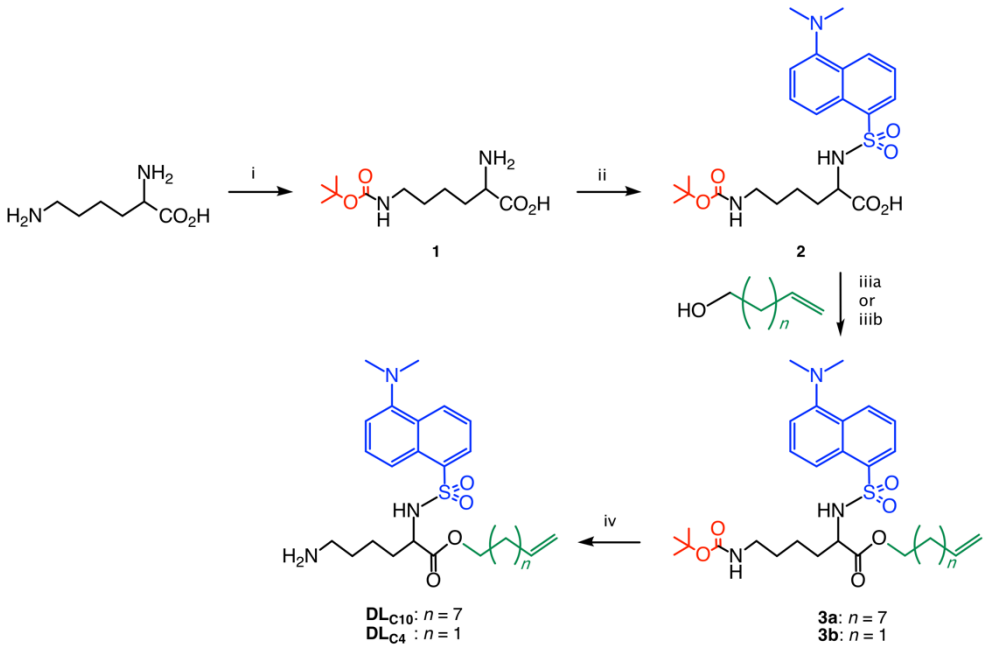

Scheme 3.2. Syntheses of the fluorogenic lysine derivatives **DL$_{C10}$** and **DL$_{C4}$**. Reagents and conditions: i) BOC-ON, H_2O/Dioxane 1:1, pH 11, r.t., 24 h; ii) dansyl-Cl, H_2O/Dioxane 1:1, pH 9.5, r.t., 20 h; iiia) *n* = 1, DCC/DMAP,[26] CH_2Cl_2, r.t., 3 h; iiib) *n* = 7, HOBt/EDCI, CH_2Cl_2, r.t., 24 h; iv) CF_3CO_2H/CH_2Cl_2, r.t., 1 h.

The affinity between **DL$_{C10}$** and **QP5$_{C10}$** was assessed by means of ^{1}H NMR spectroscopy (Figure 3.2), in deuterated 1,1,2,2-tetrachloroethane (TCE-d_2). **QP5$_{C10}$** displays a spectrum characterized, among others, by a set of seven equally-intense resonances in the high-field region (δ –1.2 to 1.8 ppm), fully consistent with the inclusion of the C(2)–C(8) methylene groups of a (dec-9-en-1-yloxy)-pendant chain inside a pillar[5]arene cavity (Figure 3.3, trace a and Figure 3.4).

Subsequent additions of increasing amounts of **DL$_{C10}$** (0.5, 1, 2, 5 equiv.) to this solution did not cause any complexation-induced shifts on the pillararene resonances. The additional signals observed in traces b–e of Figure 3.2 only account for the presence of increasing concentrations of **DL$_{C10}$** being added to the original **QP5$_{C10}$** solution (trace a).

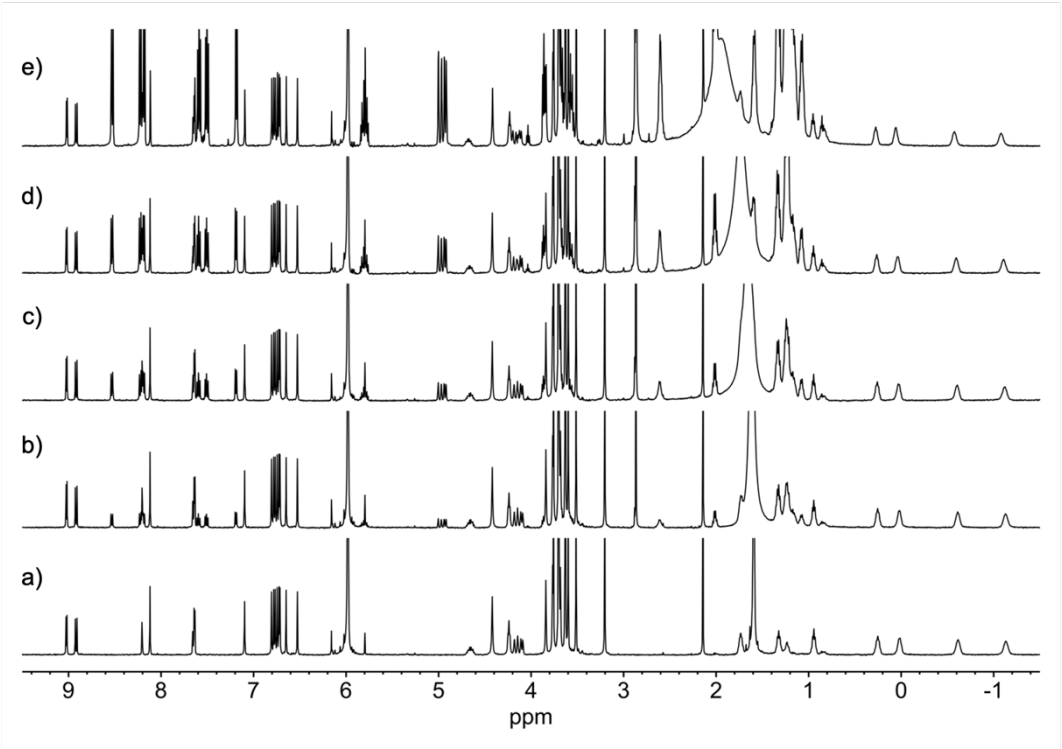

Figure 3.3. ^{1}H NMR (500 MHz, TCE-d_2, 298 K) spectra of: a) [**QP5$_{C10}$**] = 1 mM; b) [**QP5$_{C10}$**] = 1 mM and [**DL$_{C10}$**] = 0.5 mM; c) [**QP5$_{C10}$**] = [**DL$_{C10}$**] = 1 mM; d) [**QP5$_{C10}$**] = 1 mM and [**DL$_{C10}$**] = 2 mM; e) [**QP5$_{C10}$**] = 1 mM and [**DL$_{C10}$**] = 5 mM.

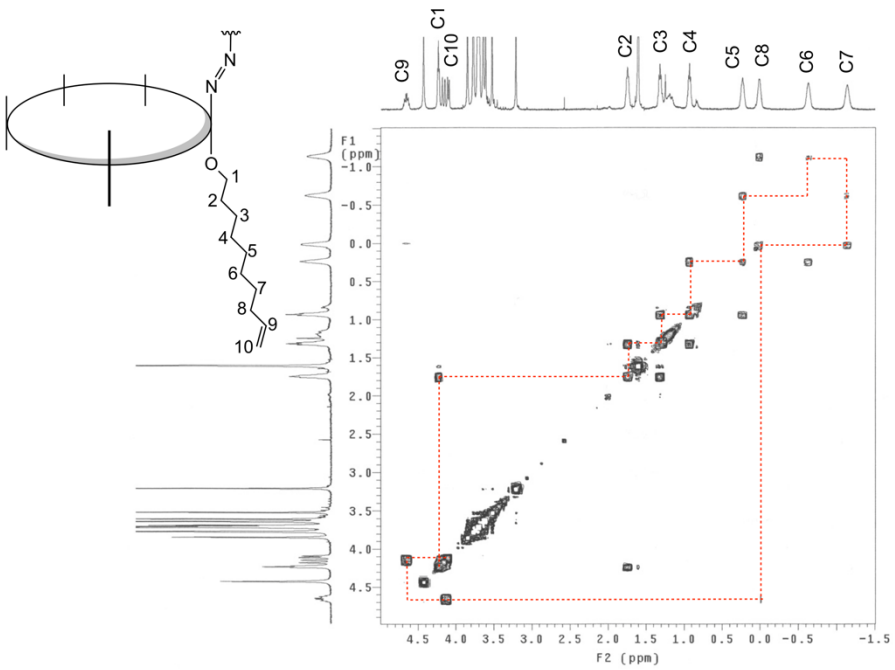

Figure 3.4. Section of the COSY spectrum (500 MHz, TCE-d_2, 298 K) of [**QP5$_{C10}$**] = 2.5 mM.

A ROESY spectrum (Figure 3.5) unambiguously confirmed the formation of an *intra*-cavity complex, by showing a number of close contacts between the hydrogen atoms of the methylene groups (C(1), C(2) and C(3)) and an aryl ring of the pillararene scaffold.

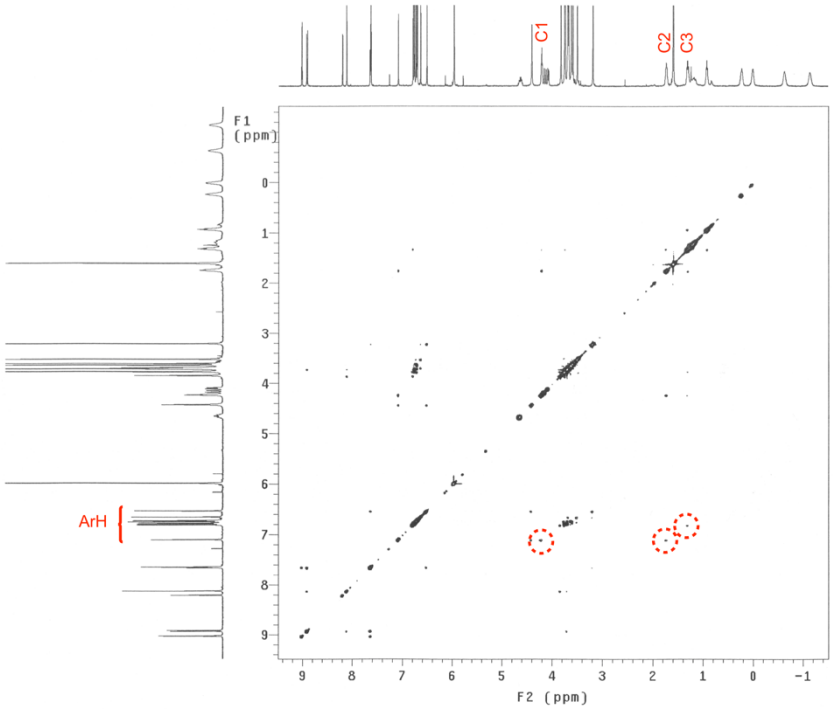

Figure 3.5. ROESY spectrum (500 MHz, TCE-d_2, 298 K) of [**QP5$_{C10}$**] = 2.5 mM.

The high-field resonances observed in Figure 3.3, may in principle arise as a result of an intramolecular inclusion process of the alkenyl moiety of a pillararene scaffold within its own

cavity (*i.e.*, self-inclusion) or an intermolecular one, between the alkenyl chain and the cavity of two different molecules. In other words, either with the formation of a pseudo[1]rotaxane structure or a head-to-tail/cyclic dimeric/oligomeric assembly (Figure 3.6). To clarify this matter, Diffusion-Ordered SpectroscopY (DOSY)[27] experiments on the model compound **QP5$_{C1}$**, available from previous studies,[13] and **QP5$_{C10}$** were carried out under the same experimental conditions (TCE-d_2, 298 K). The DOSY plots shown in Figure 3.7 demonstrate that the two macrocycles display, on average, for all their signals, diffusion coefficients (D) very similar [D_{QP5} = (1.94 ± 0.03) × 10^{-10} m^2/sec and D_{QP5C10} = (1.87 ± 0.02) × 10^{-10} m^2/sec]. This experimental evidence indicates that **QP5$_{C10}$** forms in solution a pseudo[1]rotaxane rather than a dimeric/oligomeric complex; the latter, if was present, would have most likely displayed a rather lower diffusion coefficient, because of his lager hydrodynamic radius.

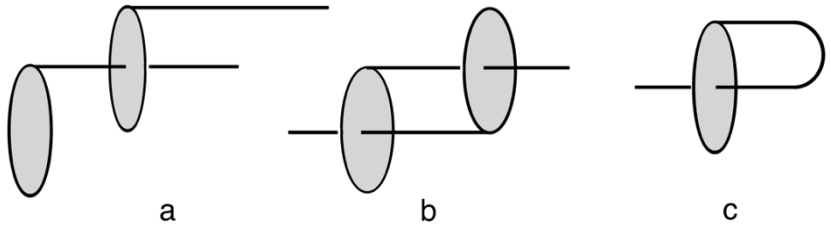

Figure 3.6. Cartoon of likely ω-alkenyl pillar[5]arene assemblies: a) linear dimer, b) daisy chain dimer and c) self-included monomer.

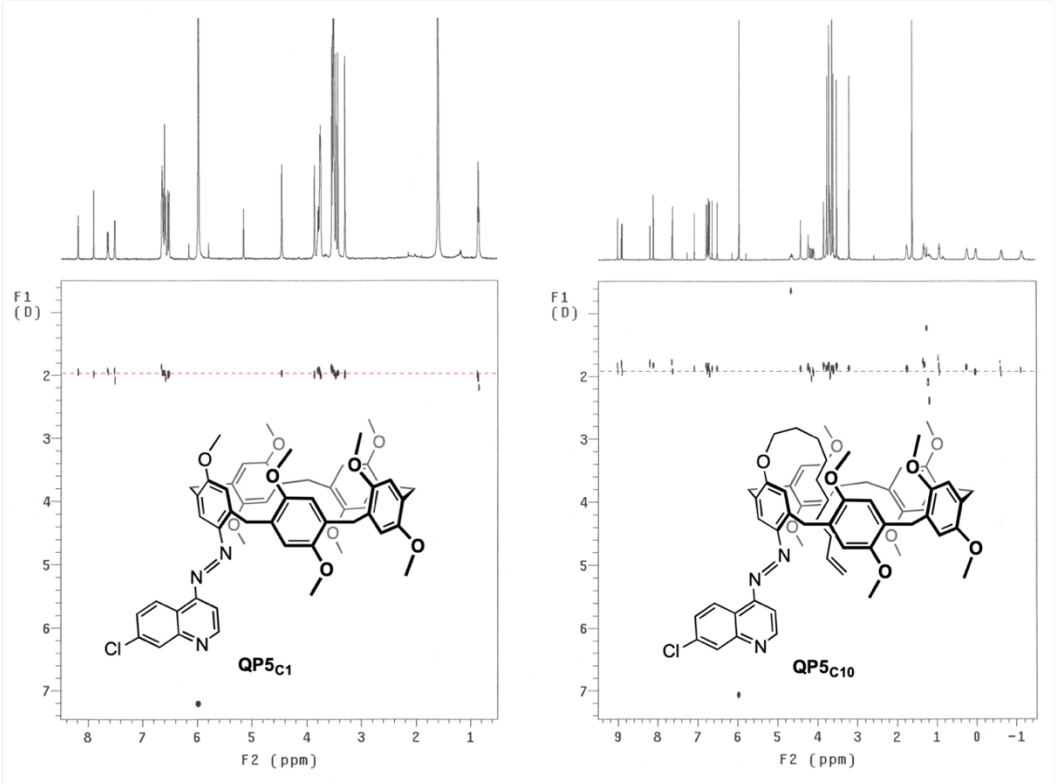

Figure 3.7. DOSY plots (500 MHz, TCE-d_2, 298 K) of **QP5$_{C1}$** and **QP5$_{C10}$**.

Tetrachloroethane plays a crucial role in the formation of the pseudo[1]rotaxane structure discussed earlier. As previously observed by Ogoshi,[28] TCE is too bulky (4.4 Å) to fit inside the cavity of a pillar[5]arene (4.7 Å)[13] (see Section 1.3, Chapter 1) and, as a result, the void inside the cavity of **QP5$_{C10}$** is filled by its own alkenyl chain. Unlike TCE, $CDCl_3$ is able to access the cavity of **QP5$_{C10}$** and in so doing displaces the pendant group out of the π-electron rich cavity (compare trace a and b of Figure 3.8).

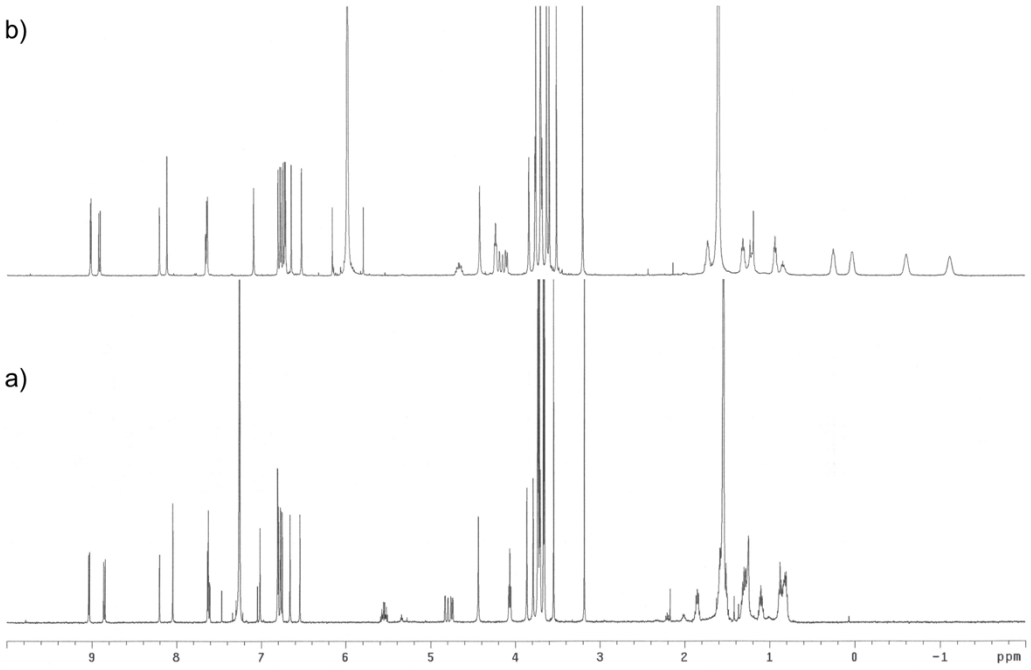

Figure 3.8. ^{1}H NMR (500 MHz, 298 K) spectra of **QP5$_{C10}$** in $CDCl_3$ and TCE-d_2, traces a and b respectively.

The solvent dependence of pillararene-based pseudo[1]rotaxane formation was first reported by Ogoshi[29] and later used in a number of occasion for the preparation of pH-responsive[30] and redox-responsive[31] supramolecular system. In another instance, the different polarities of the solvent were exploited for the separation of the threaded and included form of a stable pillar[5]arene-based pseudo[1]rotaxane.[32]

In the case under study here, the extrusion of the alkenyl chain was found to be solvent dependent. Upon addition of increasing aliquots of $CDCl_3$ (10, 20, 40, 60, 100% *v/v*) to a 1 mM TCE-d_2 solution of **QP5$_{C10}$** all the resonances of the alkenyl chain were seen to progressively shift to lower fields (Figure 3.9). This indicates that, in principle, it is possible to control the entry/exit of an alkenyl chain within the macrocycle cavity by simply varying the ratios between these two solvents. The potential of such a system is certainly vast and intriguing, ranging from the design of specific sensors for molecules capable of extruding the

chain from the cavity, up to the synthesis of molecular machines based on the controlled formation of pseudo[1]rotaxane structures.

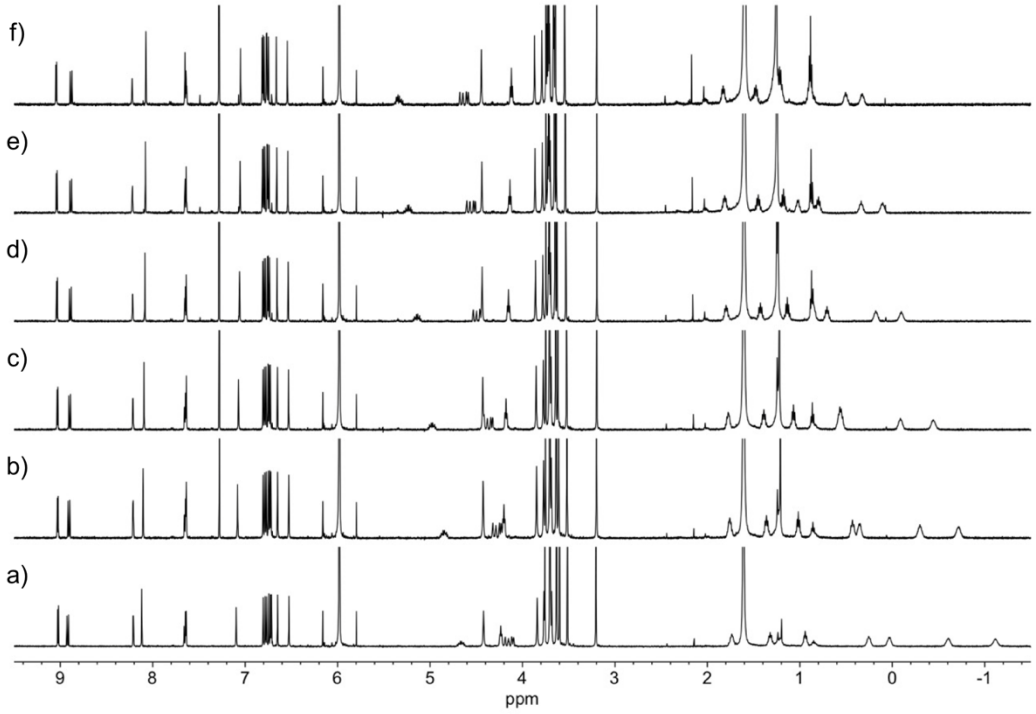

Figure 3.9. ^{1}H NMR (500 MHz, 298 K) spectra of [**QP5$_{C10}$**] = 1 mM in a) TCE-d_2; b) TCE-d_2/$CDCl_3$ 9:1; c) TCE-d_2/$CDCl_3$ 4:1; d) TCE-d_2/$CDCl_3$ 5:2 e) TCE-d_2/$CDCl_3$ 3:2 and f) TCE-d_2/$CDCl_3$ 1:1 (*v/v*).

Going back to the original target of assessing the affinity between **QP5$_{C10}$** and **DL$_{C10}$** (and to eventually test the ability of this pair to return an OFF and ON fluorescence response upon complexation and decomplexation, respectively), a ^{1}H NMR titration experiment carried out on a 1 mM $CDCl_3$ solution with increasing amounts of the lysine derivative (0.14, 0.2, 1.5, 2.0 equiv.) did not produce relevant spectral change at any given concentration (Figure 3.10), suggesting that, under these conditions, neither the 4-aminobutyl moiety nor the dec-9-ene-oxy chain of **DL$_{C10}$** or the equally-long chain present on **QP5$_{C10}$**, is able to kick out the $CDCl_3$ molecules present inside the pillararene cavity.

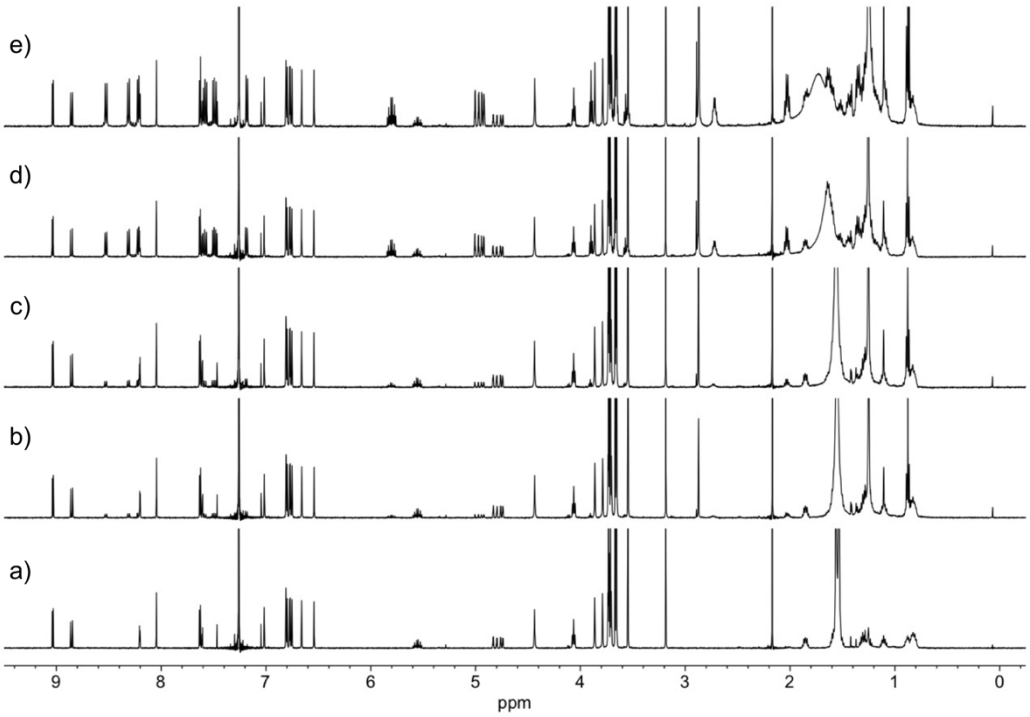

Figure 3.10. ^{1}H NMR (500 MHz, $CDCl_3$, 298 K) spectra of: a) [**QP5$_{C10}$**] = 1 mM; b) [**QP5$_{C10}$**] = 1 mM and [**DL$_{C10}$**] = 0.14 mM; c) [**QP5$_{C10}$**] = 1 mM and [**DL$_{C10}$**] = 0.2 mM; d) [**QP5$_{C10}$**] = 1 mM and [**DL$_{C10}$**] = 1.5 mM; e) [**QP5$_{C10}$**] = 1 mM and [**DL$_{C10}$**] = 2 mM.

A similar trend was also observed when either a 1:1 mixtures of TCE-d_2/$CDCl_3$, CD_3CN/CD_3OD, TCE-d_2/CD_3OD (9:1) or neat CD_2Cl_2 and CD_3CN replaced $CDCl_3$ as the titration solvent (spectra not shown). Analogously, no evidence of host-guest complex formation was detected when **QP5$_{C10}$** was titrated with increasing amounts of **DL$_{C10}$** in the protonated form (ε-$NH_3^+Cl^-$).

The findings of these titration experiments point to a strong affinity of the **QP5$_{C10}$** alkenyl chain for its own cavity in the presence of solvent too bulky to fit in. On the other hand, when the solvent is sufficiently small to be hosted inside the pillararene, neither the (dec-9-en-1-yloxy)-moiety of **QP5$_{C10}$** or **DL$_{C10}$** nor the ε-amino side-chain of the latter are recognized and bound by the pillararene.

Two structurally related analogues of **QP5$_{C10}$** and **DL$_{C10}$**, bearing a shorter alkenyl chain, namely **QP5$_{C4}$** and **DL$_{C4}$**, were then synthesized according to Schemes 3.1 and 3.2, respectively. An alkenyl residue with fewer carbon atoms was expected to prevent the host self-inclusion in one case and, possibly, favour the recognition of the lysine 4-aminobutyl moiety over a shorter (but-3-en-1-yloxy)-residue on the guest's side.

The ^{1}H NMR spectrum of a 1 mM TCE-d_2 solution of **QP5$_{C4}$** confirmed our prediction, as it did not show the phenomenon of the alkenyl chain self-inclusion previously observed for its homologue with a longer chain (Figure 3.9, trace a). No spectral changes were, however,

observed upon addition of 1 equiv. of **DL$_{C4}$** (Figure 3.11, trace b). Similarly, no host-guest interactions were detected over the course of a titration of **QP5$_{C4}$** with **DL$_{C4}$** carried out in $CDCl_3$ (Figure 3.12).

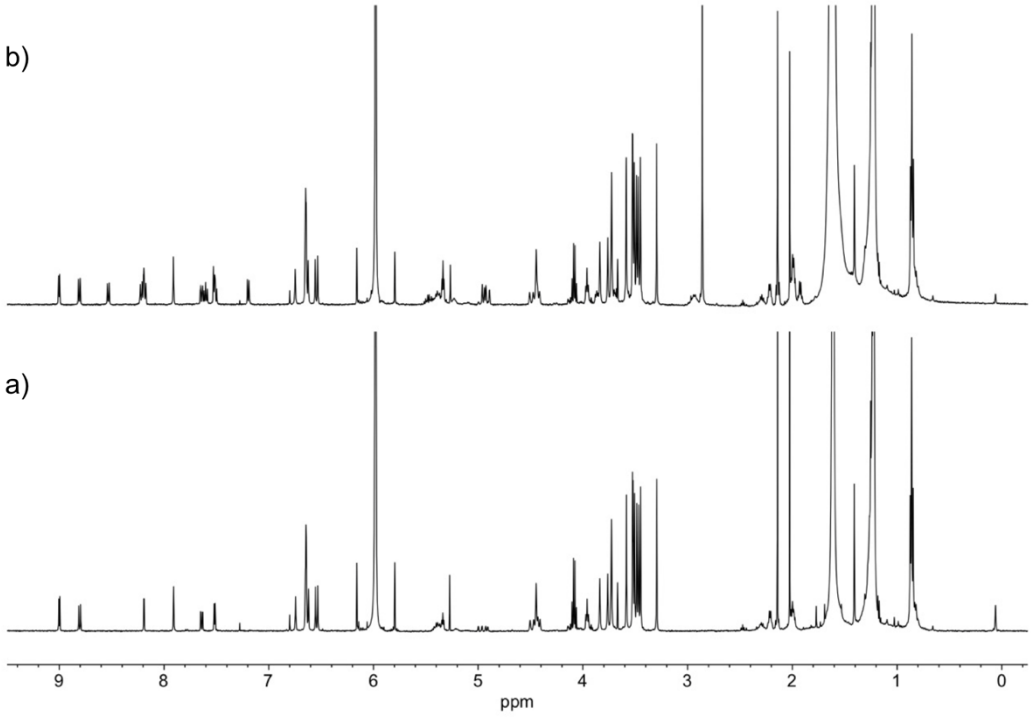

Figure 3.11. ^{1}H NMR (500 MHz, TCE-d_2, 298 K) spectra of a) [**QP5$_{C4}$**] = 1 mM and b) [**QP5$_{C4}$**] = [**DL$_{C4}$**] = 1 mM.

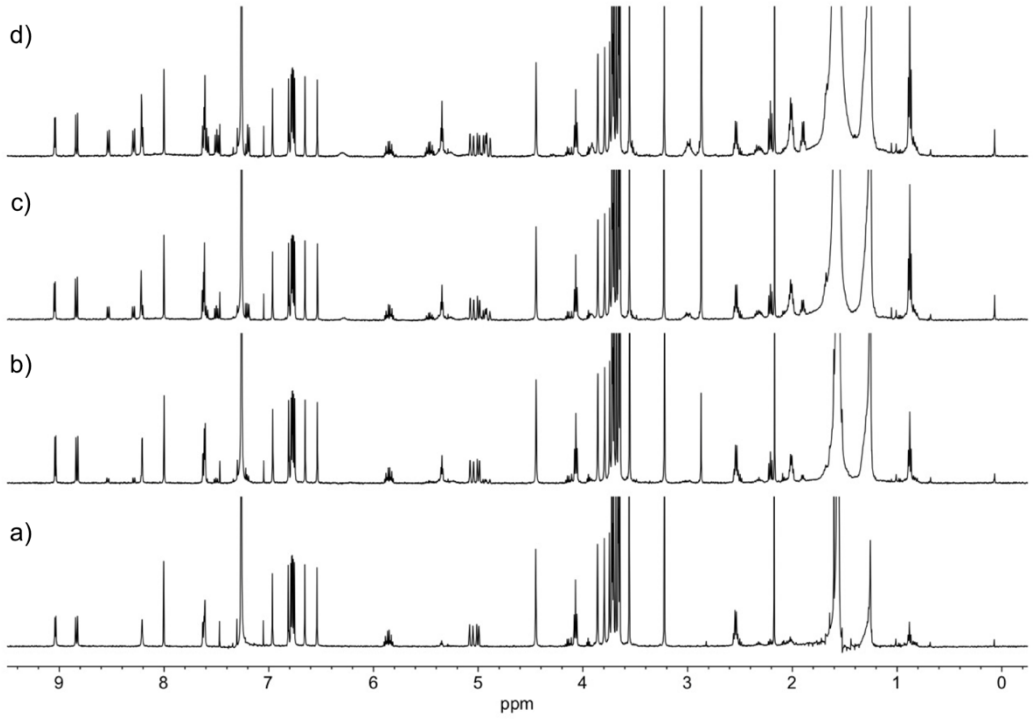

Figure 3.12. ^{1}H NMR (500 MHz, $CDCl_3$, 25 °C) spectra of: a) [**QP5$_{C4}$**] = 1 mM; b) [**QP5$_{C4}$**] = 1 mM and [**DL$_{C4}$**] = 0.25 mM; c) [**QP5$_{C4}$**] = 1 mM and [**DL$_{C4}$**] = 0.5 mM and [**QP5$_{C4}$**] = [**DL$_{C4}$**] = 1 mM.

A $CHCl_3$ spectrofluorimetric titration of $\mathbf{DL_{C10}}$ with $\mathbf{QP5_{C10}}$ (0.2, 0.6, 1, 2, 4, 6 equiv.) finally confirmed the lack of affinity between the two by showing no static quenching of the fluorescence emission up to a 1.2×10^{-6} M concentration of added pillararene (Figure 3.13).

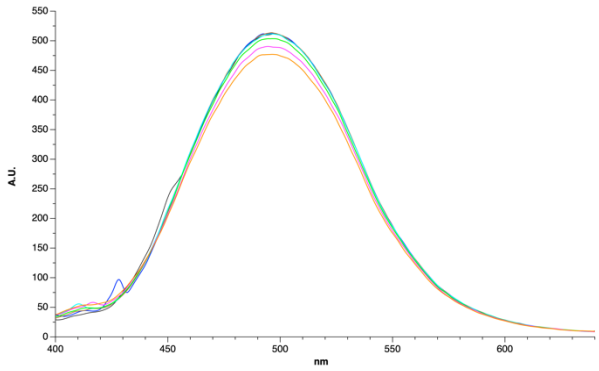

Figure 3.13. Fluorescence emission spectra at λ_{exc} = 340 nm of [$\mathbf{DL_{C10}}$] = 2×10^{-7} M (black trace) in presence of [$\mathbf{QP5_{C10}}$] = 4×10^{-8} M (blue trace); 1.2×10^{-7} M (brown trace); 2×10^{-7} M (cyan trace); 4×10^{-7} M (green trace); 8×10^{-7} M (magenta trace); 1.2×10^{-6} M (orange trace).

The unsuccessful formation of any host/guest complex between $\mathbf{DL_{C10/C4}}$ and $\mathbf{QP5_{C10/C4}}$ led us to drastically reconsider the structural feature of a new potential guest, focusing our attention onto naphthalimide derivatives. From literature studies[33] it is known that 1,8-naphthalimide derivatives (**NI**) are classical dyes/fluorophores largely used in analytical and materials chemistry as well as biochemistry because of their excellent photostability, good structural flexibility, high fluorescence quantum yield, and large Stokes shift.

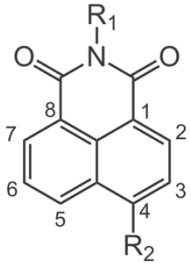

NI

The naphthalene ring acts as a π-bridge, with the R_2 (*e.g.,* –NHR, –OR) behaving as an electron-donating group and the imide moiety as a donor–π–acceptor electronic system. 1,8-naphthalimide derivatives display outstanding light and thermal stability and their fluorescence properties can be modulated by appropriately varying the substituents present at the 4-position or the imide nitrogen. Based on these characteristics, these derivatives have been widely used for the development of fluorescent chemosensors in the fields of metal ions and toxic metal ions detection, molecular recognition and imaging, in the materials chemistry

and the functional polymer area. For example, the introduction of an allyl residue directly linked to the imide function made it possible to insert this derivative within the polymer structure produced by the cross-linking of methyl methacrylate (MMA).[34] Other polymeric derivatives have been obtained by exploiting the affinity of pillararenes for naphthalimides suitably functionalized with alkylbromide substituents.[35] Water-soluble pillar[5]arene/naphthalimide host-guest complexes,[36] where the negative charge of the pillararene carboxyl substituents quench the fluorescence emission of the naphthalimide core, have also been described as optical recognition systems for non-emissive aminoacids.

Based on these considerations, we decided to prepare and test a naphthalimide derivative bearing a 6-bromohexylamino group at the 4-position and an allylic chain on the imide nitrogen as a potential guest partner for **QP5$_{C10}$**, with the idea of transferring the fluorescence properties of the resulting host-guest complex to a polymeric matrix for a later development of self-diagnostic materials.

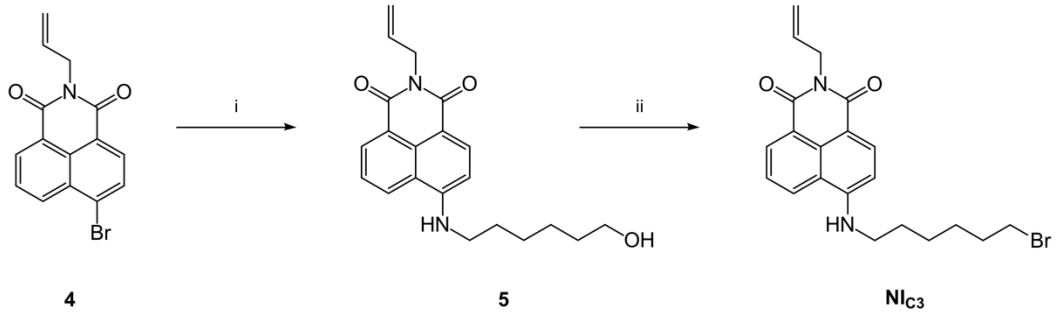

4 **5** **NI$_{C3}$**

Scheme 3.3. Synthesis of the naphthalimide guest **NI$_{C3}$**. Reagents and conditions: i) 6-amino-1-hexanol, refluxing 2-methoxyethanol, 24 h; ii) PPh_3, CBr_4 dry CH_2Cl_2, reflux, 24 h.

According to Scheme 3.3, treatment of the 4-bromo-*N*-allylnaphthalimide precursor[37] **4** with 6-aminohexanol in refluxing 2-methoxyethanol, followed by the displacement of the hydroxyl group from **5** with carbon tetrabromide in the presence of triphenylphosphine afforded derivative **NI$_{C3}$** in good yield.

Next we assessed, via standard ^{1}H NMR titration experiments, whether the 6-bromohexyl chain of **NI$_{C3}$** was recognized at all by **QP5$_{C10}$**. To this end, spectra were regularly recorded after increasing quantities of the guest (0.5, 1, 1.5 equiv.) had been added to a 1 mM $CDCl_3$ solution of the host. Unlike what seen earlier with the lysine ester derivatives, the upfield shift and broadening observed in Figure 3.14 for the resonances of **NI$_{C3}$** unambiguously revealed the inclusion of the bromoalkyl chain of the guest inside the pillararene cavity. In particular, the flattening of all the resonances relative to the guest alkyl pending group is typical for an *endo*-cavity complexation of a pillararene derivative. Minor changes were also detected for

the ArH and quinoline hydrogen atoms of **QP5$_{C10}$**, thus confirming the host-guest recognition process.

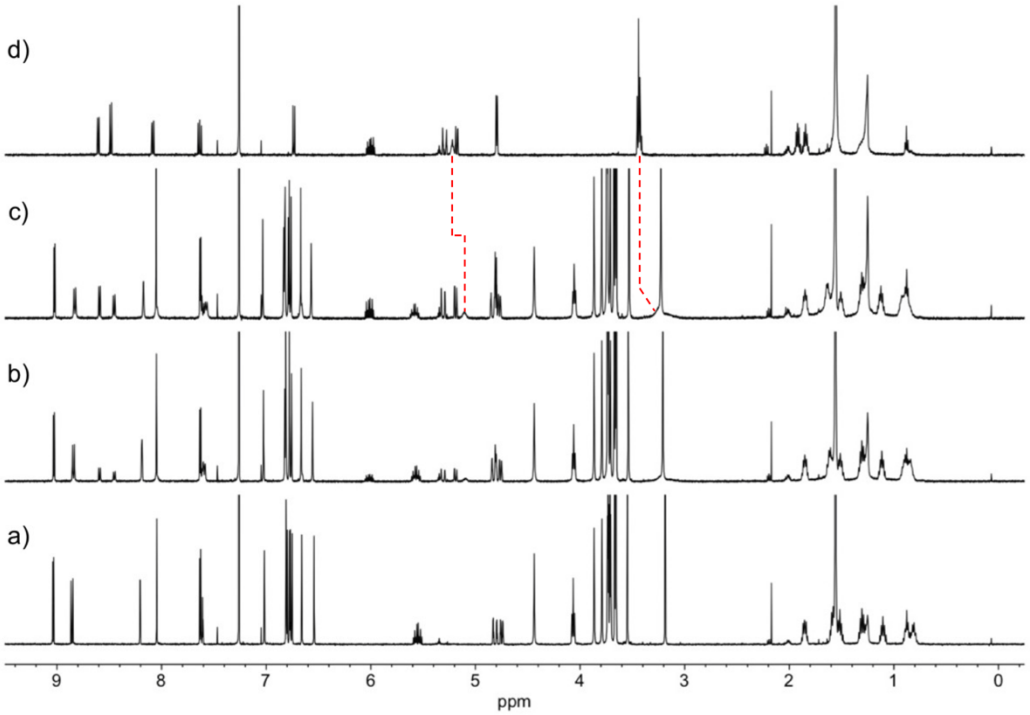

Figure 3.14. ^{1}H NMR (500 MHz, 298 K) spectra in $CDCl_3$ of a) [**QP5$_{C10}$**] = 1 mM; b) [**QP5$_{C10}$**] = 1 mM, [**NI$_{C3}$**] = 0.5 mM; c) [**QP5$_{C10}$**] = [**NI$_{C3}$**] = 1 mM; d) [**NI$_{C3}$**] = 1 mM.

These preliminary results, obtained at the very end of this doctorate research period, are extremely promising as they have provided clear-cut NMR evidence about the affinity between the naphthalimide guest **NI$_{C3}$** and the **QP5$_{C10}$** host. Further studies will have to shed light on the association constant between **NI$_{C3}$** and **QP5$_{C10}$**, the extent of quenching induced on the guest fluorescence, if any, and the ease with which this host-guest complex (in the OFF mode) can eventually be incorporated into a suitable polymeric matrix.

In conclusion, the first attempts on the use of **QP5$_{C10}$** and **QP5$_{C4}$** and the two lysine esters as potential OFF/ON fluorescent host-guest pairs were extremely disappointing. In the case of **QP5$_{C10}$** –in the presence of TCE-d_2 as a solvent– we observed a self-inclusion process of the alkenyl chain within its own cavity. Although we were able extrude this chain from the cavity by switching to $CDCl_3$, we did not observe any affinity between **QP5$_{C10}$** (or **QP5$_{C4}$**) and the two fluorescent substrates, **DL$_{C10}$** and **DL$_{C4}$**, originally designed as complementary guests. Retrospectively, with the hindsight, this is likely due to insufficient length of a 4-aminobutyl chain to protrude inside a pillar[5]arene cavity when a bulky dansyl moiety is next to it.

On the other hand, our preliminary tests between **QP5$_{C10}$** and the fluorescent naphthalimide derivative **NI$_{C3}$** have shown promising prospective for the design of fluorescence-responsive complexes.

3.3 Experimental Section†

3.3.1 General

1-hydroxybenzotriazole (HOBt), 1-ethyl-3-(3′-dimethylaminopropyl)carbodiimide (EDCI), N,N′-Dicyclohexylcarbodiimide (DCC), 2-(*tert*-butoxycarbonyloxyimino)-2-phenylacetonitrile (BOC-ON) and dansyl chloride were purchased from Sigma-Aldrich (Merck) and used without any further purification. 4-Dimethylaminopyridine (DMAP) was recrystallized following standard method.[38] N_{ε}-Boc-Lys-OH [22] and 4-bromo-*N*-allylnaphthalimide[39] were prepared according to published procedures.

3.3.2 Synthetic procedures

Synthesis of QP5 derivatives: **QP5** and K_2CO_3 (4 equiv.) were solubilised in anhydrous CH_3CN (15 mL) and allowed to reflux for 30 minutes. The alkylating agent (1.1 equiv.) was dissolved in anhydrous CH_3CN (5 mL) and added to the reaction mixture. The reaction was refluxed for 23 hours under stirring and inert atmosphere (Ar). The solvent was evaporated under reduced pressure and the solid residue formed was dissolved in CH_2Cl_2 (20 mL). The organic solution was washed with 1M HCl, H_2O and brine (3 × 20 mL of each) and then dried (Na_2SO_4). The crude product was purified by column chromatography (CH_2Cl_2/AcOEt, 95:5) and subsequently crystallized from CH_2Cl_2/CH_3OH to afford the pure derivatives **QP5$_{C10}$** and **QP5$_{C4}$**.

QP5$_{C10}$: **QP5** (68 mg, 0.076 mmol); K_2CO_3 (43.1 mg, 0.312 mmol); 9-decen-1-tosylate (25.7 mg, 0.085 mmol). Powdery red solid after crystallization: 65 mg (83%); m.p. 209–211 °C. ^{1}H NMR ($CDCl_3$) δ 9.04 (d, *J* = 4.8 Hz, 1H, *quin*-NCCH), 8.86 (d, *J* = 8.9 Hz, 1H, *quin*-NNCCCH), 8.20 (d, *J* = 2.0 Hz, 1H, *quin*-ClCCHC), 8.05 (s, 1H, ArH), 7.68–7.56 (m, 2H, *quin*-NNCCH, *quin*-ClCC*H*CH), 7.03 (s, 1H, ArH), 6.87–6.71 (m, 6H, ArH), 6.66 (s, 1H, ArH), 6.54 (s, 1H, ArH), 5.55 (ddt, *J* = 16.9, 10.1, 6.7 Hz, 1H, CH_2CHCH_2), 4.86–4.72 (m, 2H, CH_2CHCH_2), 4.44 (s, 2H, $ArCH_2Ar$), 4.07 (t, *J* = 6.4 Hz, 2H, OCH_2CH_2), 3.86 (s, 2H, $ArCH_2Ar$), 3.79 (s, 2H, $ArCH_2Ar$), 3.77–3.62 (m, 22H, 2×$ArCH_2Ar$, 6×OCH_3), 3.55 (s, 3H, OCH_3), 3.19 (s, 3H, OCH_3), 1.85 (dt, *J* = 14.2, 6.5 Hz, 2H, CH_2), 1.66–1.46 (m, 4H, 2 × CH_2), 1.40–1.19 (m, 4H, 2 × CH_2), 1.11 (p, *J* = 7.3 Hz, 2H, CH_2), 0.97–0.73 (m, 4H, 2 × CH_2) ppm; ^{13}C NMR ($CDCl_3$) δ 161.3, 153.6, 152.2, 151.2, 150.9, 150.64, 150.62, 150.57, 150.51,

† For general procedures and instrumental description see Chapter 2, Section 2.3.1.

150.48, 145.0, 144.3, 139.4, 135.7, 128.9, 128.7, 128.25, 128.19, 128.17, 128.12, 127.8, 127.6, 127.2, 126.9, 125.4, 124.3, 118.8, 114.3, 114.0, 113.95, 113.87, 113.77, 113.6, 113.5, 113.0, 104.9, 70.6, 68.0, 55.9, 55.73, 55.68, 55.60, 55.53, 55.44, 55.1, 37.1, 33.6, 32.8, 30.2, 29.8, 29.7, 29.5, 29.4, 29.1, 29.0, 28.8, 28.7, 28.6, 28.4, 27.1, 25.6, 19.7 ppm. HRMS Orbitrap) m/z: $[M–H]^{2–}$ (ESI/ Orbitrap) Calcd for $C_{62}H_{68}ClN_3O_9$, 1032.4565; Found, 1032.4584.

QP5$_{C4}$: **QP5** (48.8 mg, 0.054 mmol); K_2CO_3 (46.3 mg, 0.335 mmol); 4-bromo-1-butene (16.1 mg, 0.119 mmol). Powdery red solid after crystallization: 48 mg (94%); m.p. 179–181 °C. ^{1}H NMR ($CDCl_3$) δ 9.04 (d, *J* = 4.8 Hz, 1H, *quin*-NCCH), 8.84 (d, *J* = 8.9 Hz, 1H, *quin*-NNCCCH), 8.21 (s, 1H, *quin*-ClCCHC), 8.00 (s, 1H, ArH), 7.66–7.58 (m, 2H, *quin*-NNCCH, *quin*-ClCC*H*CH), 6.97 (s, 1H, ArH), 6.83–6.74 (m, 6H, ArH), 6.66 (s, 1H, ArH), 6.54 (s, 1H, ArH), 5.86 (ddt, *J* = 17.0, 10.2, 6.7 Hz, 1H, CH_2CHCH_2), 5.05–4.91 (m, 2H, CH_2CHCH_2), 4.45 (s, 2H,$ArCH_2Ar$), 4.07 (t, *J* = 6.6 Hz, 2H, OCH_2CH_2), 3.86 (s, 2H, $ArCH_2Ar$), 3.80 (s, 2H, $ArCH_2Ar$), 3.77–3.63 (m, 22H, 2 × $ArCH_2Ar$, 6 × OCH_3), 3.56 (s, 3H, OCH_3), 3.22 (s, 3H, OCH_3), 2.54 (q, *J* = 6.7 Hz, 2H, OCH_2CH_2CH) ppm; ^{13}C NMR ($CDCl_3$) δ 161.1, 153.6, 152.2, 151.2, 151.0, 150.74, 150.68, 150.64, 150.63, 150.54, 150.49, 145.0, 144.4, 135.7, 134.0, 128.9, 128.8, 128.34, 128.27, 128.24, 128.23, 128.20, 127.8, 127.6, 127.3, 127.0, 125.3, 124.2, 118.8, 117.3, 114.5, 114.4, 114.14, 114.06, 113.91, 113.89, 113.87, 113.7, 112.9, 105.0, 67.1, 56.0, 55.83, 55.81, 55.78, 55.72, 55.63, 55.55, 55.3, 53.3, 33.7, 31.9, 30.0, 29.7, 29.5, 29.2 ppm. HRMS (ESI/Orbitrap) m/z: $[M–H]^–$ Calcd for $C_{56}H_{56}ClN_3O_9$, 948.3626; Found, 948.3645.

N$_\alpha$-dansyl-N$_\varepsilon$-Boc-Lys-OH **(2)**: H-Lys(Boc)OH (500 mg; 2,03 mmol) was solubilized in 60 mL of aqueous carbonate buffer (pH = 9.5) and dioxane (1:1). Then, a solution of dansyl chloride (823 mg; 3.05 mmol) in dioxane (50 mL) was added dropwise in 20 minutes, while keeping the pH constant with 2N NaOH, under vigorous stirring at r.t.. After 7 h the suspension formed was extracted with diethyl ether (3 × 50 mL), and after partition, the pH of the remaining aqueous layer was lowered to 2. The solid formed was collected by suction filtration and the eluate was extracted with ethyl acetate (3 × 50 mL). The organic layers were collected, dried, evaporated to dryness and the residual oil formed was purified by column chromatography ($CHCl_3/CH_3OH$, 95:5), affording 430 mg (44%) of the dansyl lysine derivative **2**. ^{1}H NMR (CD_3OD): δ 8.55 (dt, *J* = 8.5, 1.1 Hz, 1H, SO_2CCH), 8.39 (dt, *J* = 8.6, 0.9 Hz, 1H, $((CH_3)_2NCCH$), 8.21 (dd, *J* = 7.3, 1.3 Hz, 1H, $((CH_3)_2NCCCH$), 7.63–7.52 (m, 2H, $((CH_3)_2NCCHCH$, SO_2CCHCH), 7.26 (dd, *J* = 7.6, 0.9 Hz, 1H, SO_2CCCH), 3.59 (t, *J* = 6.5 Hz, 1H, NHC*H*), 2.87 (s, 6H, $N(CH_3)_2$), 2.64 (t, *J* = 6.5 Hz, 2H, $NHCH_2$), 1.53–1.48 (m, 2H,

NHCHC*H*$_2$), 1.41 (s, 9H, OC(CH$_3$)$_3$), 1.14–0.96 (m, 4H, NHCH$_2$C*H*$_2$,NHCH$_2$CH$_2$C*H*$_2$) ppm. ^{13}C NMR (CD$_3$OD): δ 179.2 (*C*O$_2$H), 158.3 (NH*C*O$_2$), 153.1 ((CH$_3$)$_2$N*C*), 137.2 (SO$_2$*C*), 131.3 (SO$_2$C*C*), 131.2 (SO$_2$C*C*H), 131.1 ((CH$_3$)$_2$NCC*C*H), 130.2 ((CH$_3$)$_2$NCCH*C*H), 129.1 ((CH$_3$)$_2$NC*C*), 124.3 (SO$_2$CCH*C*H), 120.9 (SO$_2$CC*C*H), 116.5 ((CH$_3$)$_2$NC*C*H), 79.8 (*C*(CH$_3$)$_3$), 58.7 (NHCH), 45.8 ((CH$_3$)$_2$N), 41.1 (NHCH$_2$), 33.8 (NHCH*C*H$_2$), 30.2 (NHCH$_2$*C*H$_2$), 28.8 ((*C*H$_3$)$_3$C), 23.3 (NHCH$_2$CH$_2$*C*H$_2$) ppm.

Lysine Ester derivative 3a: **2** (220 mg, 0.46 mmol), EDCI (106 mg, 0.55 mmol) and HOBt (31 mg, 0.23 mmol) were dissolved in anhydrous CH_2Cl_2 (80 mL), then 9-decen-1-ol (78 mg, 0.51 mmol) in anhydrous CH_2Cl_2 (15 mL) was added dropwise over 30 min at 0 °C, under inert atmosphere (N_2). The reaction mixture was stirred for 24 h at r.t. and then washed with H_2O (3 × 50 mL), dried ($MgSO_4$) and concentrated under reduced pressure. The yellow glassy solid obtained was purified by column chromatography (hex/AcOEt, 2:1), providing 110 mg (39%) of the ester **3a**. ^{1}H NMR ($CDCl_3$) δ 8.53 (dt, *J* = 8.5, 1.1 Hz, 1H, SO2CH), 8.31 (d, *J* = 8.6 Hz, 1H, (CH$_3$)$_2$NCC*H*), 8.23 (dd, *J* = 7.2, 1.3 Hz, 1H, (CH$_3$)$_2$NCCC*H*), 7.59 (dd, *J* = 8.7, 7.5 Hz, 1H, (CH$_3$)$_2$NCCHC*H*), 7.50 (dd, *J* = 8.6, 7.3 Hz, 1H, SO$_2$CCHC*H*), 7.22–7.15 (m, 1H, SO$_2$CCC*H*), 5.80 (ddt, *J* = 16.9, 10.2, 6.7 Hz, 1H, CH$_2$C*H*CH$_2$), 5.40 (d, *J* = 8.8 Hz, 1H, CHN*H*), 5.06–4.87 (m, 2H, CH$_2$CH$_2$CHC*H*$_2$), 4.37 (s, 1H, CH$_2$N*H*), 3.86 (ddd, *J* = 8.9, 7.3, 5.5 Hz, 1H, NHC*H*), 3.67 (ddt, *J* = 43.1, 10.7, 6.8 Hz, 2H, OCH$_2$), 2.87 (s, 8H, (CH$_3$)$_2$N, NHC*H*$_2$), 2.10–1.96 (m, 2H, CH$_2$C*H*$_2$CHCH$_2$), 1.59–1.50 (m, 2H, NHCHC*H*$_2$), 1.44 (s, 9H, (CH$_3$)$_3$C), 1.40–1.03 (m, 14H) ppm. ^{13}C NMR ($CDCl_3$) δ 171.4 (CH*C*O$_2$), 155.9 (NH*C*O$_2$), 151.9 ((CH$_3$)$_2$N*C*), 139.1 (CH$_2$*C*HCH$_2$), 134.6 (SO$_2$*C*), 130.7 (SO$_2$C*C*H), 129.8 (SO$_2$C*C*), 129.73 ((CH$_3$)$_2$NCC*C*H), 129.67 ((CH$_3$)$_2$NC*C*), 128.4 ((CH$_3$)$_2$NCCH*C*H), 123.1 (SO$_2$CCH*C*H), 118.9 ((CH$_3$)$_2$NC*C*H), 115.3 (SO$_2$CC*C*H), 114.2 (CH$_2$CH$_2$CH*C*H$_2$), 65.7 (OCH$_2$), 55.8 (NHCH), 45.4 ((CH$_3$)$_2$N), 40.0 (NHCH$_2$), 33.7 (CH$_2$*C*H$_2$CHCH$_2$), 32.7 (NHCH*C*H$_2$), 29.3, 29.2 ((CH$_3$)$_3$*C*), 29.0, 28.97, 28.8, 28.4 ((*C*H$_3$)$_3$C), 28.1, 25.6, 22.0.

Lysine Ester derivative 3b: **2** (192 mg; 0.40 mmol), DMAP (2.5 mg; 0.02 mmol) and 3-buten-1-ol (144 mg; 2 mmol) were mixed in anhydrous CH_2Cl_2 (5 mL) at 0° C under stirring for 15 min. A solution of DCC (103 mg; 0.5 mmol) in anhydrous CH_2Cl_2 (2 mL) was then added dropwise under an inert atmosphere (N_2) and after 5 min of vigorous stirring at 0° C the mixture was let to react at room temperature. After 3 h the solid formed was filtered off and the eluate was washed with an aqueous solution of 1 M HCl (2 × 15 mL) and saturated $NaHCO_3$ (2 × 15 mL), dried over $MgSO_4$ and purified by column chromatography (hexane/ethyl acetate 2:1), to yield 141 mg (66%) of the ester **3b**. ^{1}H NMR ($CDCl_3$) δ 8.55 (d, *J* = 8.5 Hz, 1H, SO$_2$CCH), 8.31 (d, *J* = 8.7 Hz, 1H, ((CH$_3$)$_2$NCC*H*), 8.23 (dd, *J* = 7.3, 1.3 Hz,

1H, ((CH$_3$)$_2$NCCC*H*), 7.59 (dd, *J* = 8.6, 7.6 Hz, 1H, ((CH$_3$)$_2$NCCHC*H*), 7.51 (dd, *J* = 8.5, 7.3 Hz, 1H, (SO$_2$CCHC*H*), 7.20 (d, *J* = 7.5 Hz, 1H, SO$_2$CCCH), 5.55 (ddt, *J* = 17.1, 10.3, 6.7 Hz, 1H, CH$_2$C*H*CH$_2$), 5.40 (d, *J* = 8.8 Hz, 1H, N*H*CH), 4.98–4.89 (m, 2H, CH$_2$CH$_2$CHC*H$_2$*), 4.38 (s, 1H, N*H*CH$_2$), 3.86 (ddd, *J* = 8.8, 7.2, 5.5 Hz, 1H, NHC*H*), 3.73 (ddt, *J* = 39.9, 10.7, 6.8 Hz, 2H, OCH$_2$), 2.88 (s, 8H, (CH$_3$)$_2$N, NHC*H$_2$*), 2.05 (qt, *J* = 6.8, 1.5 Hz, 2H, CH$_2$C*H$_2$*CHCH$_2$), 1.57–1.43 (m, 2H, NHCHC*H$_2$*), 1.43 (s, 9H, (CH$_3$)$_3$C), 1.22–1.06 (m, 4H, NHCH$_2$C*H$_2$*, NHCH$_2$CH$_2$C*H$_2$*) ppm. ^{13}C NMR (126 MHz, CDCl$_3$) δ 171.2 (CH*C*O$_2$), 155.9 (NHCO$_2$), 149.8 ((CH$_3$)$_2$N*C*), 134.6 (SO$_2$C), 133.2 (CH$_2$*C*HCH$_2$), 130.7 (SO$_2$C), 129.8 (CH$_2$*C*HCH$_2$), 129.7(SO$_2$C*C*), 128.4 (SO$_2$C*C*H), 126.8 ((CH$_3$)$_2$NCC*C*H), 123.2 ((CH$_3$)$_2$NCCH*C*H), 119.0 ((CH$_3$)$_2$NC*C*), 117.5 (SO$_2$CCH*C*H), 115.3 (SO$_2$CC*C*H), 79.1 ((CH$_3$)$_3$*C*), 64.3 (OCH$_2$), 55.8 (NHCH), 45.4 ((CH$_3$)$_2$N), 40.0 (NHCH$_2$), 32.7 (CH$_2$*C*H$_2$CHCH$_2$), 32.5 (NHCH*C*H$_2$), 29.2 (NHCH$_2$*C*H$_2$*)*, 28.4 ((CH$_3$)$_3$C), 21.9 (NHCH$_2$CH$_2$*C*H$_2$) ppm.

DL$_{C10}$: *N*$_ε$-protected ester **3a** (100 mg, 0.16 mmol) was dissolved in 4 mL of a CH$_2$Cl$_2$/TFA (75:25) solvent mixture and then stirred for 1 h at r.t., under a nitrogen atmosphere. The solvent was stripped off under reduced pressure and the crude product was partitioned between CH$_2$Cl$_2$ and water (20 mL each). The organic layer was collected and washed with a saturated aqueous solution of NaHCO$_3$ (3 × 20 mL), dried over MgSO$_4$ and then evaporated to dryness. Purification of the resulting residue by column chromatography (CH$_2$Cl$_2$/CH$_3$OH 93:7), gave 66 mg (83%) of the ester derivative **DL$_{C10}$**. ^{1}H NMR (CDCl$_3$) δ 8.53 (dt, *J* = 8.5, 1.0 Hz, 1H, (CH$_3$)$_2$NCC*H*), 8.30 (dt, *J* = 8.7, 0.9 Hz, 1H, SO$_2$CCH), 8.22 (dd, *J* = 7.3, 1.2 Hz, 1H, SO$_2$CCC*H*), 7.58 (ddd, *J* = 8.6, 7.6, 0.7 Hz, 1H, SO$_2$CCHC*H*), 7.54–7.45 (m, 1H, (CH$_3$)$_2$NCCHC*H*), 7.18 (dd, *J* = 7.6, 0.8 Hz, 1H, (CH$_3$)$_2$NCCC*H*), 5.80 (ddt, *J* = 16.9, 10.2, 6.7 Hz, 1H, CH$_2$C*H*CH$_2$), 5.05–4.88 (m, 2H, CH$_2$CH$_2$CHC*H$_2$*), 3.96–3.84 (m, 1H, NHC*H*), 3.75 – 3.51 (m, 2H, OCH$_2$), 2.87 (s, 6H, (CH$_3$)$_2$N), 2.64–2.56 (m, 2H, NH$_2$C*H$_2$*), 2.09–1.97 (m, 2H, CH$_2$C*H$_2$*CHCH$_2$), 1.60 (ddd, *J* = 14.5, 7.6, 6.1 Hz, 2H, NHCHC*H$_2$*), 1.42–1.03 (m, 16H) ppm. ^{13}C NMR (126 MHz, CDCl$_3$) δ 171.4 (NH*C*O$_2$), 151.9 ((CH$_3$)$_2$N*C*), 139.1 (CH$_2$*C*HCH$_2$), 134.6 (SO$_2$*C*), 132.5 (SO$_2$C*C*), 130.7 ((CH$_3$)$_2$NC*C*H), 129.8 (NHC*C*), 129.7 (SO$_2$CC*C*H), 128.4 (SO$_2$CCH*C*H), 123.1 ((CH$_3$)$_2$NCCH*C*H), 119.0 (SO$_2$C*C*H), 115.3 ((CH$_3$)$_2$NCC*C*H), 114.2 (CH$_2$CH$_2$CH*C*H$_2$), 65.6 (OCH$_2$), 55.8 (NHCH), 45.4 ((CH$_3$)$_2$N), 40.9 (NH$_2$CH$_2$), 33.7 (CH$_2$*C*H$_2$CHCH$_2$), 32.6 (NHCH*C*H$_2$), 30.9, 29.3, 29.0, 29.0, 28.8, 28.1, 25.6, 21.8 ppm.

DL$_{C4}$: *N*$_ε$-protected ester **3b** (100 mg; 0.187 mmol) was dissolved in 4 mL of a CH$_2$Cl$_2$/TFA (75:25) solvent mixture and then stirred for 1 h at r.t., under a nitrogen atmosphere. The solvent was stripped off under reduced pressure and the crude product was partitioned between CH$_2$Cl$_2$ and water (30 mL each). The organic layer was collected and washed with a

saturated aqueous solution of $NaHCO_3$ (3 × 30 mL), dried over $MgSO_4$ and then evaporated to dryness. Purification by column chromatography ($CHCl_3/CH_3OH$, 95:5 → 9:1 → 85:15) of the residue formed gave 70 mg (86%) of the final product. ^1H NMR ($CDCl_3$) δ 8.53 (dt, *J* = 8.5, 1.1 Hz, 1H, SO_2CCH), 8.32 (d, *J* = 8.6 Hz, 1H, $(CH_3)_2NCCH$), 8.23 (dd, *J* = 7.4, 1.3 Hz, 1H, $(CH_3)_2NCCCH$), 7.58 (dd, *J* = 8.7, 7.6 Hz, 1H, $(CH_3)_2NCCHCH$), 7.50 (dd, *J* = 8.5, 7.3 Hz, 1H, SO_2CCHCH), 7.19 (d, *J* = 7.5 Hz, 1H, SO_2CCCH), 5.99 (br s, 1H, NH), 5.55 (ddt, *J* = 17.1, 10.4, 6.7 Hz, 1H, CH_2CHCH_2), 4.99–4.86 (m, 2H, $CH_2CH_2CHCH_2$), 3.88 (dd, *J* = 7.3, 5.4 Hz, 1H, NHCH), 3.72 (ddt, *J* = 43.6, 10.7, 6.8 Hz, 2H, CO_2CH_2), 2.87 (s, 8H, $N(CH_3)_2$ + NH_2), 2.54 (tt, *J* = 6.7, 3.9 Hz, 2H, CH_2NH_2), 2.04 (qt, *J* = 6.8, 1.4 Hz, 2H, $CH_2CH_2CHCH_2$), 1.59 (m, 2H, $NHCHCH_2$), 1.24 (m, 4H, $NH_2CH_2CH_2CH_2$,$NH_2CH_2CH_2CH_2$) ppm. ^{13}C NMR ($CDCl_3$) 174.3 (CO_2CH_2), 151.7 ($(CH_3)_2NC$), 134.7 (SO_2C), 133.3 (CH_2CHCH_2), 130.6 (SO_2CC), 130.4 (SO_2CCH), 129.6 ($(CH_3)_2NCCHCH$), 128.6 ($(CH_3)_2NCC$), 128.4 ($(CH_3)_2NCCHCH$), 123.1 (SO_2CCHCH), 119.2 (SO_2CCH), 115.4 (SO_2CCCH), 117.4 ($CH_2CH_2CHCH_2$), 64.3 (CO_2CH_2), 55.6 (NHCH), 45.4 ($N(CH_3)_2$), 40.4 (CH_2NH_2), 32.4 ($CH_2CH_2CHCH_2$), 32.3 ($NHCHCH_2$), 28.6, 27.9 ($NH_2CH_2CH_2CH_2$ + $NH_2CH_2CH_2CH_2$) ppm. HRMS (ESI/Orbitrap) m/z: $[M–H]^-$ Calcd for $C_{22}H_{31}N_3O_4S$, 432.1956; Found, 432.1964.

Naphthalimide derivative 5: 4-bromo-*N*-allylnaphthalimide **4** (140 mg, 0.44 mmol) was dissolved in 2-methoxyethanol (15 mL). To this solution, 6-amino-1-hexanol (521 mg, 4.4 mmol) was added and the mixture was allowed to react for 24 hours under reflux and vigorous stirring. The solvent was evaporated under reduced pressure and the solid obtained was purified by column chromatography (hexane/acetone 2:1) to give 60 mg (39%) of **5**. ^1H NMR ($CDCl_3$) δ 8.60 (d, J = 7.3 Hz, 1H), 8.48 (d, J = 8.4 Hz, 1H), 8.09 (d, *J* = 8.4 Hz, 1H), 7.63 (t, *J* = 7.9 Hz, 1H), 6.73 (d, J = 8.4 Hz, 1H), 6.00 (ddt, J = 16.2, 10.7, 5.7 Hz, 1H), 5.38–5.11 (m, 4H), 4.80 (dd, J = 5.5, 1.6 Hz, 2H), 3.74–3.65 (m, 3H), 3.42 (q, J = 6.9 Hz, 2H), 1.84 (p, *J* = 7.2 Hz, 2H), 1.63 (p, *J* = 6.7 Hz, 2H), 1.55–1.46 (m, 2H); ^{13}C NMR ($CDCl_3$) δ 164.6, 164.0, 149.6, 134.8, 132.8, 131.4, 130.0, 126.0, 124.9, 123.2, 120.4, 117.2, 110.4, 104.6, 62.9, 43.8, 42.3, 32.7, 29.1, 27.1, 25.7.

NI$_{C3}$: **5** (60 mg, 0.16 mmol), PPh_3 (164 mg, 0.63 mmol) and CBr_4 (207.8 mg, 0.63 mmol) were dissolved in anhydrous CH_2Cl_2 (20 mL) and the solution left to react for 24 h under reflux and an inert atmosphere (Ar). The solvent was removed under reduced pressure and the solid obtained was dissolved in CH_2Cl_2 (40 mL) and washed with water (3 × 40 mL). The organic layer was dried ($MgSO_4$), concentrated to dryness and the solid residue formed was purified by column chromatography (CH_2Cl_2 → hexane/acetone 1:1) to afford 40 mg (46%) of the titled compound. ^1H NMR ($CDCl_3$) δ 8.61 (dd, *J* = 7.3, 1.0 Hz, 1H), 8.49 (d, *J* = 8.4 Hz,

1H), 8.08 (dd, *J* = 8.3, 1.1 Hz, 1H), 7.64 (dd, *J* = 8.4, 7.3 Hz, 1H), 6.74 (d, *J* = 8.4 Hz, 1H), 6.13–5.87 (m, 1H), 5.40–5.09 (m, 2H), 4.80 (dt, *J* = 5.6, 1.5 Hz, 2H), 3.44 (t, *J* = 6.8 Hz, 2H), 1.88 (dp, *J* = 38.1, 6.9 Hz, 4H), 1.36–1.20 (m, 4H) ppm; ^{13}C NMR ($CDCl_3$) δ 164.5, 164.0, 149.5, 134.7, 132.8, 131.4, 130.0, 126.0, 124.9, 123.3, 120.4, 117.2, 110.4, 104.6, 43.7, 42.3, 33.8, 32.6, 29.0, 28.0, 26.5.

3.4 References

[1] Brighenti R., Li Y., Vernerey F.J., *Front. Mater.*, **2020**, *7*, 196.

[2] Wang Y., Ping G., Li C., *Chem. Commun.*, **2016**, *52*, 9858.

[3] (a) Li J., Harada A., Kamachi M., *Polym. J. (Tokyo)*, **1994**, *26*, 1019; (b) Harada A., Kawaguchi Y., Nishiyama T., Kamachi M., *Macromol. Rapid Commun.*, **1997**, *18*, 535; (c) Hernandez R., Rusa M., Rusa C.C., Lopez D., Mijangos C., Tonelli A.E., *Macromolecules*, **2004**, *37*, 9620; (d) Fleury G., Schlatter G., Brochon C., Travelet C., Lapp A., Lindner P., Hadziioannou G., *Macromolecules*, **2007**, *40*, 535; (e) Zhao Y.L., Stoddart J.F., *Langmuir*, **2009**, *25*, 8442.

[4] Appel E.A., Biedermann F., Rauwald U., Jones S.T., Zayed J.M., Scherman O.A., *J. Am. Chem. Soc.*, **2010**, *132*, 14251; (b) Appel E.A., Loh X.J., Jones S.T., Biedermann F., Dreiss C.A., Scherman O.A., *J. Am. Chem. Soc.*, **2012**, *134*, 11767; (c) Appel E.A., Loh X.J., Jones S.T., Dreiss C.A., Scherman O.A., *Biomaterials*, **2012**, *33*, 4646.

[5] Früh A.E., Artoni F., Brighenti R., Dalcanale E., *Chem. Mater.*, **2017**, *29*, 7450.

[6] (a) Zadmard R., Hokmabadi F., Jalali M.R., Akbarzadeh A., *RSC Adv.*, **2020**, *10*, 32690; (b) Guo D., Liu Y., *Chem. Soc. Rev.*, **2012**, *41*, 5907.

[7] (a) Xia B.Y., Xue M., *Chem. Commun.*, **2014**, *50*, 1021; (b) Yu G.C., Hua B., Han C.Y., *Org. Lett.*, **2014**, *16*, 2486.

[8] (a) Wang P., Li Z.T., Ji X.F., *Chem. Commun.*, **2014**, *50*, 13114; (b) Li C.J., Ma J.W., Zhao L., Zhang Y.Y., Yu Y.H., Shu X.Y., Li J., Jia X.S., *Chem. Commun.*, **2013**, *49*, 1924; (c) Hua B., Zhou J., Yu G.C., *Tetrahedron Lett.*, **2015**, *56*, 986.

[9] Wang Y., Xu J.F., Chen Y.Z., Niu L.Y., Wu L.Z., Tung C.H., Yang Q.Z., *Chem. Commun.*, **2014**, *50*, 7001.

[10] (a) Xia B., Heb J., Abliz Z., Yu Y., Huang F., *Tetrahedron Lett.*, **2011**, *52*, 4433; (b) Gao L., Han C., Zheng B., Dong S., Huang F., *Chem. Commun.*, **2013**, *49*, 472; (c) Ma Y., Xue M., Zhang Z., Chi X., Huang F., *Tetrahedron*, **2013**, *69*, 4532; (d) Guan Y., Ni, M., Hu X., Xiao T., Xiong S., Lin C., Wang L., *Chem. Commun.*, **2012**, *48*, 8529; (e) Zhang H., Nguyen K.T., Ma X., Yan H., Guo J., Zhu L., Zhao Y., *Org. Biomol. Chem.*, **2013**, *11*, 2070; (f) Li C., Han K., Li J., Zhang Y., Chen W., Yu Y., Jia X., *Chem. Eur. J.*, **2013**, *19*, 11892; (g) Song N., Chen D.X., Qiu Y.C., Yang X.Y., Xu B., Tian W., Yang Y.W., *Chem. Commun.*, **2014**, *50*, 8321; (h) Shi B., Xia D., Yao Y., *Chem. Commun.*, **2014**, *50*, 13932.

[11] (a) Ogoshi T., Shiga R., Yamagishi T., *J. Am. Chem. Soc.*, **2012**, *134*, 4577; (b) Li H., Chen D.X., Sun Y.L., Zheng Y.B., Tan L.L., Weiss P.S., Yang Y.W., *J. Am. Chem. Soc.*, **2013**, *135*, 1570; (c) Zhang H., Ma X., Nguyen K.T., Zhao Y., *ACS Nano*, **2013**, *7*, 7853; (d) Duan Q., Cao Y., Li Y., Hu X., Xiao T., Lin C., Pan Y., Wang L., *J. Am. Chem. Soc.*, **2013**, *135*, 10542; (e) Ogoshi T., Kida K., Yamagishi T., *J. Am. Chem. Soc.*, **2013**, *135*, 20146; (f) Li Z.Y., Zhang Y., Zhang C.W., Chen L.J., Wang C., Tan H., Yu Y., Li X., Yang H.B., *J. Am. Chem. Soc.*, **2014**, *136*, 8577; (g) Cao Y., Hu X.Y., Li Y., Zou X., Xiong S., Lin C., Shen Y.Z., Wang L., *J. Am. Chem. Soc.*, **2014**, *136*, 10762; (h) Chang Y., Yang K., Wei P., Huang S., Pei Y., Zhao W., Pei Z., *Angew. Chem. Int. Ed.*, **2014**, *53*, 13126; (i) Yang Y.W., Sun Y.L., Song N., *Acc. Chem. Res.*, **2014**, *47*, 1950.

[12] (a) Kardelis V., Li K., Nierengarten, I., Holler M., Nierengarten J.F., Adronov A., *Macromolecules*, **2017**, *50*, 9144; (b) Chang J., Zhao Q., Kang, L., Li H., Xie M., Liao X., *Macromolecules*, **2016**, *49*, 2814.

[13] Pisagatti I., Gattuso G., Notti A., Parisi M.F., Brancatelli G., Geremia S., Greco F., Millesi S., Pappalardo A., Spitaleri L., Gulino A., *RSC Adv.*, **2018**, *8*, 33269.

[14] (a) Strutt N.L., Forgan R.S., Spruell J.M., Botros Y.Y., Stoddart J.F., *J. Am. Chem. Soc.*, **2011**, *133*, 5668; (b) Deng H., Shu X., Hu X., Li j., Jia X., Li C., *Tetrahedron Lett.*, **2012**, *53*, 4609; (c) Yu G., Hua B., Hac C., *Org. Lett.*, **2014**, *16*, 2486.

[15] (a) Dasgrupta S., Mukherjee P.S., *Org. Biomol. Chem.*, **2017**, *15*, 762; (b) Cheng W., Tang H., Wang R., Wang L., Meier H., Cao D., *Chem. Commun.*, **2016**, *52*, 8075.

[16] Früh A.E., Artoni F., Brighenti R., Dalcanale E., *Chem. Mater.*, **2017**, *29*, 7450.

[17] Santa T., *Biomed Chromatogr.*, **2011**, *25*, 1.

[18] (a) Walker J.M., *Methods Mol. Biol.*, **1994**, *32*, 321; (b) Walker J.M., *ibid.*, **1994**, *32*, 329.

[19] Xue G., Bradshaw J.S., Song H., Bronson R.T., Savage, P.B., Krakowiak K.E., Izatt, R.M., Prodi L., Montalti, M., Zaccheroni N., *Tetrahedron*, **2001**, *57*, 87.

[20] Ocak Ü., Ocak M., Bartsh R.A., *Inorg. Chim. Acta*, **2012**, *381*, 44.

[21] Kumar N., *Comprehensive Supramolecular Chemistry II*, **2017**, *8*, 197.

[22] Heimer E.P., Wang C., Lambros T.J., Felix A.M., *Org. Prep. Proced. Int.*, **2009**, *15*, 6, 379.

[23] Tapuhi Y., Schmidt D.E., Lindner W., Karger B.L., *Anal. Biochem.*, **1981**, *115*, 123.

[24] Sheehan J.C., Cruickshank P.A., Boshart G.L., *J. Org. Chem.*, **1961**, *26*, 2525.
[25] Wuts P.G.M., *Greene's Protective Groups in Organic Synthesis – Fifth Edition*, **2014**, Wiley. For a "green" method see: Zinelaabidine C., Souad O., Zoubir J., Malika B., Noue-Eddine A., *Int. J. Chem.*, **2012**, *4*, 73.
[26] Neises B., Steglich W., *Angew. Chem. Int. Ed. Engl.*, **1978**, *17*, 552.
[27] Cohen Y., Avram L., Frish L., *Angew. Chem. Int. Ed.*, **2005**, *44*, 520.
[28] Ogoshi, T.; Furuta, T.; Hamada, Y.; Kakuta, T.; Yamagishi, T.; *Mater. Chem. Front.* 2018, **2**, 597.
[29] Ogoshi T., Demachi K., Kitajima K. Yamagishi T., *Chem. Commun.,* **2011**, *47*, 7164.
[30] Xia B., Zheng B., Han C., Dong S., Zhang M., Hu B., Yu Y., Huang F., *Polym. Chem.*, **2013**, *4*, 2019.
[31] Zhang R., Wang C., Long R., Chen T., Yan C., Yao Y., *Front. Chem.*, **2019***, 7,* 508.
[32] Guan Y., Liu P., Deng C., Ni M., Xiong S., Lin C., Hu X., Ma J., Wang L., *Org. Biomol. Chem.*, **2014**, *12*, 1079.
[33] Dong H., Wei T., Ma X., Yang Q., Zhang Y., Sun Y., Shi B., Yao H., Zhang Y., Lin Q., *J. Mater. Chem. C*, **2020**, *8*, 13501.
[34] Konstantinova T.N., Miladinova P.M., *J. Appl. Polym. Sci.*, **2009**, *111*, 1991.
[35] Wei Y., Wang N., Li D., Wang G., He Y., *React. Funct. Polym.*, **2019**, *144*, 104351.
[36] Bojtár M., Paudics A., Hessz D., Miklos K., Bitter I., *RSC Adv.*, **2016**, *6*, 86269.
[37] Konstantinova T.N., Meallier P., Grabchev I., *Dyes and Pigments*, **1993**, *22*, 191.
[38] Armarego
[39] Konstantinova T.N., Meallier P., Grabchev I., *Dyes and Pigments*, **1993**, *22*, 191.

CHAPTER 4

4.1 The "wet" supramolecular chemistry: host-guest complex formation in water

Water is, perhaps, the most important molecule on our planet. Life, indeed, is strictly dependent on its presence, since even the simplest living organisms need this polar molecule to carry out their biological functions. The cells, structural basis of all living beings, possess a cytoplasmic medium highly rich in water, which makes H_2O a widely used solvent for studies in the clinical field, also from a chemical point of view, for transporting substances or sequestering toxic agents in the body. The concepts of molecular recognition and self-organization rely on inspiration from water-evolved natural systems: natural receptors, such as enzymes and antibodies, display strong and selective host-guest complexation through multiple weak and non-covalent interactions between the functional groups of the binding partners. Therefore, the design and the study of new synthetic supramolecular assemblies in water are more and more intriguing goals.[1] Indeed, because of the need for a host molecule to be water-soluble, severely setting a limit on the type of building blocks that can be used for such design, specific types of interactions and approaches must be chosen to overcome the competitive influence of the water. Another important feature of large water-soluble receptors is the encapsulation of several guests, allowing molecular interactions to be studied within a confined space as well as to carry out chemical reactions in aqueous media. The self-assembly processes in water, for most of these supramolecular architectures, either biological or synthetic, are mainly driven by hydrophobic effects.[2] Furthermore, other important interactions take place in the formation of the aforementioned assemblies, such as hydrogen bonding, ion-ion and ion-dipole interaction. It's important to note that self-assembly processes in aqueous solutions depend on the concentration and the type of salts present in solution.[3] For example, salt effects are rather important for self-assembly systems based on ion-ion interactions, but negligible for those mainly driven by hydrophobic effect. As a result, most of the supramolecular systems involved with biological targets feature a strong hydrophobic assembly component, in combination with polar interactions taking part in the formation of the structure.

During the past few decades, a series of macrocyclic molecules have been developed, including cyclodextrins, cucurbit[*n*]urils, calix[*n*]arenes, pillar[*n*]arenes (see Chapter 1), which have gained increasing popularity for their application in the biomedical field. In particular

pillar[*n*]arenes, inherently water insoluble, when adequately functionalised, may become water-soluble species (Section 4.2 in this Chapter). Among them, carboxylatopillar[*n*]arenes[4] represent a class of water-soluble derivatives that have been extensively investigated because of their ability to interact with pharmacologically active water-soluble molecules through the formation of host-guest complexes. In addition, they can rely on the presence of hydrophobic moieties not only to directly bring poorly soluble drug molecules into aqueous solution, or after micelle or vesicle formation, but also to increase the permeability of such molecules across the cell barrier (see the Enhanced Permeability and Retention (EPR) effect)[5], or for their controlled release in target areas.

As part of this PhD project, the search for new macrocyclic-based systems able to bind and carry biologically and pharmacologically active molecules and eventually release them upon an external stimulus (pH change, concentration gradient, etc.) has been one of the objectives of interest. To this end, a new water-soluble pillar[6]arene (**WSP6**) was synthetized and its proclivity to bind two model drugs has been shown. In one instance, the target antibiotic was loaded on a 'smart' surface, decorated with **WSP6**, with final aim of constructing, down the line, biomedical devices coated with antimicrobial and anti-adhesive layer. In the other, the new pillararene was tested as such, as a potential carrier of an anticancer drug.

*4.2 Water-soluble pillar[*n*]arenes*

The ever-increasing development of technologies, combined with the versatility of these compounds, has led to the use of macrocyclic hosts in aqueous solution, with the intention of exploiting their peculiar receptor properties, which can be modulated according to the size of the cavity provided by the macrocyclic scaffold and its functionalization. The insertion of positively or negatively charged groups is the most frequently used strategy for this purpose.

The properties of pillar[*n*]arenes have already been discussed (Section 1.3, Chapter 1), including the ease of functionalization at both edges of the macrocyclic cavity. It was precisely by inserting ten carboxylate groups into the pillararene structure that the first water-soluble pillar[5]arene (**WP5**) was obtained,[6] which demonstrated high complexing properties towards the toxic paraquat molecule in the aqueous medium. Moreover, **WP5** has been shown to act as a supramolecular container capable of directly encapsulate a bioactive molecule and the release of drug has been controlled by pH variations.

Water solubility can be achieved by providing these macrocycles with positively charged functionalities, such as ammonium groups,[7] or with protonable functionalities, as in the case of tryptophan-modified pillar[5]arenes.[8]

Furthermore, due to the simultaneous presence of hydrophilic and hydrophobic functions in the structure, water-soluble pillararenes can act as surfactants, with the possibility of forming higher aggregates such as micelles or vesicles,[9] which have been widely used for the capture of drugs or poorly water-soluble molecules.

4.3 The synthesis of pillar[6]arene WSP6

Similar to pillar[5]arenes, pillar[6]arene rims may also be derivatized with suitable functional groups capable of making the resulting macrocycle soluble in water. The first reported water-soluble pillar[6]arene (**WP6**) was synthetized by introducing twelve 2-carboxyethyl moieties.[10] **WP6** proved to be very effective as sequestering agent for paraquat, its association constant with this dicationic pesticide being higher than that observed for the analogous pillar[5]arene.[11] This greater affinity was attributed to the size of the pillar[6]arene cavity (6.7 Å), where the pesticide (6.3 Å) could fit much better than the pillar[5]arene one (4.7 Å). This dodeca-anionic pillararene also forms very stable inclusion complexes in water with many other cationic species, including a number of pyridinium derivatives.[12] **WP6** is able to host *trans*-azobenzene guests but fails to form complexes with the corresponding *cis*-azobenzene.[13]

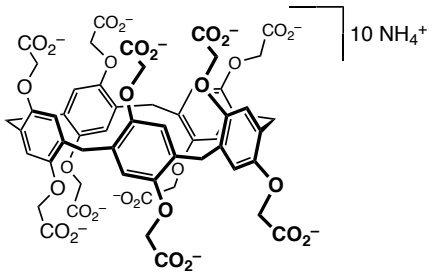

WP5

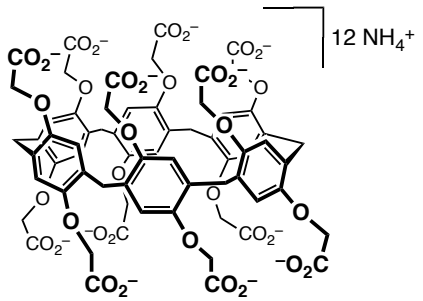

WP6

Carboxylatopillar[*n*]arenes combine a π-electron rich hydrophobic cavity with two hydrophilic portals bearing anionic carboxylate groups, useful for the recognition of cationic guests. Appropriately sized hydrophobic analytes can be hosted inside this cavity with the positively charged end-groups protruding outward for favourable electrostatic interactions with the anionic groups. As a result, carboxylatopillar[*n*]arenes are ideal candidates for host-guest binding with cationic guests and have been used as cargo molecules for the fabrication of responsive supramolecular systems for the trapping and releasing of specific analytes.[4] Photo- and redox-responsive host-guest systems capable of selectively undergoing dissociation in aqueous media could also be used as drug-responsive systems.[13,14]

Water-soluble pillararenes have therefore been widely investigated as carrier for pharmacologically active molecules and have, over the years, gained much attention as essential building blocks in the preparation of drug delivery systems.[15] For example, **WP5** has been shown to act, upon pH variations, as a supramolecular container for the reversible binding and release of norharmane (**NHM**) a poorly water-soluble antiviral and antibacterial alkaloid.[16]

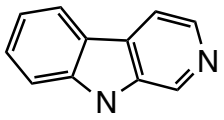

NHM

In the light of these observations, the research group where this thesis was carried out, by taking into account that: a) the microenvironment of an infection site is acidic because of lactic acid accumulation [17] and b) carboxylato-substituted water-soluble pillar[*n*]arenes [18] display a good biocompatibility, a low toxicity and a proclivity to bind alkylammonium guests,[19] has recently tested the affinity of **WP5** towards the drug amikacin (**Ami**) with the aim of using this macrocycle as a carrier for the targeted delivery of **Ami** to a given site of infection. [20] This semisynthetic antibiotic because of its activity against Gram-negative bacteria, especially *Pseudomonas aeruginosa*, is commonly used to cure several bacterial infections, but its antibiotic efficacy often relies on rather high dosages.

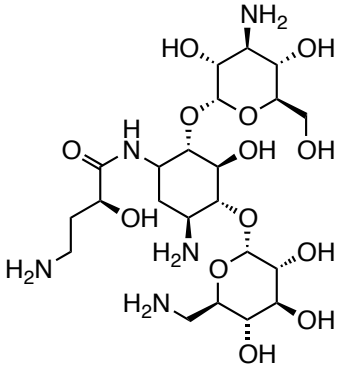

Amikacin

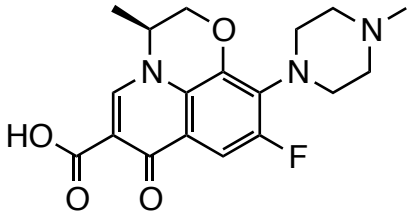

Levofloxacin

Barbera *et al.*[20] demonstrated that: a) **WP5** strongly binds amikacin (K_{ass} = (9.90 $\pm$ 1.28) $\times$ 10^3 M^{-1}) in a 50 mM phosphate-buffered saline (PBS) solutions in D_2O (pH 7.2); b) the antimicrobial activity of this pillararene-based drug-transport system tested against *Pseudomonas aeruginosa* ATCC27853, shows remarkable activity towards these bacteria,

exclusively prompted by amikacin; c) since the solubility of **WP5** is pH-dependant,[21] amikacin may readily be released back into solution as a result of a pH variation.

In a following account, Barbera *et al.*,[22] were also able to show that **WP5** recognizes and binds levofloxacin (**Lev**), a fluoroquinolone antibiotic used to treat a number of bacterial infections, including acute bacterial sinusitis, pneumonia, urinary tract infections, chronic prostatitis, and some types of gastroenteritis.[23] This drug is also commonly used, in conjunction with other drugs, for the treatment of tuberculosis, meningitis or pelvic inflammatory disease.[24] In this case, NMR titration experiments, carried out in a 50 mM PBS solution in D_2O (pH 7.2) indicated an association constant one order of magnitude lower (K_{ass} = (5.47 $\pm$ 1.16) $\times$ 10^2 M^{-1}) than that seen for amikacin.

In an attempt to find a better host molecule for levofloxacin, pillar[6]arene derivative **WSP6** became the synthetic target of the present study.

The structural features of this new water-soluble pillararene include a wider cavity, longer alkyl chains and two additional carboxylate moieties. As part of the design of cargo molecules for the complexation and subsequent release of pharmacologically active molecules, and in view of the results previously obtained by the research group in the manufacture of a multilayer system based on **WP5**, the structural changes made to the **WSP6** derivative are part of a screening process aimed at the selective recognition of drugs with antibacterial properties, in order to improve affinity and thus control over release. To this end, the effect of a larger cavity, provided by the six aromatic units as opposed to the five previously used in the cyclic adduct, was investigated. The choice of a functionalization with longer alkyl residues, on the other hand, lies in the possibility, at a later stage, of increasing the distance between the individual layers of the *Layer-by-Layer* (LbL) system (Section 4.4), with the intention of being able to trap a greater quantity of drug within the interstitial structure. With this in mind, the new **WSP6** derivative was synthesised.

In principle there are two different synthetic pathways for the preparation of **WSP6**: a) the direct cyclo-oligomerization of monomer **5** or b) the exhaustive alkylation of the preformed *per*-hydroxylated pillar[6]arene[32] **4** (Scheme 4.1).

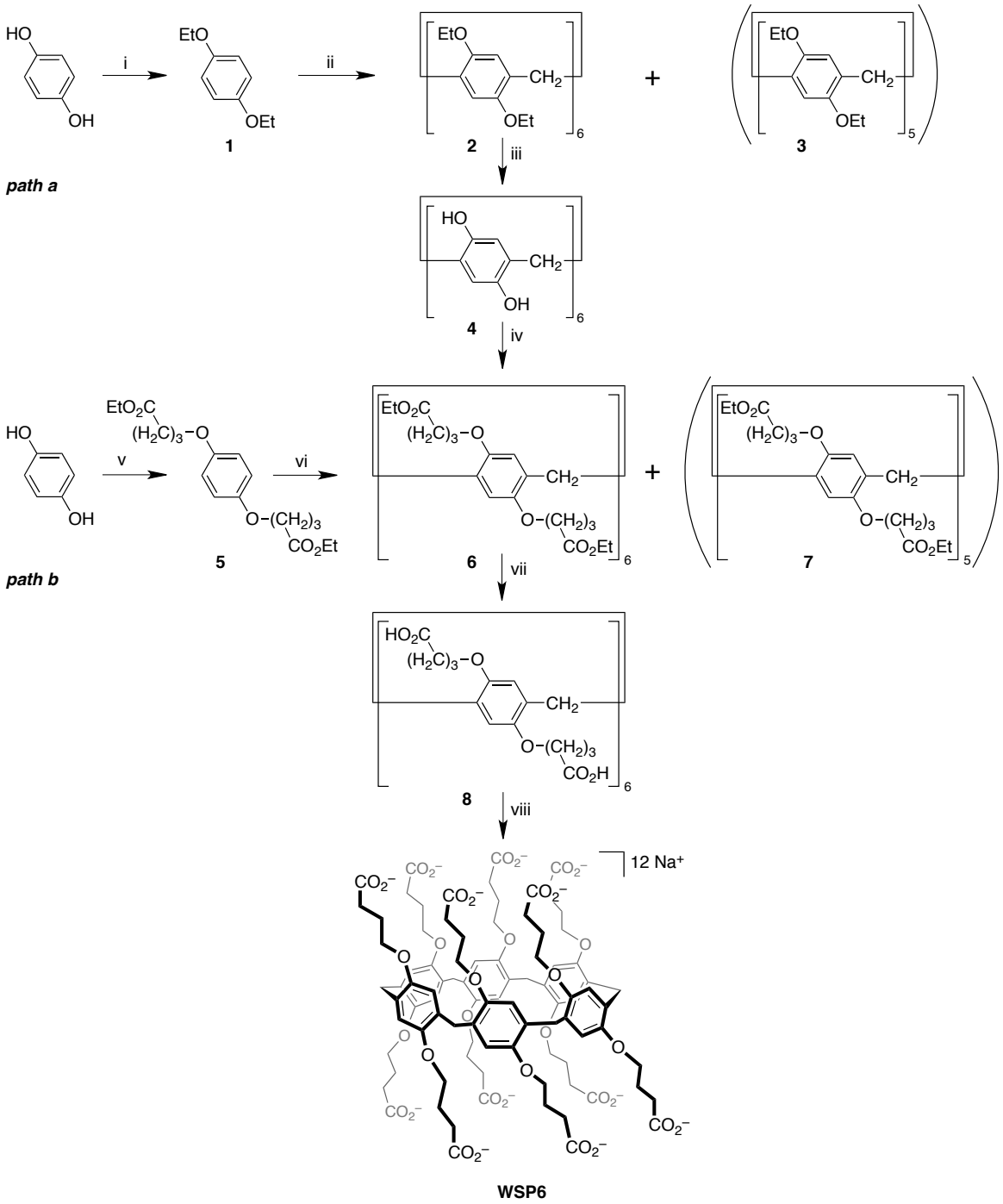

Scheme 4.1. The synthesis of dodeca-carboxylatopillar[6]arene **WSP6**. Reagents and conditions, path a: v) ethyl 4-bromobutyrate, K_2CO_3, refluxing CH_3CN, 24 h ; vi) $–(CH_2OH)_n–$, $FeCl_3$, dry CH_2Cl_2, r.t., 5 h; vii) 1. $NaOH_{(aq.)}$, EtOH, r.t., 15 h; 2. HCl 37%; viii) $NaOH_{(aq.)}$, THF/CH_3OH 1:1, r.t., 2 h. Path b: i) EtI, NaOH, DMSO, r.t., 2 h; ii) $–(CH_2OH)_n–$, $BF_3•OEt_2$, dry $CHCl_3$, r.t., 20 min; iii) BBr_3 dry CH_2Cl_2, r.t., 16 h; iv) ethyl 4-bromobutyrate, K_2CO_3, refluxing CH_3CN, 24 h.

The former involves the preliminary synthesis of diethyl 4,4′-(1,4-phenylenebis(oxy))dibutyrate (**5**) by treatment of hydroquinone with 4-ethyl-bromobutyrate using potassium carbonate as a base, the subsequent cyclo-oligomerization of monomer **5** in the presence of an appropriate Lewis acid catalyst and a suitable chlorinated solvent, followed by a base-catalysed hydrolysis of the resultant dodeca-ester **6** (Scheme 4.1, *path*

b). The latter requires a four-step procedure to obtain dodeca-ester **6** consisting in: a) the initial macrocyclization of 1,4-diethoxybenzene (**1**), to afford **2**; b) the cleavage of the alkyl groups with formation of the *per*-hydroxylated pillar[6]arene **4**; c) the conversion of **4** into the dodeca-ester **6** (Scheme 4.1, *path a*). Dodeca-ester **6** was then hydrolysed under basic conditions to provide the required dodeca-carboxylatopillar[6]arene **WSP6**.

In both instances, the pillararene macrocyclization reaction was found to be the critical step of the entire synthesis, as the pentamer (**3** and **7** in *path a* and *b*, respectively) is the thermodynamic product whereas the hexamer is the kinetic one when reaction is carried out in chloroform.[25,27] In the case of *path b*, in order to maximize the formation of the desired **WSP6** over its narrower analogue, different reaction times, solvents and acid catalysts were initially screened (Table 4.1). As far as *path b* is concerned, according to our data –in the presence of $FeCl_3$ as a catalyst and CH_2Cl_2 as the solvent– the longer is the reaction time, the lower are the yields of isolated pillar[6]arene (Table 4.1, entries 1–3). The best yields were obtained when the reaction was run for 5 hours.

Table 4.1. Reaction conditions[a] and relative isolated yields of dodecaester **6** and decaester **7**

Entry	catalyst	solvent	time (h)	**6** (%)	**7** (%)
1	$FeCl_3$	CH_2Cl_2	5	9	11
2	$FeCl_3$	CH_2Cl_2	17.5	4	9
3	$FeCl_3$	CH_2Cl_2	22	4	8
4	$FeCl_3$	$CHCl_3$	5	3	6
5	BF_3•OEt_2	$C_6H_{11}Cl$	5	n.d.	n.d.
6	$FeCl_3$	$C_6H_{11}Cl$	18	n.d.	n.d.

[a] All reactions were carried out at room temperature.

In the presence of $FeCl_3$, the use of chloroform instead of dichloromethane was unsatisfactory as the solvent templating-effect, attributed to CH_2Cl_2, went missing (compare entry 1 and 4).[26] Chlorocyclohexane –a solvent successfully used by Ogoshi and co-workers[27] for the synthesis of a dicyclohexylmethoxy-pillar[6]arene derivative– gave, in our hands, disappointing results in the presence of either $FeCl_3$ or BF_3•OEt_2 as the reaction catalyst (entries 5 and 6). In chloroform, the replacement of $FeCl_3$ with a different Lewis acid[28] (BF_3•OEt_2) or a Brønsted acid ($MeSO_3H$) catalyst[29] did not lead to any increment in the yields of the desired cyclic hexamer.

According to *path a* of Scheme 4.1, the cyclo-oligomerization of the less hindered 1,4-diethoxybenzene,[30] previously obtained from 1,4-hydroquinone and iodoethane,[31] proceeds

more efficiently. By carrying out this cyclization in anhydrous $CHCl_3$, in the presence of BF_3•OEt_2 as a catalyst,[26] dodeca-ethoxypillar[6]arene **2** and deca-ethoxypillar[5]arene **3**, were readily formed (20 min.) and easily isolated after column chromatography in 20 and 12% yield, respectively. Hexamer **2** was de-alkylated with BBr_3[32] to afford *per*-hydroxylated pillar[6]arene **4** quantitatively, and the latter subsequently converted to dodeca-ester **6** (30%), upon treatment with an excess of ethyl 3-bromopropionate. Despite the greater number of steps, *path a* affords **6** in higher overall yield than *path b*.

Direct and indirect (*via* the isolation of dodeca-carboxylic derivative **8**) hydrolysis of **6** to **WSP6** were both tested. In the first case, the use of a stoichiometric amount of NaOH –with respect to each ester group present in **6**– turned out to be rather laborious in terms of isolation and purification of dodeca-carboxylate **WSP6**. On the other hand, a similar treatment of **6** with an excess of base, followed by HCl addition, isolation of dodeca-acid **8**, and then quantitative conversion to the corresponding sodium salt **WSP6** turned out to be a more convenient procedure.[33]

With the new water-soluble pillar[6]arene **WSP6** in hands, the affinity towards **Lev** was preliminarily tested by ^{1}H NMR spectroscopy, by adding increasing aliquots of the antibiotic (0.5, 1.0 and 2.0 equiv. of [**Lev**] = 25 mM in the same PBS solution, see below) to a 1.0 mM solution of **WSP6** dissolved in a 60 mM PBS solution in D_2O (pH 7.2), to assess whether host-guest binding took place at all and whether this eventually occurred in a fast or slow regime on the NMR timescale (Figure 4.1).

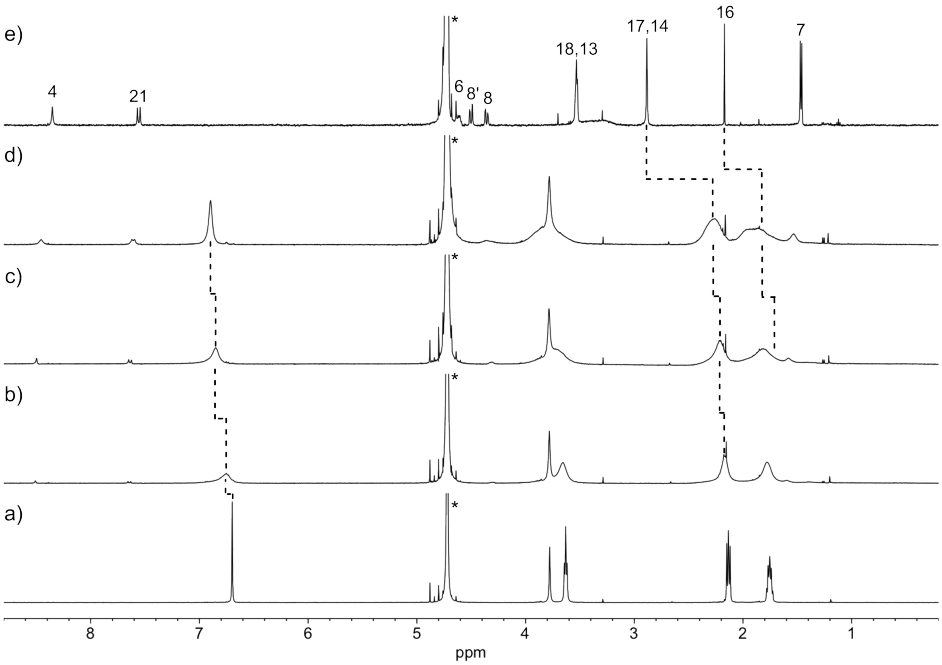

Figure 4.1. ^{1}H NMR spectra (500 MHz, D_2O, 298 K) of: a) [**WSP6**] = 1.0 mM; b) [**WSP6**] = 1.0 mM and [**Lev**] = 0.5 mM; c) [**WSP6**] = [**Lev**] = 1.0 mM; d) [**WSP6**] = 1.0 mM and [**Lev**] = 2.0; and e) [**Lev**] = 1.0 mM solutions. The asterisks indicate the residual solvent peak (HDO).

The choice of recording the NMR spectra in PBS derives not only from the intention to mimic the physiological conditions for release, but also from the need of having to analyse sharper host peaks in the course of the titration experiments. **WSP6** shows in neat D_2O rather broad peaks, which could, in principle, complicate the spectral analysis of the following host-guest binding process. Upon complexation, the hydrogen atoms of the guest piperazine ring underwent substantial upfield complexation-induced shifts (CIS). The extent of these CIS progressively decreased as the titration went on. These results are in agreement with the formation of an inclusion complex undergoing fast association/dissociation, in which the piperazine moiety of levofloxacin is located within the magnetic shielding region of the **WSP6** cavity. Peak assignments for the included moiety of **Lev** derive from a COSY NMR spectrum (Figure 4.2).

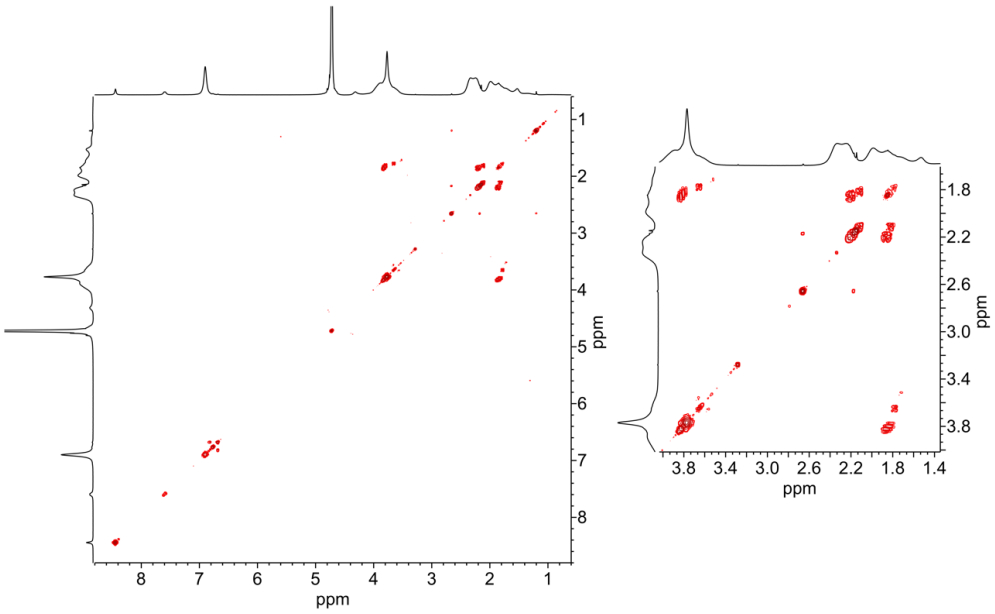

Figure 4.2. COSY spectrum (500 MHz, D_2O, 298 K) of [**WSP6**] = 7.5 mM and [**Lev**] = 15.0 mM solution in PBS 60 mM.

The inclusion of levofloxacin within the cavity of **WSP6** was additionally confirmed by a NOESY experiment (Figure 4.3) –carried out in the presence of an excess of guest– which showed intermolecular correlation peaks between the aromatic hydrogen atoms of the pillararene scaffold and H_{14}, H_{16} and H_{17} of **Lev**. The piperazine ring signals undergo conspicuous shifts and broadening, thus suggesting a strong host-guest affinity between **WSP6** and **Lev**. NMR titration experiments were later carried out to assess the association constant (K_{ass}) in PBS solution.

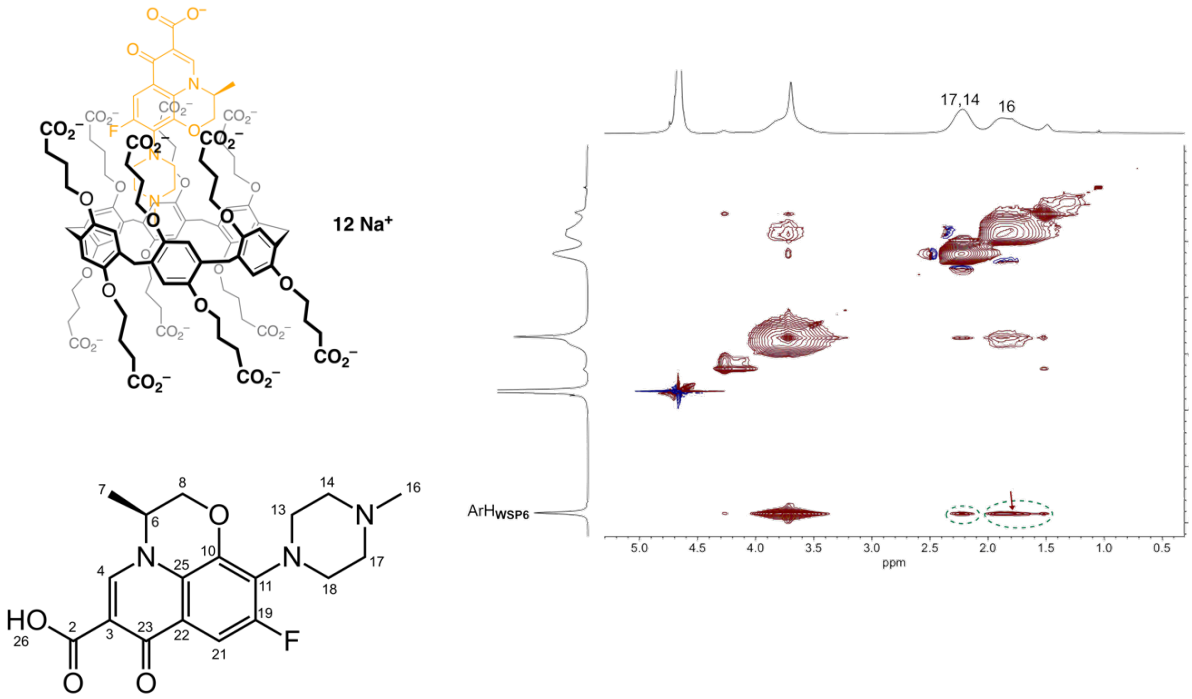

Figure 4.3. NOESY spectrum (500 MHz, D_2O, 298 K) of [**WSP6**] = 7.5 mM and [**Lev**] = 15.0 mM solutions in PBS 60 mM.

To this end, increasing amounts of levofloxacin ([**Lev**] = 0.05–2 mM) were added to a 1.0 mM solution of **WSP6** and the chemical shift values of the ArH resonance at different guest concentrations were tallied and interpolated, assuming both a 1:1 and a 1:2 complexation model for **WSP6/Lev**. Only in the former case we found a cogent fitting curve. In addition, a 1:1 binding stoichiometry was further confirmed by the inflection point derived from the tangent method[34] (Figure 4.4).

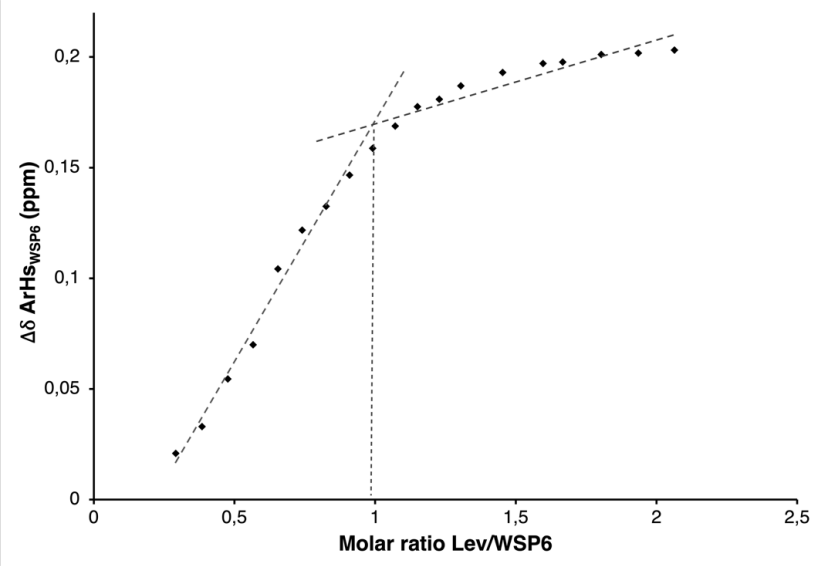

Figure 4.4. ArH downfield shifts for [**WSP6**] = 1 mM upon successive additions of increasing amounts of **Lev**; the point of inflection determines the guest/host molar ratio.

The association constant was derived from the *Nelder-Mead* nonlinear optimization method of the experimental δ_{ArH} values of **WSP6** observed upon addition of **Lev** (Figure 4.4), using the BindFit v0.5 program.[35] Accordingly, in a 60 mM PBS solution **WSP6** and **Lev** were found to bind with a $K_{ass} = (1.94 \pm 0.34) \times 10^3\ M^{-1}$.

The successive task was the development of levofloxacin@**WSP6**-based multi-layered films with antibiotic loading-and-releasing properties similar to those previously described by Barbera *et al.*[20]

4.4 Layer-by-layer assembly of WSP6/levofloxacin films

Over the past few decades layer-by-layer (LbL) assembly has emerged as a powerful technology for fabricating nanostructured multi-layered films and nanocomposites with tailored composition, structure and thickness, and various functions.[36] The LbL strategy, when carried out in aqueous media, represents a simple, low-cost and mild method to obtain functional surface modification. LbL assemblies are formed by stepwise alternate adsorption of complementary building blocks of different nature (such as polyelectrolytes,[37] DNA, dendrimers,[38] nanoparticles (NPs),[39] polypeptides,[40] macrocycles,[41] etc.) on a substrate of any shape and size, occurring either via electrostatic or non-electrostatic interactions (hydrogen bonding, metal-ion coordination, host-guest interaction, covalent bonds, and so on).

LbL films have shown potential applications in the areas of nanoreactors, electrochemical devices, separation membranes, biosensors, surface modification, coatings and drug delivery. LbL-based drug delivery systems are able to exploit many of their unique features synergistically:[42] (i) both water-soluble/non-soluble substrates can be loaded onto these devices; (ii) they can be designed in a way that can retain their original sturdiness and stability within a wide range of temperature, pH and ionic strength as well as under physiological conditions; (iii) drug release can be controlled by external stimuli; (iv) the release can be further controlled by assembling a variable number of layers, which act as a controllable barrier against drug diffusion; (v) multiple drug delivery is achievable by incorporating different drugs within the layers of the film, owing to the possibility of selecting the type of materials deposited along the vertical axis; (vi) multi-layered films can be loaded with growth factors and stored for long periods of time as high as one year without extensive degradation or bioactivity loss; (vii) finally, the versatility of LbL allows the construction of systems with the more appropriate shape to the desired end. However, LbL construction is

not without disadvantages. It involves long construction times, with the assembly of a single layer taking typically a few minutes depending on the nature of the component used.

Bioactive molecules such as drugs, proteins, peptides, and even nucleic acids can be incorporated within a LbL film following two main routes. One involves the direct inclusion of the drug as one of the building blocks during the construction of the film. Thus, changing the number of layers can regulate the amount and the nature of the loaded bioactive agents. However, in multi-layered structures the building blocks may exhibit interlayer diffusion, which may be difficult to control over their subsequent release.[43] A second route for drug loading within thin films involves an immobilization step where the film anchoring the carrier is exposed to a concentrated solution of the drug to be loaded. Such an approach is viable for low molecular weight drugs, which diffuse easily through the pores of the film.[44] Alternatively, both strategies can be used simultaneously.[45] The fabrication of multi-layered functional systems incorporating bioactive molecules may also proceed via the pre-assembly of suitable host-guest complexes, by taking advantage of cargo macrocycles (such as pillar[*n*]arenes). These complexes are then used as building blocks for the assembly of the required film. As **WSP6** is able to tightly bind levofloxacin under physiological conditions, the next step was to integrate the host-guest ability of this water-soluble pillar[6]arene with a LbL film coating, characterized by biocidal and anti-fouling activity, to generate a system capable of preventing bacterial adhesion and proliferation on a given surface (*e.g.*, a medical implant/device). To this end, glass and quartz substrates were coated with prototype LbL films, via the electrostatic interaction method. Layers of polyallylamine hydrochloride (**PAH**) and dodeca-carboxylatopillar[6]arene **WSP6** –as the cationic and anionic components, respectively– were alternated with the final aim of obtaining, after levofloxacin loading, functional surfaces coated with a film endowed with antibacterial properties.

As mentioned earlier, LbL films were obtained by successive deposition of **WSP6** and **PAH** on glass or quartz (for UV-Vis measurements) slides. Experimentally, slides were initially treated with concentrated nitric acid to eliminate any organic remains,[46] and then alternatively dipped in appropriate solutions (1–3 mg/mL) of the cationic and anionic component (see Experimental Section). An aqueous solution of cationic polyethylenimine **PEI** was used for the initial amination step of the pre-treated slides. Then, multi-layered films (**WSP6/PAH**)$_8$ were obtained by repeating alternate immersion steps in **WSP6** and **PAH** solutions (Figure 4.5a) and by thoroughly washing the final multi-layer surface with a large amount of water to remove any excess of adsorbed material.

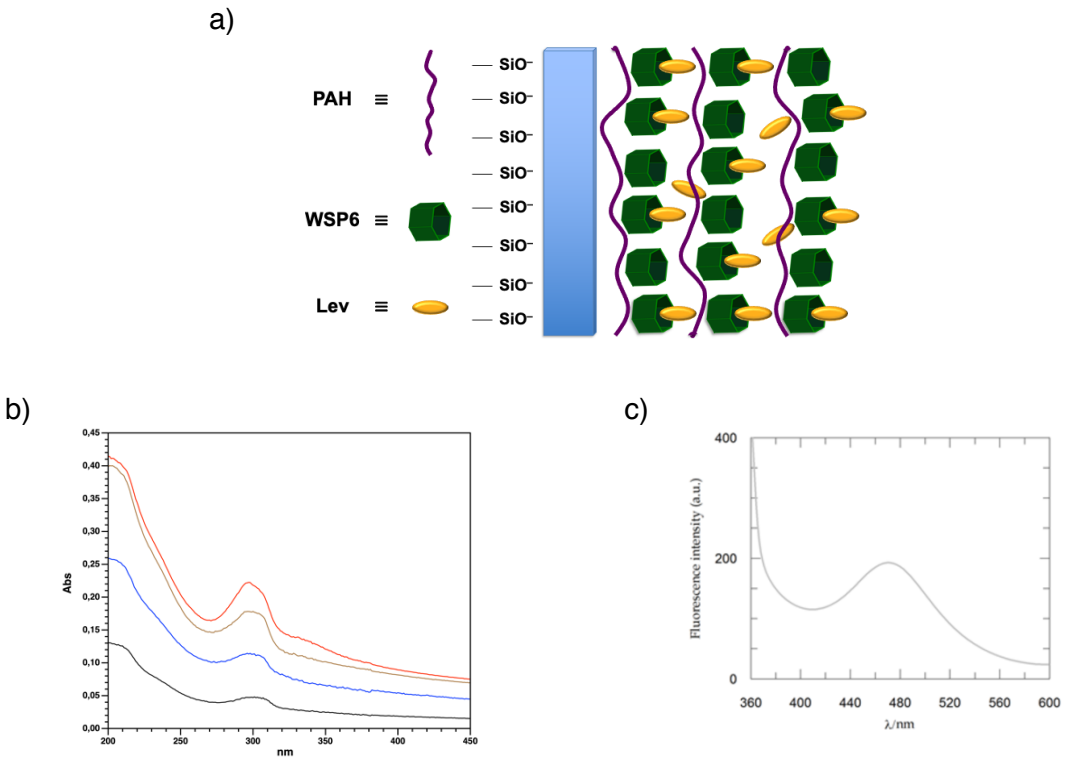

Figure 4.5. a) Cartoon representation of **Lev**@(**WSP6/PAH**)$_n$ film coating; b) UV-Vis spectra of: (**WSP6/PAH**)$_2$ (black trace), (**WSP6/PAH**)$_4$ (blue trace), (**WSP6/PAH**)$_6$ (maroon trace), (**WSP6/PAH**)$_8$ (red trace) ; c) fluorescence emission spectrum (λ_{exc} = 289 nm) of (**WSP6/PAH**)$_8$ after levofloxacin loading.

The growth of the multi-layered coated surface was monitored by UV-Vis spectroscopy, after each immersion step in the **WSP6** solution (Figure 4.5b). The absorbance of **WSP6** (λ = 292 nm) increases as the number of pillararene layers grows, thus confirming the deposition of the oppositely charged electrolytes on the slide surface.

Finally, to load the antibiotic, the glass (or quartz) slide coated with the (**WSP6/PAH**)$_8$ multilayer film was dipped in an aqueous solution of levofloxacin (2.2 mg/mL) for 2 hours, thoroughly rinsed with water and then let to dry at 60° C. Subsequent to this treatment, levofloxacin loading was conveniently confirmed by UV-Vis and fluorescence measurements carried out on the quartz slides. Thus, LbL-coated quartz plates, when excited at λ_{exc} = 289 nm, displayed the typical fluorescence emission spectrum of levofloxacin (λ_{max} = 470 nm, Figure 4.5c). In a similar fashion, the kinetic profile of the *in vitro* release of levofloxacin from (**WSP6/PAH**)$_8$ and **Lev**@(**WSP6/PAH**)$_8$ was assessed spectrophotometrically in a 60 mM aqueous solution of PBS at pH 7.2, kept at 37±1 °C. Levofloxacin release was monitored (λ = 289 nm) at specific intervals, over a period of 8 hours, under experimental conditions deliberately set to mimic the physiological conditions.

Figure 4.6 shows an initial burst of levofloxacin release into the medium within 20 minutes, followed by a steady release in the subsequent 8 hours.

Compared to previous results, reported by Barbera *et al.*,[22] related to the use of the analogous (**WP5/PAH**)$_8$ multi-layered film, this new pillar[6]arene-based coating is able to load and release a higher dose of levofloxacin (4.8 *vs.* 3.0 μg/mL for (**WSP6/PAH**)$_8$ and (**WP5/PAH**)$_8$, respectively, the latter measured in a 50 mM PBS solution) as shown in Figure 4.6. In addition, the release from the **Lev**@(**WSP6/PAH**)$_8$ system is slightly slower in the same aqueous medium compared to **Lev**@(**WP5/PAH**)$_8$.

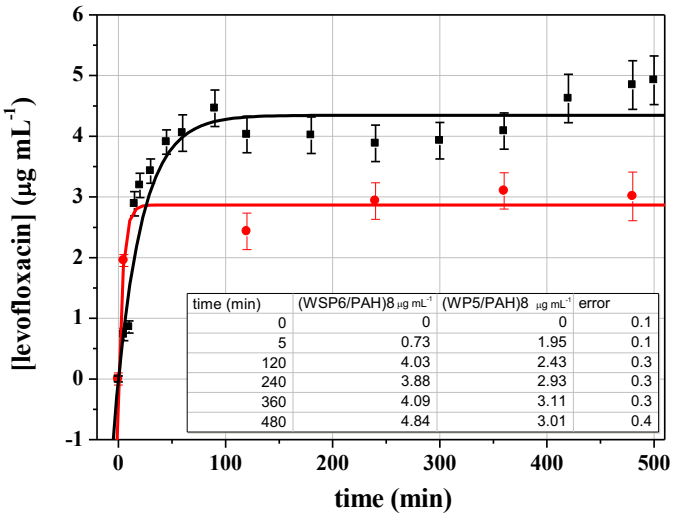

time (min)	(WSP6/PAH)8 μg mL-1	(WP5/PAH)8 μg mL-1	error
0	0	0	0.1
5	0.73	1.95	0.1
120	4.03	2.43	0.3
240	3.88	2.93	0.3
360	4.09	3.11	0.3
480	4.84	3.01	0.4

Figure 4.6. Comparison of the *in vitro* release profile of levofloxacin from a **Lev**@(**WSP6/PAH**)$_8$ (black line) and a **Lev**@(**WP5/PAH**)$_8$ multilayer film (red line)[22] in 60 and 50 mM PBS solution, respectively (pH 7.2, T = 37 °C). Data are fitted to pseudo first order kinetic model (see Materials and Methods in Experimental Section).

A different outcome is observed when levofloxacin is loaded onto the multi-layer film along the way during LbL deposition as a **Lev**⊂**WSP6** complex. In this case, the absorption to the multi-layer is not as efficient as the one described above (*i.e.*, **Lev** loaded onto the pre-formed (**WSP6/PAH**)$_8$ multilayer film); the *plateau* is reached in just 1 minute because of the exiguous amount of antibiotic released (0.85 μg/mL) by the LbL, probably as a result of an overall lower amount of levofloxacin loaded in the first place.

To experimentally quantify the influence of a number of coating layers on the performance of the drug-releasing system, a **Lev**@(**WSP6/PAH**)$_4$ multi-layer was also prepared. Figure 4.7 clearly shows that the quantity of drug released in this case was just over half of the one previously freed (2.5 μg/mL for **Lev**@(**WSP6/PAH**)$_4$ *vs.* 4.8 μg/mL for **Lev**@(**WSP6/PAH**)$_8$). So, the quantity of drug released by the system is strictly dependant on the number of the coating layers present on material's surface.

On the other hand, the trend is quite different when the release from **Lev**@(**WSP6/PAH**)$_8$ is measured in ultrapure water with the temperature set at 29 °C (Figure 4.8). Over a period of 8 hours, the drug is released from the system much more slowly.

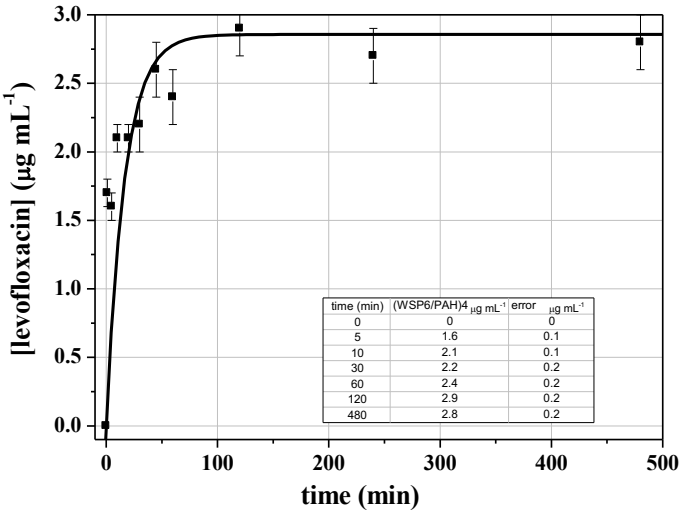

Figure 4.7. In vitro release profile of levofloxacin in PBS (60 mM at pH 7.2) from a (**WSP6/PAH**)$_4$ multilayer film at T = 37 °C. Data are fitted to pseudo first order kinetic model (see Materials and Methods in Experimental Section).

Therefore, by changing the temperature, pH, and number of layers in the coating film it is possible to control the timing and quantity of drug released in solution by the multi-layers system. Such a material, thus providing on request a sudden availability of the drug, could in principle be useful for the coating of medical equipment for surgical use, in which there is a need to have a fair amount of antibiotic in the limited time of the intervention. On the other hand, a slow and constant release would certainly make these materials useful for hospitalization purposes and long-term care, allowing a more effective prevention of nosocomial infections.

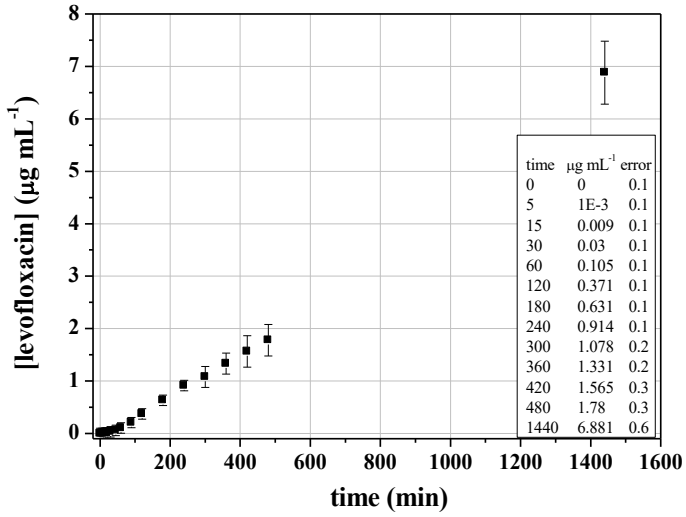

Figure 4.8. In vitro release profile of levofloxacin in ultrapure water from a (**WSP6/PAH**)$_8$ multilayer film at T = 29 °C.

4.5 Antimicrobial studies on the WSP6/levofloxacin films

The *in vitro* antimicrobial activity of the new pillararene-based drug-transport system was tested against *Staphylococcus aureus* ATCC29213 at a fix sub-MIC concentration of levofloxacin. To this end, we firstly determined the Minimum Inhibitory Concentration (MIC), namely the lowest concentration of an antimicrobial agent able to prevent the growth of a bacterial strain. In order to determine the MIC of levofloxacin, cultures of *S. aureus*, at a final inoculum of approximatively 10^4–10^5 bacteria per mL, were cultured with increasing aliquots of levofloxacin, ranging between 0.25 and 64 μg/mL. The MIC_{90}, *i.e.*, the lowest concentration of a drug required to prevent 90% of microbial growth of levofloxacin, was found to be 1 μg/mL. For antimicrobial susceptibility testing medium was used a Mueller-Hinton broth (MHB), containing *S. aureus* (4.5×10^4 bacteria per mL) and bacterial growth was then monitored by counting the Colony Forming Units (CFUs) in the bacterial suspension, at given time intervals (6, 24, 48 h).

Figure 4.9 shows the microbial culture medium after incubation with **Lev**@(**WSP6/PAH**)$_8$ and (**WSP6/PAH**)$_8$ films.

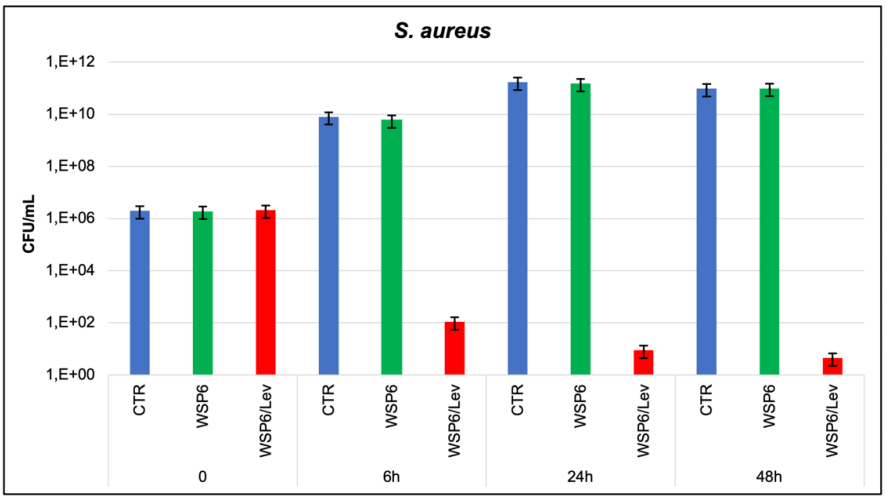

Figure 4.9. Colony-forming units (CFUs) of *S. aureus* grown in a Mueller-Hinton broth (MHB) as the testing medium after 6, 24, 48 h of incubation, carried out in the presence of: (**WSP6/PAH**)$_8$ films as such, **Lev**@(**WSP6/PAH**)$_8$ films, and the control culture (green, red and blue bars, respectively).

In agreement with previous findings on the lack of any biocidal activity of **WP5** against *S. aureus*, also **WSP6** and (**WSP6/PAH**)$_8$ films, cultured in the above-mentioned bacterial suspension, showed no toxic effects on the microorganism growth. Conversely, **Lev**@(**WSP6/PAH**)$_8$ films were found to be extremely efficient in inhibiting bacterial colonizations, causing dramatic (~10^4 fold), steady and persistent CFU decrease after 6 hours. The bacterial activity exerted by **Lev**@(**WSP6/PAH**)$_8$ lasts up to 48 hours.

Live/Dead staining test carried out on the free bacteria in the culture medium (Figure 4.10) further confirmed results obtained from the Colony Forming Units (CFU) assay. Bacteria present in the control culture (CTR) and in the well containing the (**WSP6/PAH**)$_8$ slides were found to have intact cellular membranes (green fluorescent) at given incubation time. On the contrary, a low number or hardly any cells were detected in the presence of **Lev**@(**WSP6/PAH**)$_8$ films after 6–24 and 48 h, respectively. Moreover, in presence of the **Lev**@(**WSP6/PAH**)$_8$ system, bacteria with damaged cellular membranes were seen to significantly increase in the 6 to 24 h incubation time period.

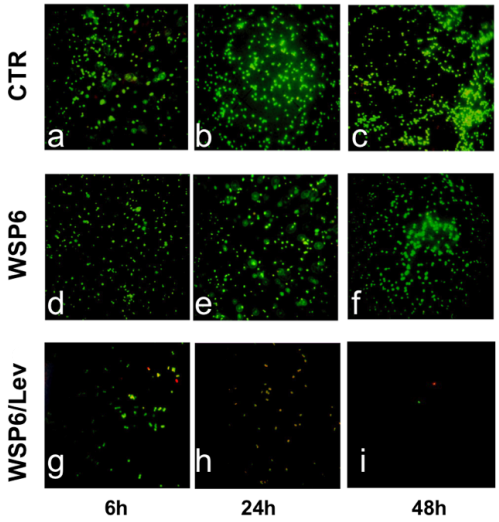

Figure 4.10. Fluorescence images of bacteria in suspension after 6 (a,d,g), 24 (b,e,h) and 48 (c,f,i) hours. The green and red stains indicate the presence of live or dead bacteria, respectively.

The contact-killing and adhesion resistance properties of the **Lev**@(**WSP6/PAH**)$_8$ films were also screened with the *Live/Dead Bac*Light™ bacterial viability kit (Figure 4.11). To this end after a period of 6, 24 and 48 hours of incubation in bacterial cultures, quartz-coated plates were stained by using *Live/Dead kit* and fluorescence images were recorded.

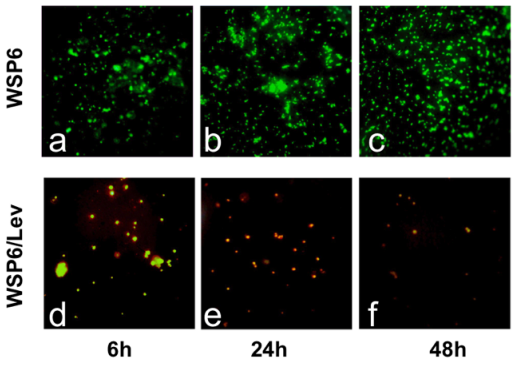

Figure 4.11. Fluorescence images of adhered bacteria after 6 (a,d), 24 (b,e) and 48 (c,f) hours. The green and red stains indicate the presence of live or dead bacteria, respectively.

Antibiotic-free samples ((**WSP6/PAH**)$_8$) showed a high density of live cells (green stains) while substrates coated with the **Lev**@(**WSP6/PAH**)$_8$ film displayed rare zones of dead bacteria (red stains) thus demonstrating the strong biocidal activity of the surface. These findings were also confirmed by quantitative analysis of the surface coverage, in terms of Integrate Density (I.D.) (Table 4.2).

Table 4.2. Adhesion of *S. aureus* cells on **Lev**@(**WSP6/PAH**)$_8$ and (**WSP6/PAH**)$_8$ films in terms of I.D. mean values

		Lev@(**WSP6/PAH**)$_8$	(**WSP6/PAH**)$_8$
Incubation period	**6h**	6.9×10^4	3.4×10^5
	24h	4.1×10^4	5.9×10^5
	48h	2.4×10^4	7×10^5

In fact, by comparing the I.D. values of **Lev**@(**WSP6/PAH**)$_8$ and (**WSP6/PAH**)$_8$, it is possible to observe that the rate of *S. aureus* adhesion was reduced by 80, 93 and 97%, after 6, 24 and 48 hours, respectively (Figure 4.12).

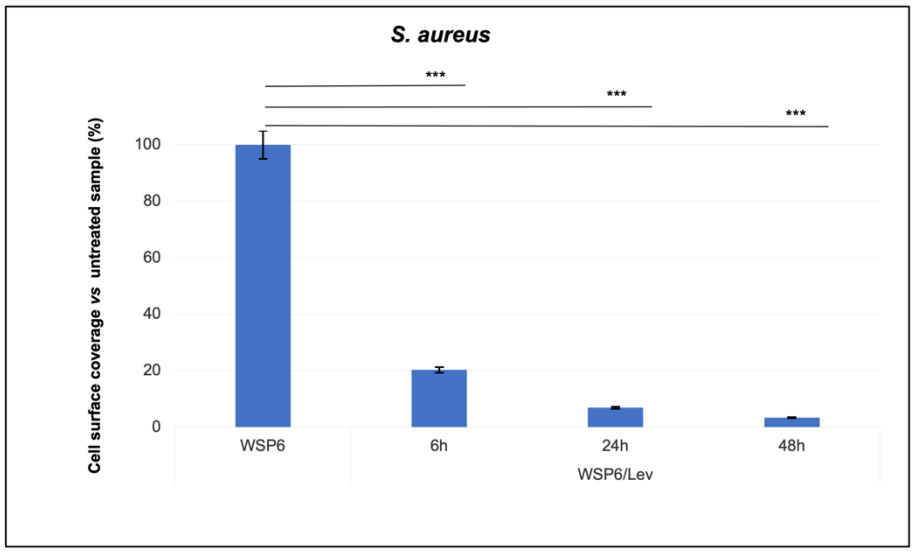

Figure 4.12. Percentage of cell surface coverage of treated samples *vs*. untreated sample. For ANOVA test from Bonferroni's multiple comparisons test, three (***) asterisks identify adjusted p-value between 0.001 and 0.0001 (for additional details see Antibacterial activity assessment in Experimental Section).

These preliminary findings indicate that the new **WSP6** receptor is a good candidate for the development of multi-layered films with antibiotic loading/releasing and antibiofilm properties and open up new avenues for the engineering of antiadhesive and antibacterial surfaces for medical devices.

4.6 Recognition and solubilization of doxorubicin

In a more comprehensive search for additional bioactive targets to be loaded onto pillar[6]arene-based multilayers, rhodamine B, amikacin sulphate, histamine, and ciprofloxacin were screened by ^{1}H NMR spectroscopy, both in water and in PBS solution, for their affinity towards **WSP6**. In all these instances, however, unsatisfactory results in terms of binding constants were detected and further investigations were abandoned. Next, **WSP6** was tested as a potential cargo macrocycle for doxorubicin (**Dox**).

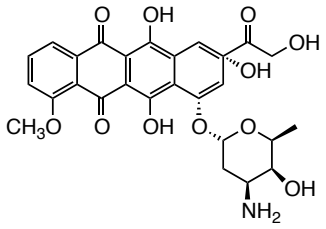

Doxorubicin

Doxorubicin, on its own or in combination with other chemotherapeutic agents, is a common first line therapy for numerous cancers including breast, ovarian, bladder, and lung. Although the mechanism of action for **Dox** is still being studied, proposed mechanisms include intercalation into DNA disrupting gene expression, generation of reactive oxygen species, and inhibition of topoisomerase II, a gyrase important for DNA synthesis and replication.[47] Notably, the delivery method may influence the pathway activated by **Dox**, which is not free from side effects. The most serious long-term adverse effect of **Dox** therapy is irreversible cardiomyopathy, which is highly affected by increased levels of reactive oxygen species, resulting in apoptosis in the heart. Formulations of doxorubicin with cyclodextrins, with which this drug has a high affinity, have been extensively studied, for tumour-selective cancer chemotherapy.[48] On the other hand, release systems based on nanoparticles are widely used, as they are capable of encapsulating the drug and delivering it selectively.[49] Multilayer release systems obtained LbL assembly technique have also been developed.[50]

Recently, this anticancer drug has been combined with water-soluble pillar[*n*]arenes. Particularly, interesting systems have been obtained with the water-soluble pillar[6]arene **WP6** and doxorubicin, in which the ability of the macrocycle to form micelles in a basic environment is exploited to convey and subsequently release the drug in an acid environment, following a change in the pH.[51] However, in this case doxorubicin is not included as such in the pillararene cavity, but in the form of a prodrug, and it is precisely the added moiety that binds the water-soluble pillar[6]arene. A more complex formulation has

involved the use of a spacer covalently linked to doxorubicin, for the formation of a supramolecular prodrug micelles based on the host-guest interaction between water-soluble pillar[6]arene (**WP6**) and novel doxorubicin-based prodrugs.[52] In this case, upon a pH variation, the carboxylic functionalities, present on **WP6**, trigger the cleavage of the bond between the spacer and the drug, allowing the release of **Dox** in solution after the separation from the nanoparticle.

Up to now, unlike the case of cyclodextrins,[48] no evidence of host-guest complex formation between any water-soluble pillar[6]arene and **Dox** have been reported. The low affinity of the pillararenes tested so far and the poor solubility of **Dox** in water and aqueous buffer solutions being probably the reason why these molecules do not recognize each other efficiently. Doxorubicin (hydrochloride) has a solubility of approximately 0.5 mg/mL in a 1:1 solution of DMSO/PBS (pH 7.2). It is known that the affinity between a macrocycle and a poorly soluble substrate/molecule can in principle be exploited for enhancing the solubility of the latter in a given media –where the macrocycle is soluble– as a result of the formation of stable macrocycle-substrate intra-cavity complexes. For example, **WP6** was used as a solubilizing agent to enhance the solubility and bioactivity of tamoxifen, a well-known anticancer drug poorly water-soluble anticancer drug.[53] In our case, we found that the new **WSP6** is able to form a host-guest complex with doxorubicin and in so doing enhance its solubility in water. The affinity between the two was studied by ^{1}H NMR spectroscopy by adding increasing amounts of **Dox** (0.5, 1.0 and 2.0 equiv.) to a 1 mM solution of **WSP6** in D_2O (Figure 4.13).

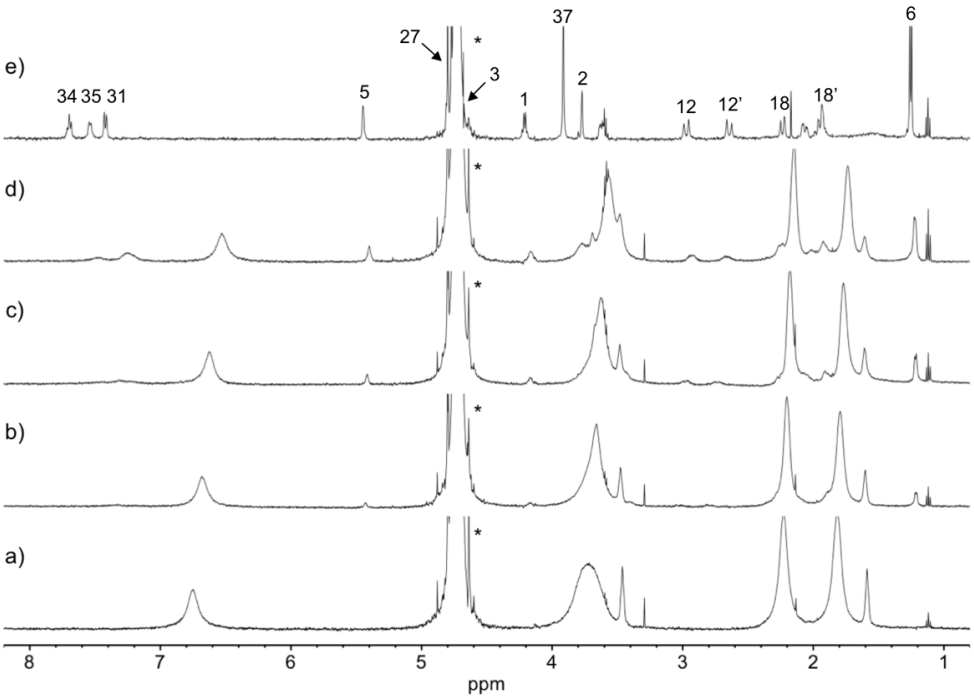

Figure 4.13. ^{1}H NMR spectra (500 MHz, D_2O, 298 K) of: a) [**WSP6**] = 1.0 mM; b) [**WSP6**] = 1.0 mM and [**Dox**] = 0.5 mM; c) [**WSP6**] = [**Dox**] = 1.0 mM; d) [**WSP6**] = 1.0 mM and [**Dox**] = 2.0; and e) [**Dox**] = 1.0 mM solutions. The asterisk identifies the HDO peak.

The complexation process was found to be fast on the NMR timescale and, accordingly, an association constant of $8.25 \times 10^2 \pm 3.38$ M^{-1} was determined (WinEQNMR [54]), by monitoring the progressive upfield shifts of the **WSP6** ArH resonances.

Peak assignment for the included moieties of doxorubicin took advantage of NOESY and COSY experiments (Figure 4.14 and 4.15, respectively). In particular, the NOESY spectrum of a 0.7:1 mixture of **WSP6** and **Dox**, obtained after centrifugation of the initial suspension, showed among others, correlation peaks between the OMe group of **Dox** and the ArHs and $CH_2CH_2CO_2^-$ resonances of **WSP6**.

A DOSY experiments carried out in D_2O on a 1:1 **WSP6**/**Dox** mixture revealed that host and guest form a discrete 1:1 complex as the diffusion coefficient of such a species is very close to the one recorded for the deca-carboxylatopillar[5]arene obtained from **7** ($D_{WSP6@Dox}$ = 1.8 × 10^{-10} m^2/s and D_{WSP5} = 2.0 × 10^{-10} m^2/s).

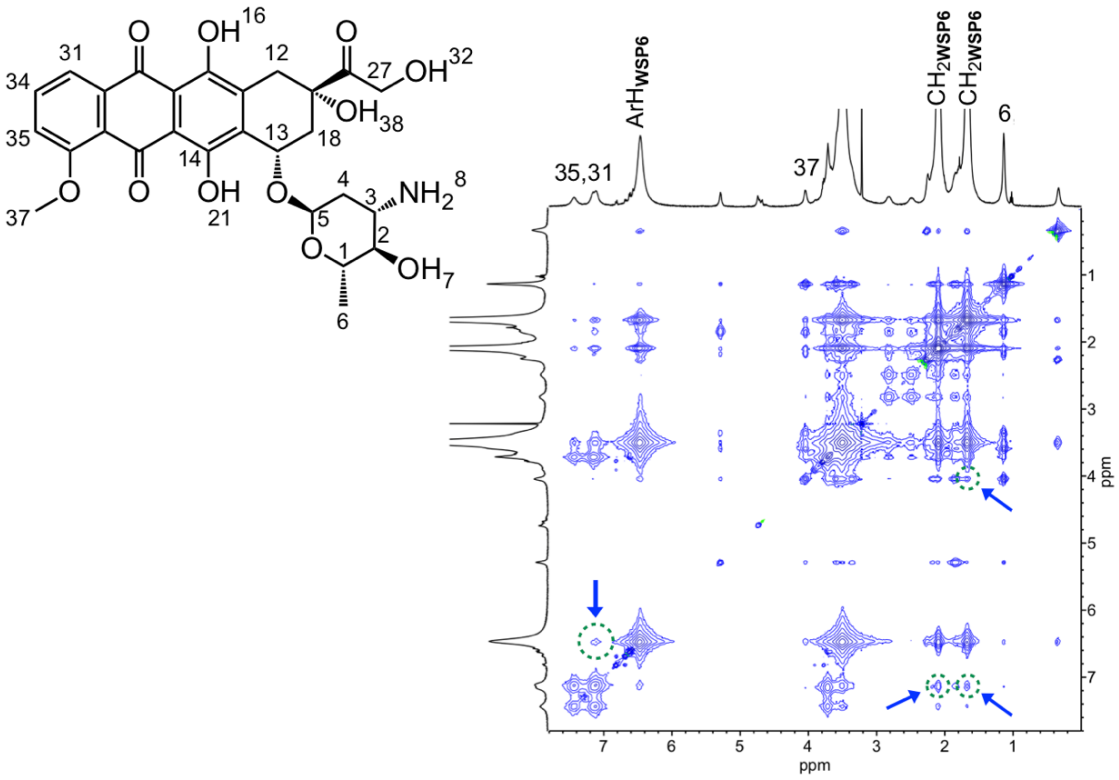

Figure 4.14. 2D NOESY spectrum (500 MHz, D_2O, 298 K) of a [**WSP6**] = 10 mM [**Dox**] = 15 mM solution.

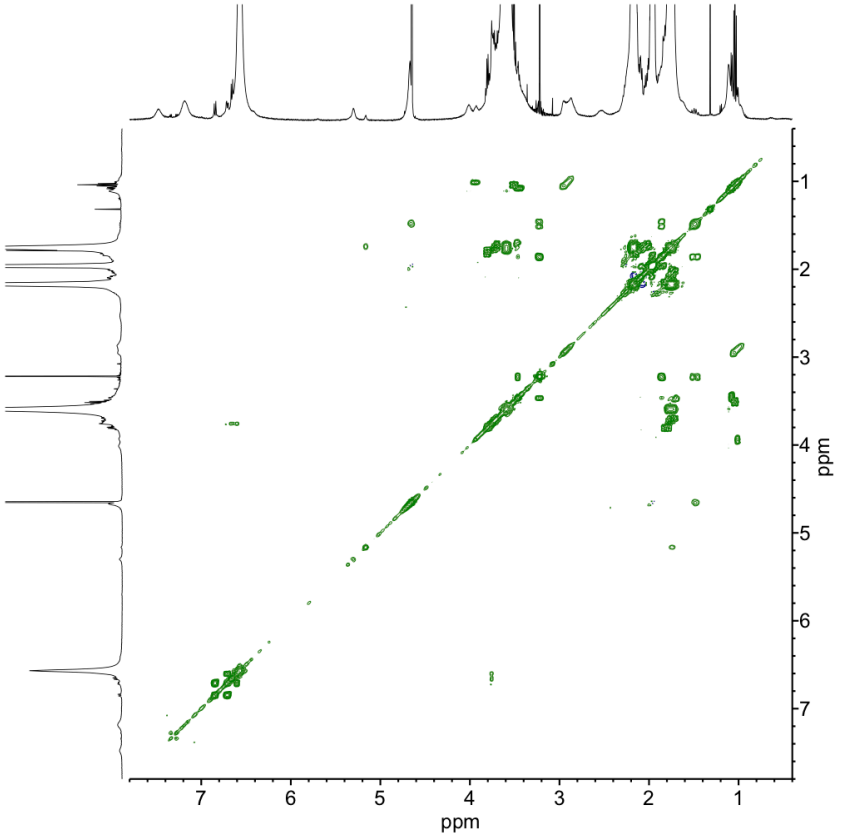

Figure 4.15. COSY spectrum (500 MHz, D_2O, 298 K) of a [**WSP6**] = [**Dox**] = 2 mM solution.

To assess whether **WSP6** was able to enhance the solubility of doxorubicin in an aqueous solution, we carried out a solid-liquid extraction experiment in which a fix amount of **Dox** (5 μmol) was initially suspended in a 60 mM PBS D_2O solution and then extracted for 4 hours at 25 °C with PBS solutions containing increasing concentrations of **WSP6** (0, 0.5, 1.4, 3.1 and 6.6 mM). The five suspensions were then centrifuged to remove the excess of undissolved doxorubicin and the supernatant was quantitatively transferred in an NMR equipped with a coaxial tube, containing a 40 mM solution of maleic acid as an internal quantitative standard. As shown by the phase solubility diagram reported in Figure 4.16, the highest concentration of **Dox** that a 60 mM PBS solution of **WSP6** is able to extract was found to be 3.8 mM. This value was obtained by plotting the values of doxorubicin concentrations, calculated by ^{1}H NMR analysis (*Henderson equation*),[55] *versus* the concentrations of a given **WSP6** extracting solution.

Interestingly, only the doxorubicin solutions containing **WSP6** survived to prolonged storage (up to two months) at 4 °C. On the contrary, a control solution of **Dox** on its own, kept under identical conditions, showed (^{1}H NMR) extensive decomposition. This means that **WSP6** is also able to stabilize solutions of this drug preventing their decomposition, a property that undoubtedly could in principle be exploited for the preparation of solutions for medical use.

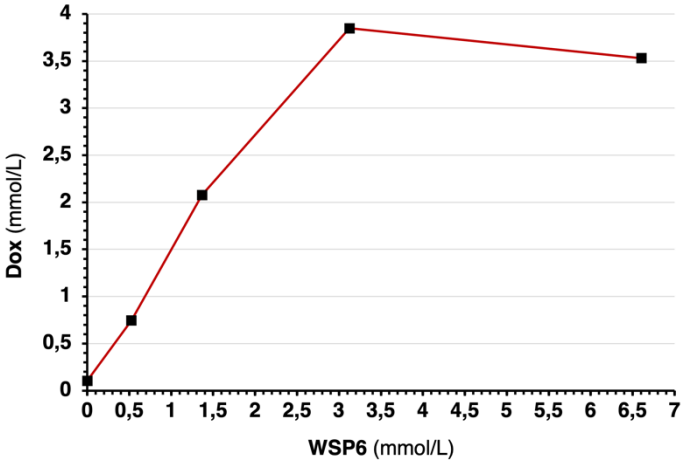

Figure 4.16. Phase solubility diagram of solid **Dox** (2,9 mg; 5 µmol) extracted with **WSP6** solutions of increasing concentration in PBS 60 mM.

In the light of these data, the **Dox⊂WSP6** complex may be seen as a promising drug delivery system, providing the pillararene scaffold is not cytotoxic and it is able to act as a cargo molecule for the selective release of doxorubicin inside tumour cells. The markedly acidic environment found inside neoplastic cells could, in principle, induce the protonation of the pillararene carboxylic functions and, as a result, favour the intra-cellular release of the drug.

To assess the anti-angiogenic properties of the **Dox⊂WSP6** complex, *in vitro* tests were carried out on different tumour cell lines. The preliminary data reported in Table 4.3 were conducted on breast (BT474), lung (A549) and ovarian (A2780) cancer cells.

Table 4.3. Cancer cell concentration after treatment with **WSP6**, **Dox**, and **Dox⊂WSP6**.

	WSP6	**Doxorubicin**	**Dox⊂WSP6**	**t-stud**
A2780	>30 μM (4)	7.1±2.4 nM (6)	12.0±4.5 nM (6)	p<0.05
A549	>30 μM (4)	46.0±12.8 nM (6)	74.4±21.4 nM (5)	p<0.05
BT474	>30 μM (4)	1.244±238 μM (5)	1.422±244 μM (5)	n.d.

(in round brackets is the number of proves for each experiment.)

Our very preliminary findings show that **WSP6** is not cytotoxic against the cancer cells tested and, as a result, the anti-tumoural activity observed is only provided by the release of doxorubicin inside of tumour tissue.

In conclusion, the new water-soluble pillar[6]arene **WSP6** was successfully synthetized in good yields. This macrocycle proved to be a better host partner for levofloxacin than **WP5**, with a binding constant an order of magnitude higher under physiological conditions. This binding affinity prompted us to develop a multilayer system using the layer-by-layer technique with antibiotic drug loading and release properties. The relevance of this study rests on the prospect of using the present approach for the fabrication of smart medical

equipment (*e.g.*, catheters, endotracheal tubes) featuring antibacterial multilayer coatings for the release of specific antibiotics. The fabrication of multi-layers system capable of rapid drug release is particularly appealing as it paves the way for the development of ready-to-use medical equipment, useful in those cases where large quantities of drug a required in a short time (*e.g.*, surgeries).

As a further line of research, the receptor abilities of **WSP6** were also tested with the poorly water-soluble drug doxorubicin, with the intention of using the macrocyclic scaffold as a cargo molecule for selective drug delivery into cancer cells. **WSP6** was found to have the ability to complex doxorubicin and increase its solubility in the physiological environment, forming an aggregate of discrete molecules that is, to the best of our knowledge, the first example of a system in which the doxorubicin molecule is released from a single pillararene molecule.

4.7 Experimental Section†

Materials and Methods. Dodeca-ethoxypillar[6]arene was prepared according to literature procedures.[26] Hydroquinone, levofloxacin (**Lev**), doxorubicin (**Dox**), poly(ethyleneimine) (**PEI**, average MW 750000, 50% in water) and poly(allylamine) hydrochloride (**PAH**, average MW 50000) were purchased from Sigma-Aldrich. Anhydrous solvents were either obtained commercially or dried by standard methods prior to use,[56] while other chemicals were reagent grade, routinely used without any further purification.

The strain of *Staphylococcus aureus* ATCC29213 used in the microbiological studies was acquired from the American Type Culture Collection (LGCPromochem, Milan, Italy). *S. aureus* microorganisms were stored at -80 °C in a Trypti-case Soy broth (TSB) containing 20% (*v/v*) glycerol. Quartz slides were obtained from Alfa Aesar.

Chemical shifts are reported in ppm and are referenced to the residual solvent used ($CDCl_3$: δ_H 7.26 and δ_C 77.0 ppm; DMSO-d_6: δ_H 2.50 and δ_C 39.5 ppm), spectra recorded in D_2O were referenced to external 1,4-dioxane (δ_H 3.53 and δ_C 66.7 ppm). NMR titration studies were carried out at a fixed **WSP6** concentration (1 mM) and samples were routinely prepared by dissolving solid **WSP6** in D_2O or a D_2O phosphate buffer solution (60 mM $Na_2HPO_4 \cdot 7H_2O/NaH_2PO_4 \cdot H_2O$, pH 7.2). The stock solution of levofloxacin ([**Lev**] = 25 mM) was prepared by using the above-mentioned 1 mM **WSP6** solution as the solvent, so as to maintain a constant host concentration after addition of aliquots of the guest, while all doxorubicin solutions were freshly prepared using the same **WSP6** solution. The association constants were calculated by a nonlinear regression method using the WinEQNMR program,[54] and BindFit v0.5 program.[35] UV-Vis absorption spectra were taken on a Varian Cary 50 spectrophotometer (additionally equipped with a fiber optic probe with a 1cm fixed-length path) and on a Perkin-Elmer Lambda 45 spectrophotometer. A Perkin-Elmer LS-45 fluorescence spectrometer equipped with a Hamamatsu R928 phototube was used to collect the emission spectrum of the **Lev**@(**WSP6/PAH**)$_8$ films (λ_{exc} = 289 nm). *In vitro* release data are fitted to pseudo first order kinetic non-linear equation: $q_t = q_e \cdot (1 - e^{K_1 \cdot t})$

Releasing device	q_e (μg mL^{-1})	K_1 (L min^{-1})	R^2
(WP5/PAH)$_8$	2.9 ± 0.1	0.23 ± 0.06	0.95
(WSP6/PAH)$_8$	4.35 ± 0.25	0.042 ± 0.006	0.95
(WSP6/PAH)$_4$	2.86 ± 0.25	0.060 ± 0.06	0.94

† For general procedure and instrumental description see Chapter 2, Section 2.3.1.

Microbial assays were performed by Dr. Domenico Franco, Dr. Laura M. De Plano and Prof. Salvatore Guglielmino, Dipartimento di Scienze Chimiche, Biologiche, Farmaceutiche ed Ambientali, Università di Messina.
Anti-tumoural assays were carried out by Dr. Camillo Rosano and Dr. Maurizio Viale, IRCCS Policlinico San Martino, National Institute for Cancer Research, Genova.
In vitro release data fitting was performed by Prof. Gabriele Lando, Università di Messina.

Preparation of multi-layers system (WSP6/PAH)$_{4/8}$ by LbL technique. The glass/quartz slides were sonicated in concentrated nitric acid (98%) for 30 minutes, washed first with deionized water and then degreased with absolute ethanol, and finally dried for 24 h at 60 °C. Only in the case of the first layer the glass surface was immersed in an aqueous solution of polyethylenimine **PEI** (3 mg/mL) for 15 minutes, to introduce positively charged molecules onto the anionic substrate surface, the subsequent cationic layers were formed by dipping the solid support in an aqueous solution of polyallylamine hydrochloride **PAH** (3 mg/mL) for the same time. Then, each new-formed layer is washed with a large amount of water to remove the excess of unmodified positive polyelectrolyte, and finally dried to obtain the cationic monolayer. Afterwards, this cationic coated slide was immersed in an aqueous solution of **WSP6** (1.3 mg/mL) for 15 minutes to introduce negatively charged molecules, washed also in this case with a large amount of water and dried, resulting in a bilayer with an anionic external surface.

Determination of the minimum inhibitory concentration (MIC) of Levofloxacin. The MIC of levofloxacin for *Staphylococcus aureus* ATCC29213 was determined by adding increasing aliquots of the antibiotic (0.25–0.64 μg/mL) to cultures of *S. aureus* in a Mueller Hinton broth (MHB) at a semi-exponential growth and a final inoculum of approximately 10^4–10^5 bacteria per mL. The MIC_{90} –*i.e.*, the lowest concentration of a drug required to prevent 90% of microbial growth–of levofloxacin for *S. aureus* was found to be 1 μg/mL.

Antibacterial activity assessment. Bacterial semi-exponential cultures were used for all bactericidal assays. Specifically, *S. aureus* overnight cultures were inoculated in fresh medium and incubated for 6–8 h at 37 °C under shaking (150 rpm). Bacteria were then centrifuged and re-suspended in a 60 mM PBS solution (pH 7.2) three times. Starting from this bacterial solution having an equivalent turbidity (McFarland standard) of 0.5 (approximately 2×10^8 CFU/mL), serial dilutions were made to finally obtain 2×10^6 bacteria/mL in the MHB medium.

Glass slides coated with the (**WSP6**/**PAH**)$_8$ film and the (**WSP6**/**PAH**)$_8$ film loaded with levofloxacin (**Lev**@(**WSP6**/**PAH**)$_8$), were placed into a sterile 6-well microplate, filled with 4 mL of the bacterial culture and incubated for 6, 24 and 48 h at 37 °C under gentle shaking (100 rpm, orbital shaker KS-15, Edmund Buhler GmbH). Normal bacterial growth without glass-slide substrates was used as positive control (CTR).

The antibacterial effect of the levofloxacin released from the **Lev**@(**WSP6**/**PAH**)$_8$ substrates in the culture medium was evaluated by the Colony Forming Units (CFU) assay and the Live/Dead staining (*Bac*Light™ Bacterial Viability Kit, for microscopy). The Live/dead viability assay was also use to evaluate of the bacteria in adhered on the substrates coated with **Lev**@(**WSP6**/**PAH**)$_8$ and the (**WSP6**/**PAH**)$_8$ films. Specifically, after a given incubation period, each substrate was placed in a new well, washed three times with a 60 mM PBS solution, to remove non-adherent bacteria, then stained with the Live/Dead kit for 15 min. in the dark at 37 °C.

Fluorescent images were visualized by using a Leica DMRE epifluorescence microscope (Leica Microsystems, Heerbrugg, Switzerland) with a Leica C Plan 100x objective and a BP 515–560 nm excitation filter in combination with a LP 590 nm suppression filter. A quantitative evaluation of cells adhering onto the surface was performed using the Scion Image software (Windows version of NIH Image software). This software allows to evaluate the bacterial cell coverage in terms of integrated density (ID):

$$ID = N \times (M - B)$$

where *N* is the number of pixels in the selection, *M* is the average grey value of the pixels, and *B* is the most common pixel value).

4.7.1 Synthetic procedures

*diethyl 4,4'-(1,4-phenylenebis(oxy))dibutyrate **5**:* A suspension of hydroquinone (5.0 g, 45.6 mmol) and K_2CO_3 (13.5 g, mmol) were stirred in 200 mL of CH_3CN. After 10 minutes at r.t., ethyl 4-bromobutyrate (26.7 g, 136.7 mmol) was added and the mixture was refluxed for 24 h. Solvent was removed by rotary evaporation and the resulting brown solid was dissolved in AcOEt (100 mL) and then washed with HCl (3×50 mL) and H_2O (3×50 mL). The organic layer was collected and dried over $MgSO_4$, and the solvent was removed under reduced pressure. The resulting brownish oil was purified by column chromatography (hexane/ethyl acetate 5:1) and subsequently recrystallized from hexane/AcOEt 5:1, providing pure **5** as white crystals (13.0 g, 84%); m.p. 145–147 °C; ^{1}H NMR ($CDCl_3$): δ 1.26 (t, *J* = 7.1 Hz, 6H), 2.08 (m, 4H), 2.50 (t, *J* = 7.3 Hz, 4H), 3.94 (t, *J* = 6.1 Hz, 4H), 4.14 (q, *J* = 7.3 Hz, 4H), 6.80 (s, 4H) ppm.

Other spectroscopic data were in full agreement with those previously reported by Q. Jin *et al*.[57]

Dodeca-ethylbutyrate pillar[6]arene ***6*** *and deca-ethylbutyrate pillar[5]arene* ***7*** (direct method): Diester **5** (1,41 g; 4,16 mmol) and paraformaldehyde (380 mg; 12,48 mmol) were stirred at 0° C in anhydrous CH_2Cl_2 (80 mL), at 0 °C for 10 min. $FeCl_3$ (114 mg; 0,7 mmol) was added at once and the mixture was stirred for 1 h at 0° C under inert atmosphere (Ar). Over this period the solution turned from a bright yellow to a dark green. The reaction mixture was let to warm a r.t. and it was then stirred for further 4 h. The dark-green solid formed was collected by suction filtration and the filtrate was washed with brine (100 mL), water (3×50 mL) and then dried over $MgSO_4$. The brownish oil obtained after solvent evaporation was purified by column chromatography (hexane/ethyl acetate 3:2) to yield **6** (133,5 mg, 9%) and **7** (160,4 mg, 11%), (ratio **6** : **7** = 1 : 1.2):

For **6**: R_f 0.14; m.p. 101–103 °C. ^{1}H NMR ($CDCl_3$): δ 6.79 (s, 10 H, Ar*H*), 4.09 (q, *J* = 7.2 Hz, 20 H, $CO_2CH_2CH_3$), 3.90 (br s, 20 H, $ArOCH_2$), 3.72 (s, 10 H, $ArCH_2Ar$), 2.56 (t, *J* = 7.6 Hz, 20 H, $CH_2CO_2CH_2$), 2.09–2.14 (m, 6 H, $OCH_2CH_2CH_2$), 1.16 (t, *J* = 7.1 Hz, 30 H, $CO_2CH_2CH_3$) ppm; ^{13}C NMR ($CDCl_3$): δ 173.2 (CO_2Et) 149.7 (1,4-Ar*C*), 128.4 (3,6-Ar*C*), 115.0 (2,5-Ar*C*), 67.6 ($ArOCH_2$), 60.4 ($CO_2CH_2CH_3$), 31.3 ($CH_2CO_2CH_2$), 29.5 ($ArCH_2Ar$), 25.5 ($OCH_2CH_2CH_2$), 14.2 ($CH_3CH_2CO_2$) ppm. HRMS (ESI/Orbitrap) m/z: $[M–H]^-$ Calcd for $C_{114}H_{156}O_{36}$, 2100.0297; Found, 2100.0259.

For **7**: R_f 0.21; m.p. 105–107 °C. ^{1}H NMR ($CDCl_3$): δ 6.79 (s, 10H, Ar*H*), 4.09 (q, *J* = 7.2 Hz, 20H, $CO_2CH_2CH_3$), 3.90 (bs, 20H, $ArOCH_2$), 3.72 (s, 10H, $ArCH_2Ar$), 2.56 (t, *J* = 7.57 Hz, 20H, $CH_2CO_2CH_2$), 2.09-2.14 (m, 6H, $OCH_2CH_2CH_2$), 1.16 (t, *J* = 7.1 Hz, 30H, $CO_2CH_2CH_3$) ppm. ^{13}C NMR ($CDCl_3$): δ 173.2 (*C*OOEt) 149.7 (Ar*C*O), 128.4 (Ar*C*CH_2), 115.0 (Ar*C*H), 67.6 ($PhOCH_2$), 60.4 ($CO_2CH_2CH_3$), 31.3 ($CH_2CO_2CH_2$), 29.5 ($ArCH_2Ar$), 25.5 ($OCH_2CH_2CH_2$), 14.2 ($CH_3CH_2CO_2$) ppm.

Dodeca-ethylbutyrate pillar[6]arene ***6*** (indirect method): a suspension of **5** (254 mg; 0.35 mmol) and K_2CO_3 (1,16 g; 8,4 mmol) was refluxed in anhydrous $CHCN_3$ (40 mL) for 20 minutes under an inert atmosphere (Ar). 4-Ethylbromobutyrate (432 mg; 2.21 mmol) was added and the mixture was refluxed under vigorous stirring for 24 hours. The solid present in the reaction mixture was filtered off and the filtrate was concentrated to dryness under reduced pressure. The oily residue obtained was purified by column chromatography (toluene/AcOEt 9:1 to 8:2) to afford 215 mg (30%) of the title compound.

*Dodeca-butanoic pillar[6]arene **8***: 5 mL of an aqueous solution of NaOH (42.6 mg, 1.07 mmol) was added dropwise to an ethanol solution (10 mL) of doceca-ester **8** (150 mg, 0.071 mmol).The mixture was heated under reflux for 15 hours and then cooled to r.t.. The solvent was reduced to about half of its original volume, under reduced pressure, and the acid thus formed was precipitated by addition of 12.5 M HCl. The white powdery solid was filtered and repeatedly washed with H_2O to afford 122 mg (97%) of the pure compound **8**; m.p. 238–240 °C; ^{1}H NMR (DMSO-d_6) δ 12.10 (br s, 12 H, CO_2H), 6.64 (s, 12 H, ArH), 3.74 (t, J = 6.1 Hz, 24 H, $ArOCH_2$), 3.64 (s, 12 H, $ArCH_2Ar$), 2.36 (t, J = 7.6 Hz, 24 H, CH_2CO_2H), 1.87 (m, 24 H, $CH_2CH_2CH_2$) ppm; ^{13}C NMR (DMSO-d_6) δ 174.5 (CH_2CO_2H), 149.8 (ArCO), 126.7 ($ArCCH_2$), 114.4 (ArCH), 67.1 ($PhOCH_2$), 39.5 (CH_2CO_2H), 30.8 ($ArCH_2Ar$), 25.0 ($CH_2CH_2CH_2$) ppm. HRMS (ESI/Orbitrap) m/z: $[M–H]^–$ Calcd for $C_{90}H_{108}O_{36}$, 1763.6541; Found, 1763.6542.

*Dodeca-carboxylate pillar[6]arene **WSP6**:* 0,5 mL of aqueous solution of NaOH (32.6 mg, 0.82 mmol) was added dropwise to a stirred solution of **8** (120 mg, 0.068 mmol) was dissolved in a 1:1 THF/CH_3OH mixture (5 mL). After two hours the solvent was stripped off under reduced pressure, quantitatively yielding **WSP6** as a pure white solid; m.p > 300 °C. ^{1}H NMR (D_2O) δ 1.83 (p, J = 6.6 Hz, 24 H, $CH_2CH_2CH_2$), 2.20 (t, J = 7.8 Hz, 24 H, $CH_2CO_2^–$), 3.70 (t, J = 6.2 Hz, 24 H, $ArOCH_2$), 3.85 (s, 12 H, $ArCH_2Ar$), 6.77 (s, 12 H, ArH) ppm; ^{13}C NMR (D_2O) δ 181.9 (CH_2CO_2Na), 150.4 (ArCO), 128.8 ($ArCCH_2$), 116.3 (ArCH), 69.2 ($PhOCH_2$), 33.6 (CH_2CO_2Na), 31.3 ($ArCH_2Ar$) 25.8 ($CH_2CH_2CH_2$) ppm.

*Deca-carboxylate pillar[5]arene **WSP5***: m.p. > 300 °C. ^{1}H NMR (D_2O, δ 4.79 ppm) δ 6.79 (s, 10H, ArH), 3.84 (s, 10H, $PhCH_2$), 3.71 (bs, 20H, $PhOCH_2$), 2.37–2.31 (m, 20H, CH_2CO_2Na), 1.90 (q, J = 7.1, 6.7 Hz, 20H, $CH_2CH_2CH_2$) ppm. ^{13}C NMR (D_2O) δ 182.3 (CO_2Na), 150.1 ($COCH_2$), 129.3 (CCH_2), 116.2 (ArCH), 69.3 (OCH_2), 34.2 (CH_2CO_2Na), 29.6 ($ArCH_2Ar$), 26.0 ($CH_2CH_2CH_2$).

*1,4-Diethoxybenzene **1**:* According to the published procedure by Scarso *et al.*[31] treatment of 1,4-hydroquinone with CH_3CH_2I in NaOH and DMSO gave **1** (5.8 g; 70%) as a white solid after recrystallization from warm EtOH. ^{1}H NMR ($CDCl_3$) δ 6.82 (d, J = 0.5 Hz, 4H), 3.98 (q, J = 7.0 Hz, 4H), 1.38 (td, J = 7.0, 0.6 Hz, 6H).

*Dodeca-ethoxypillar[6]arene **2***: According to the method reported by Hu *et al.*[26] the cyclooligomerization of **1** in presence of paraformaldehyde and BF_3•OEt_2 in dry $CHCl_3$

provided **2** (537 mg; 20%) as a white solid. ^{1}H NMR ($CDCl_3$) δ 6.69 (s, 12H), 3.93–3.69 (m, 32H), 1.28 (t, J = 7.0 Hz, 36H).

*per-hydroxylated pillar[6]arene **4***: Following the procedure reported by Ma *et al.*,[32] the reaction of **2** and BBr_3 in dry CH_2Cl_2 afforded **4** (310 mg; 92%) as a white solid after recrystallization from acetone. ^{1}H NMR (Acetone-d_6) δ 7.69 (bs, 12H), 6.54 (s, 12H), 3.67 (s, 12H).

4.8 References

[1] (a) Chen X.M., Hou X.F., Bisoyi H.K., Feng W.J., Cao Q., Huang S., Yang H., Chen D., Li Q., *Nat. Commun.*, **2021**,*12*, 4993; (b) Chen Y., Huang F., Li Z.T., Liu Y., *Sci. China Chem.*, **2018**, *61*, 979; (c) Zhang Y., Liu Y., Liu Yu, *Adv. Mater.*, **2020**, *32*, 1806158; (d) Kakuta T., Yamagishi T., Ogoshi T., *Acc. Chem. Res.* **2018**, *51*, 1656; (e) Schrader T., Hamilton A.D., *Functional Synthetic Receptors*, Wiley-VCH, Weinheim, **2005**, Schrader T., Hamilton A.D., (Eds.); (f) Ariga K., Kunitake T., *Supramolecular Chemistry— Fundamentals and Applications: Advanced Textbook*, Springer, Berlin, **2006**. (g) Kubik S., Reyheller C., Stuwe S., *J. Inclusion Phenom. Macrocyclic Chem.*, **2005**, *52*, 137.

[2] (a) van der Vegt N.F.A., Nayar D., *J. Phys. Chem. B*, **2017**, *121*, 43, 9986; (b) Lipshutz B.H., Ghorai S., Cortes-Clerget M., *Chem. Eur.J.*, **2018**, *24*, 6672.

[3] Schneider H.J., Kramer R., Simova S., Schneider U., *J. Am. Chem. Soc.,* **1988**, 110, 6442.

[4] Dasgupta S., Mukherjee P.S., *Org. Biomol. Chem.,* **2017**, *15*, 762.

[5] (a) Shi Y., van der Meel R., Chen X., Lammers T., *Theranostics*, **2020**, *10*, 7921; (b) Maeda H., *J. Pers. Med*, **2021**, *11*, 229.

[6] Ogoshi T., Hashizume M., Yamagishi T.A., Nakamoto Y., *Chem. Commun.*, **2010**, *46*, 3708.

[7] (a) Ma Y.J., Ji X.F., Xiang F., Chi X.D., Han C.Y., He J.M., Abliz Z., Chen W.X., Huang F., *Chem. Commun.*, **2011**, *47*, 12340; (b) Yao Y., Xue M., Chi X.D., Ma Y.J., He J.M., Abliz Z., Huang F., *Chem. Commun.*, **2012**, *48*, 6505.

[8] Yang K., Chang Y., Wen J., Lu Y., Pei Y., Cao S., Wang F., Pei Z., *Chem. Mater.*, **2016**, *28*, 1990.

[9] (a) Duan Q., Cao Y., Li Y., Hu X., Xiao T., Lin C., Pan Y., Wang L., *J. Am. Chem. Soc.*, **2013**, *135*, 10542; (b) Cao Y., Zou X., Xiong S., Li Y., Shen Y., Hu X., Wang L., *Chin. J. Chem.,* **2015**, *33*, 329; (c) Chang Y., Yang K., Wei P., Huang S., Pei Y., Zhao W., Pei Z., *Angew. Chem. Int. Ed.*, **2014**, *53*, 13126.

[10] Yu G., Xue M., Zhang Z., Li J., Han C., Huang F., *J. Am. Chem. Soc.*, **2012**, *134*, 13248.

[11] Yu G.C., Zhou X.R., Zhang Z.B., Han C.Y., Mao Z.W., Gao C.Y., Huang F., *J. Am. Chem. Soc.*, **2012**, *134*, 19489.

[12] (a) Wang P., Yan X.Z., Huang F., *Chem. Commun.*, **2014**, *50*, 5017; (b) Yang J., Yu G.C., Xia D.Y., Huang F., *Chem. Commun.*, **2014**, *50*, 3993.

[13] Xia D.Y., Yu G.C., Li J.Y., Huang F., *Chem. Commun.*, **2014**, *50*, 3606.

[14] (a) Xia W., Hu X.Y., Chen Y., Lin C., Wang L., *Chem. Commun.*, **2013**, *49*, 5085; (b) Yu G., Han C., Zhang Z., Chen J., Yan X., Zheng B., Liu S., Huang F*., J. Am. Chem. Soc.*, **2012**, *134*, 8711.

[15] (a) Yao Y., Xue M., Chen J., Zhang M., Huang F., *J. Am. Chem. Soc.,* **2012**, 134, 15712; (b) Duan Q., Cao Y., Li Y., Hu X., Xiao T., Lin C., Pan Y., Wang L., *J. Am. Chem. Soc.,* **2013**, 135, 10542; (c) Cao Y., Hu X.Y., Li Y., Zou X., Xiong S., Lin C., Shen Y.Z., Wang L., *J. Am. Chem. Soc.,* **2014**, 136, 10762.

[16] Qi Z., Achazi K., Haag R., Dong S., Schalley C.A., *Chem. Commun.*, **2015**, 51, 10326.

[17] Torres I.M., Patankar Y.R., Shabaneh T.B., Dolben E., Hogan D.H., Leib D.A., Berwin B.L., *Infect. Immun.,* **2014**, 82, 4689.

[18] (a) Sun Y.L., Yang Y.W., Chen D.X., Wang G., Zhou Y., Wang C.Y., Stoddart J.F., *Small*, **2013**, 9, 3224; (b) Zhang H., Ma X., Nguyen K.Y., Zhao Y., *ACS Nano*, **2013**, 7, 7853; (c) Wu X., Gao L., Yu X., Wang H., Wang L., *Chem. Rec.,* **2016**, 1216.

[19] Dasgupta S., Chowdhury A., Mukherjee P.S., *RSC Adv.*, **2015**, 5, 85791.

[20] Barbera L., Franco D., De Plano L.M., Gattuso G., Guglielmino S.P.P., Lentini G., Manganaro N., Marino N., Pappalardo S., Parisi M.F., Puntoriero F., Pisagatti I., Notti A., *Org. Biomol. Chem.*, **2017**, *15*, 3192.

[21] Wang P., Li Z., Ji X., *Chem. Commun.,* **2014**, *50*, 13114.

[22] Barbera L., De Plano L.M., Franco D., Gattuso G., Guglielmino S.P.P., Lando G., Notti A., Parisi M.F., Pisagatti I., *Chem. Commun.,* **2018**, *54*, 10203.

[23] (a) Poole M., Anon J., Paglia M., Xiang J., Khashab M., Kahn J., *Otolaryngol Head Neck Surg.,* **2006**, *34*, 7; (b) Noreddin A.M., Elkhatib W.F., *Expert Rev Anti Infect Ther.,* **2010**, *8*,14; (c) McGregor J.M., Allen G.P., Bearden D.T., Ther Clin Risk Manag., **2008**, *4*, 843; (d) Schaeffer A.J., Wu S.C., Tennenberg A.M., Kahn J.B., *J. Urol.,* **2005**, *174*, 4; (d) Zamir D., Weiler Z., Kogan E., Ben-Valid E., Hay E., Reitblat T., Polishchuk I., *J. Clin. Gastroenterol.,* **2006**, *40*, 90.

[24] Marra F., Marra C.A., Moadebi S., Shi P., Elwood R.K., Stark G., FitzGerald J.M., *Chest.*, **2005**, *128*, 13.

[25] Cao D., Kou Y., Liang J., Chen Z., Wang L., Meier H., *Angew. Chem. Int. Ed.*, **2009**, *48*, 9721.

[26] Hu X.B., Chen Z.X., Chen L., Zhang L., Hou J.L., Li Z.T., *Chem. Commun.*, **2012**, *48*, 10999.

[27] Ogoshi T., Ueshima N., Akutsu T., Yamafuji D., Furuta T., Sakakibara F., Yamagishi T., *Chem. Commun.*, **2014**, *50*, 5774.
[28] Ogoshi T., Kanai S., Fujinami S., Yamagishi T., Nakamoto Y. J., *Am. Chem. Soc.*, **2008**, *130*, 5022.
[29] Mirzaei S., Wang D., Lindeman S.V., Sem C.M., Rathore R., *Org. Lett.*, **2018**, *20*, 6583.
[30] Shangguan L., Chen Q., Shi B., Huang F., *Chem. Commun.*, **2017**, *53*, 9749.
[31] Da Pian M., Schalley C.A., Fabris F., Scarso A., *Org. Chem. Front.*, **2019**, *6*, 1044
[32] Ma Y., Chi X., Yan X., Liu J., Yao Y., Chen W., Huang F., Hou J., *Org. Lett.*, **2012**, *14*, 6, 1532.
[33] Yu G., Xue M., Zhang Z., Li J., Han C., Huang F., **2012**, *134*, 32, 13248.
[34] (a) Basilio N., García-Río L., Martín-Pastor M., *J. Phys. Chem. B*, **2010**, *114*, 14, 4816; (b) Gómez B., Francisco V., Nieto F.F., Garcia-Rio L., Pastor M.M., Paleo M.R., Sardina F.J., *Chem. Eur. J.*, **2014**, *20*, 12123.
[35] (a) Thordarson P., *Chem. Soc. Rev.*, **2011**, *40*, 1305; (b) Hibbert D.B., Thordarson P., *Chem. Commun.*, **2016**, *52*, 12792. Available on http://supramolecular.org/
[36] (a) Richardson J.J., Bjornmalm M., Caruso F., *Science*, **2015**, *348*, 2491; (b) Xiao F.X., Pagliaro M., Xu Y.J., Liu B., *Chem. Soc. Rev.*, **2016**, *45*, 3088.
[37] Decher G., Hong J.D., *Makromol. Chem., Macromol. Symp.*, **1991**, *46*, 321.
[38] Liu Z., Wang X., Wu H., Li C., *J. Colloid Interface Sci.*, **2005**, *287*, 604.
[39] Srivastava S., Kotov N.A., *Acc. Chem. Res.*, **2008**, *41*, 1831.
[40] Boulmedais F., Ball V., Schwinte P., Frisch B., Schaaf P., Voegel J.C., *Langmuir,* **2003**, *19*, 440.
[41] Crespo-Biel O., Dordi B., Reinhoudt D.N., Huskens J., *J. Am. Chem. Soc.,* **2005**, *127*, 7594.
[42] (a) Crouzier T., Sailhan F., Becquart P., Guillot R., Logeart-Avramoglou D., Picart C., *Biomaterials*, **2011**, *32*, 7543; (b) Gilde F., Maniti O., Guillot R., Mano J.F., Logeart- Avramoglou D., Sailhan F., *Biomacromolecules*, **2012**, *13*, 3620; (c) Guillot R., Gilde F., Becquart P., Sailhan F., Lapeyrere A., Logeart-Avramoglou D., *Biomaterials*, **2013**, *34*, 5737.
[43] Wood K.C., Chuang H.F., Batten R.D., Lynn D.M., Hammond P.T., *Proc. Natl. Acad. Sci. USA*, **2006**, *103*, 10207.
[44] Sukhishvili S.A., *Curr. opin. Colloid Interface Sci*, **2005**, *10*, 37.
[45] Zhang D., Zhang K., Yao Y.L., Xia X.H., Chen H.Y., *Langmuir*, **2004**, *20*, 7303.
[46] (a) Richardson J.J., Cui J., Björnmalm M., Braunger J.A., Ejima H., Caruso F., *Chem. Rev.*, **2016**, *116*, 14828; (b) Zhu G.H., Cho S., Zhang H., Zhao M., Zacharia N.S., *Langmuir*, **2018**, *34*, 4722.
[47] (a) Chatterjee K., Zhang J., Honbo N., Karliner J.S., *Cardiology*, **2010**, *115*, 155 – 162; (b) Patel S., Sprung A.U., Keller B.A., *et al.*, *Mol. Pharmacol.*, **1997**, *52*, 4, 658 – 666; (c)Lorenzo E., Ruiz-Ruiz C., Quesada A.J., *et al.*, *J. Biol. Chem.*, **2002**, *277*, 17, 10883.
[48] (a) Bekers O., Beijnen J.H., Otagiri M., A Bult., Underberg W.J.M., *Journal of Pharmaceutical&BiomedicalAnalysis*, **1990**, *8*, 671 – 674; (b) Y. Bakkour, Vermeersch G., Morcellet M., Boschin F., Martel B., Azaroual N., *Journal of Inclusion Phenomena and Macrocyclic Chemistry*, **2006**, *54*, 109; (c) Motoyama K., Onodera R., Okamatsu A., Higashi T., Kariya R., Okada S., Arima H., *J Drug Target*, **2014**, *22*, 3, 211.
[49] Zhao N., Woodle M.C., Mixson A.J., *J. Nanomed. Nanotechnol.*, **2018**, *9*, 5.
[50] Mohanta V., Madras G., Patil S., *Appl. Mater. Interfaces*, **2014**, *6*, 20093.
[51] Cao Y., Zou X., Xiong S., Li Y., Shen Y., Hu X., Wang P.L., *Chin. J. Chem.*, **2015**, *33*, 329.
[52] Cao Y., Li Y., Hu X., Zou X., Xiong S., Lin C., Wang L., *Chem. Mater.*, **2015**, *27*, 1110.
[53] Shangguan L., Chen Q., Shi B., Huang F*., Chem. Commun.,* **2017**, *53*, 9749.
[54] Hynes M.J., *J. Chem. Soc.*, *Dalton Trans.*, **1993**, 311.
[55] Henderson T.J., *Anal. Chem.*, **2002,** *74*, 191.
[56] Armarego W.L.F., *Purification of Laboratory Chemicals – Eighth Edition*, Butterworth-Heinemann (Elsevier), **2017**.
[57] Zhang T., Fan H., Zhou J., Jin Q.; *Journal of Polymer Science, Part A: Polymer Chemistry*, **2009**,*47*, 12, 3056.